Dust storms over South Africa: synoptic weather patterns and evolution of meteorological variables associated with significant dust storm events

by

Mbavhalelo Maliage

Submitted in partial fulfilment of the requirements for the degree

Master of Science (Meteorology)

In the Faculty of Natural & Agricultural Sciences

University of Pretoria

DECLARATION

I, Mbavhalelo Maliage, declare that the dissertation which I hereby submit for the degree Master of Science (Meteorology) at the University of Pretoria, is my own work and has not previously been submitted by me for a degree at this or any other tertiary institution.

Signature: 

Date: June 2024

SUMMARY

Student:	Mbavhalelo Maliage
Supervisor:	Dr Rebecca Garland
Co-Supervisor:	Dr Liesl L. Dyson
Department:	Geography, Geoinformatics and Meteorology
Faculty:	Natural & Agricultural Sciences
University:	University of Pretoria
Degree:	Master of Science (Meteorology)

Dust storms (DS) are common in semi-arid and arid regions, with the majority of the natural dust source regions located in the Northern Hemisphere. Although there are some significant source regions in the Southern Hemisphere, South Africa is not a major contributor to dust emissions. Consequently, very little research has been conducted on DS in South Africa. However, there has been an increase in anthropogenic source regions linked to agricultural activities over the central parts of South Africa. With the expected increase in DS frequency over South Africa, it is therefore important to understand the meteorological factors associated with these DS. The study aims to first identify the main synoptic weather systems that produce DS over the country, separating the findings according to DS along the coast and DS over the interior of the country. Secondly, the study aims to identify how meteorological variables evolve before, during, and after a DS.

Ten DS are selected for analysis, five from coastal regions and five from the interior. The weather systems associated with coastal DS are similar for all five DS: a surface trough extending along the west or adjacent interior. This often results in offshore flow along the west coast, also known as berg wind conditions. For interior DS, three are a result of thunderstorm activity, with one DS associated with a cut-off low. Two DS were triggered by cold fronts, one being a prefrontal dust storm and the other a post-frontal dust storm.

The meteorological variables analysed are temperature, focussing on the diurnal temperature range (ΔT) and the maximum temperature (T_{max}), wind speed and direction, relative humidity (RH), dew point temperature (T_d), rainfall, and soil moisture. All coastal DS had an easterly component to the wind direction, which is caused by the location weather systems that caused the DS. The DS that

lasted the longest, did not have the lowest RH, T_d, or temperature, but had the strongest wind gusts and strongest high-pressure system. The results indicate how DS are associated with drier atmospheric conditions, which are depicted by low RH and T_d. This is observed with synoptic scale-induced DS, where the RH and T_d gradually decrease, being the lowest on the day of the DS. However, the opposite was observed for mesoscale-induced DS. The presence of thunderstorms associated with the mesoscale-induced DS meant that there was enough moisture in the atmosphere for their development, indicated by higher T_d and RH values. The results also show that the behaviour of the meteorological variables is influenced by several factors such as whether it is a synoptic-scale or mesoscale weather system, the duration, and strength of the weather system associated with the DS, the season in which the DS occurred, as well as the location or source region of the DS. Overall, this study is a base study for DS over South Africa, to contribute to the research necessary for a decision tree for forecasting DS in the future.

ACKNOWLEDGEMENTS

- My supervisors, Dr Rebecca Garland and Dr Liesl Dyson – for your patience and support, and all the encouragement. Thank you very much.
- Mom and dad – thank you for every single sacrifice you have made for me. I honour you.
- My family – the greatest support system I have been blessed with. Thank you for always believing in me and encouraging me throughout.
- My sisters – Thank you for the long conversations, the empowerment sessions, the prayers that gave me the extra boost I needed in the end, and just being the sound board I needed.
- To Andani – No words can express how thankful I am for you. Thank you for being there for me and being so dependable. Truly a blessing.
- Ofunwa – You changed my perspective completely, and you were my weekly boost of joy and laughter. Thank you.
- My colleagues at South African Weather Services – Thank you for the words of support, especially Venetia Phakula, for the random check-in calls and messages, and for being the push I always needed.
- South African Weather Services for the time off and the data provided.
- National Centre for Environmental Prediction for the use of the reanalysis data;
- EUMETSAT and NASA for the satellite imagery;

Most important of all, I am so grateful to my Lord Jesus Christ. When I was weak and almost gave up, You reminded me of Your promises to me, and gave me the strength I needed to carry this out. I owe my whole life to You Lord.

Previous publications:

Maliage, M., Garland, R. and Dyson, L. (2023). Synoptic Weather Patterns Associated with Significant Dust Storm Events Over South Africa. *Proceeds of 54th Annual Conference of the National Association for Clean Air (NACA)*. ISBN: 978-0-7961-0569-1. 6 to 8 September 2023, Polokwane, South Africa, pp.SP3.1–SP3.5. Available online: https://drive.google.com/file/d/18G2HZAlXHhn3X20j_z2kd4fYOiyt7OMD/view?usp=drive_web [Accessed 25 Nov. 2023].

Contents

LIST OF FIGURES

LIST OF TABLES

Table 4.9: indicates the amount of rainfall in mm that the stations received prior to the interior DS events, as well as during the DS event. The cells highlighted in blue indicate the stations that have received rainfall. The area blocked out in black indicates that there was no rainfall data available. 99

ACRONYMS, ABBREVIATIONS AND SYMBOLS

AMS	American Meteorology Society
AWS	Automatic Weather Stations
CCN	Cloud Condensation Nuclei
DNC	Day Natural Colour
DS	Dust storm (s)
EUMETSAT	European Organisation for Exploitation of Meteorological Satellites
ENSO	El Niño Southern Oscillation
GES-DISC	Goddard Earth Sciences Data and Information Services Centre
Giovanni	Geospatial Interactive Online Visualization And Analysis Infrastructure
IPCC	Intergovernmental Panel on Climate Change
METAR	Meteorological Terminal Aerodrome Report
MSG	Meteosat Second Generation
NASA	National Aeronautics and Space Administration
NCEP	National Centre for Environmental Prediction
RH	Relative humidity
SAWS	South African weather service
SEVIRI	Spinning Enhanced Visual and InfraRed Imager
TWV	Threshold wind velocity
WMO	Word Meteorological Organisation

Chapter 1: Background and introduction

1.1. Introduction

Dust storms (DS) are common in semi-arid and arid regions, with most of the natural dust source regions located in the Northern Hemisphere. The Southern Hemisphere also has some significant source regions, although smaller in spatial extension, located in South America, southern Africa, and Australia (Middleton and Kang, 2017, NIDIS, n.d.). DS have several impacts, both long and short-term, on human society as well as on the Earth System. These impacts cannot only affect the immediate region where the DS originate, but also the surrounding countries due to the long-range transport of dust particles (Middleton and Kang, 2017). DS can also influence the climate of an area as they also affect the total energy budget of the atmosphere. Dust particles directly influence the radiation balance by scattering and absorbing solar and terrestrial radiation, as well as inducing or strengthening the local thermal inversion. Dust particles can also indirectly modify the microphysics of clouds, either suppressing precipitation, or invigorating the development of convective clouds, which can contribute to the overall rainfall of a region (Andreae and Rosenfeld, 2008).

There are several factors that impact DS formation and frequency such as precipitation, temperature, humidity, vegetation type and cover, as well as soil moisture to mention a few. Understanding the relationship between dust aerosols and meteorological conditions in the planetary boundary layer is important for improving DS model simulation as well as for forecasting DS (Zhang et al., 2010).

1.2. Dust Storms

According to the World Meteorological Organization (WMO), Sand and DS (SDS) are a meteorological hazard that can threaten human health, agriculture, aviation, ground transportation, solar energy industry, air quality, as well as aquatic and terrestrial ecological systems (UNEP et al., 2016). Sand and DS are common in arid and semi-arid regions and play a vital role in the Earth System. These DS events occur when strong winds blow over loose, unprotected soil, lifting the particles into the atmosphere. The WMO has classified dust events according to McTainsh and Pitblado (1987) , who classified them into 4 main categories:

I. DS, which is the result of turbulent winds raising large quantities of dust into the air and reducing visibility to less than 1000m,

II. Blowing dust, which is dust raised by winds to moderate height above the ground reducing visibility to eye level (i.e. between 1000m and 1800m) ,

III. Dust haze produced by dust particles in suspended transport which have been raised from the ground by a DS prior to the time of observation,

IV. Dust whirls (or dust devils) are whirling columns of dust that move with the wind and are usually less than 30m high (but can extend to 300m) and of narrow dimensions.

Currently, 75% of global dust emissions are emitted from natural source regions, with more than 55% of emissions coming from the dust belt in the Northern Hemisphere (Ginoux et al., 2012, UNEP et al., 2016). Although anthropogenic dust emissions only account for 25% of total global emissions (Ginoux et al., 2012), most of the anthropogenic dust source regions emerge from the Southern Hemisphere. In South Africa, new dust sources have been identified over the central parts, due to the recent drought experienced over the country coupled with affected agricultural activities (Eckardt et al., 2020b).

1.3. Motivation for the study

Little research has been conducted in South Africa regarding DS as it is not a major contributor to global dust emissions. However, they can still have a significant impact on the local environment. Previously, dust source regions were mainly identified based on the location of deserts, which are considered to be natural source regions. However, vegetation cover reduction due to land use and climate change created the potential for new anthropogenic dust source regions to emerge globally. The emergence of anthropogenic dust source regions could also potentially impact weather as well as the global and regional climate and can lead to large uncertainties in quantitative estimations of dust emission in numerical modelling (Chen et al., 2019).

Previous studies (Bhattachan et al., 2012, Vickery et al., 2013) on dust source regions in South Africa indicated that the southern part of the Kalahari Desert shown in figure 1.1, considered a natural dust source region, had the highest emission frequency in South Africa. Recent studies (Bekiswa, 2019, Eckardt et al., 2020b) have now identified major dust source regions associated with anthropogenic activities such as commercial agriculture, concentrated over the Free State and North West provinces of South Africa, with minor source regions identified over the Northern Cape and Mpumalanga provinces.

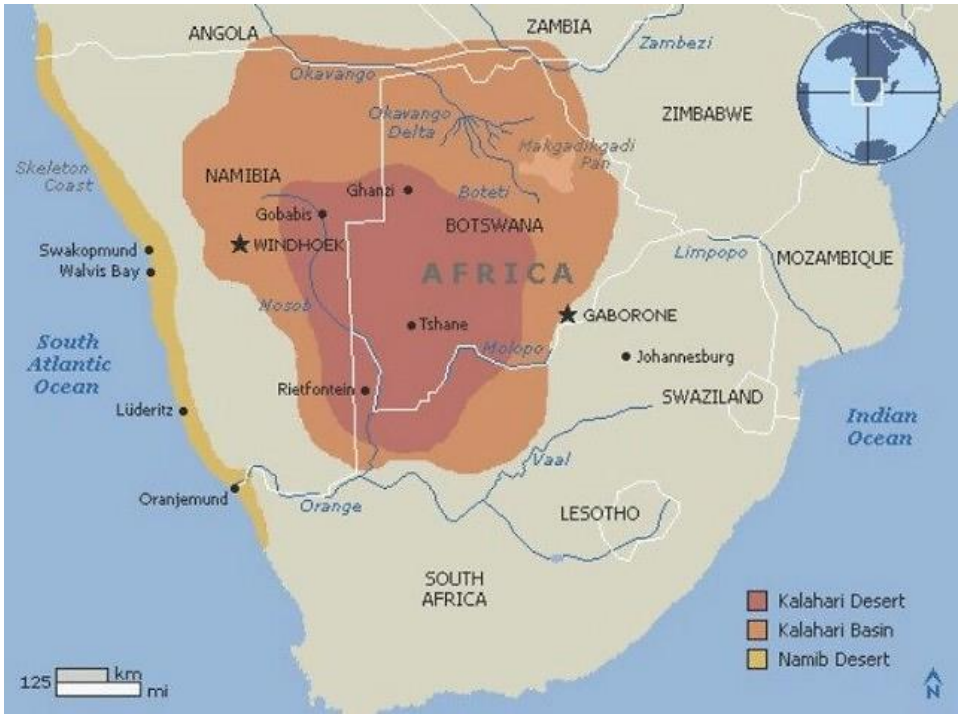

Figure1.1: Location of the Namib desert and the Kalahari Desert. (image retrieved from https://geography.name/kalahari-desert-2/)

The emergence of these new dust source regions over South Africa was exacerbated by the severe drought that occurred between 2015 and 2016, where some provinces received less than 50% of their normal annual rainfall (Simpson and Dyson, 2018). It is therefore important to understand the processes that lead to DS formation and evolution. These factors include the local dominant weather patterns that produce winds strong enough to entrain dust, as well as the development and change in meteorological elements during the occurrence of DS, focusing on South Africa.

This research aims to provide an observational basis for the evolution of meteorological parameters associated with DS. This will contribute to the limited research conducted over the Southern Hemisphere regarding the links between DS formation and evolution and meteorological parameters. This will ultimately assist in accurately modelling the global dust budget and its impacts on the environment. In addition, with increased information about DS and associated weather, more accurate DS forecasting processes and systems can be developed. Using these forecasts, the appropriate efforts to mitigate damage can be put into place and effective early warning can be communicated (UNEP, 2013).

1.4. Aims and objectives

The focus of this dissertation is to identify the synoptic circulation associated with significant DS events over South Africa, as well as how meteorological variables evolve before, during and after significant DS over South Africa. The aims of the research are as follows:

Aim 1: Identify the synoptic systems associated with different coastal and interior DS events.
The objectives needed to meet Aim 1 are as follows:

i. Classify DS according to mesoscale or synoptic scale weather events.
ii. Identify the surface and mid-level circulation systems associated with DS for interior DS and coastal DS.

Aim 2: Determine the behaviour of meteorological variables during DS events
The objectives needed to meet Aim 2 are as follows:

i. Determining the spatial distribution of DS events using satellite imagery, and media sources
ii. Identify the wind speed and direction, temperature, rainfall, dewpoint temperature and humidity trends before, during and after a DS event. This will be done for 3 days before and 2-3 days after the event;
iii. Analyse soil moisture data for the DS events. This will be done for 2 days before and during the event

1.5. Dissertation outline

The dissertation outline will be divided into 5 chapters. The summary of the chapters is as follows:

Chapter 2 introduces DS and their source regions, zooming into South African source regions. The general circulation of South Africa is discussed, focussing on weather systems strong enough to entrain dust, as well as the seasonal variability of the weather systems in association with the seasonal variability of dust emissions over South Africa. The last section gives an overview of the current understanding of the relationship between DS and weather parameters. The focus is on temperature, humidity, precipitation, wind speed, and wind direction, which are the parameters investigated in this study. The influence of soil moisture on the occurrence of DS is also explored.

Chapter 3 begins by outlining the selection process of the events used in this study, as well as the data and sources used to identify the DS events. The methodology of classifying the DS is also explained, highlighting the criteria used to classify the DS. The section that follows outlines the data used to identify the surface and mid-level synoptic circulation associated with the selected DS events weather

systems. Finally, the last section explains how the meteorological data is used to analyse the evolution of each meteorological variable.

In **chapter 4**, the weather systems identified for the DS events are discussed. The behaviour of each of the meteorological parameters are then also reviewed for each DS event selected. The discussions are done according to the classification highlighted in chapter 3 (i.e. interior DS and coastal DS).

Chapter 5 summarises the findings. The limitations of the research are also highlighted, are well as the key questions and recommendations to consider in future research.

2. Chapter 2: Literature Review

2.1. Introduction

The occurrence of DS is dependent on several meteorological factors. In this chapter, the DS cycle is detailed, as well as the global source regions and source regions in South Africa. The mean circulation over South Africa is explained to understand the weather systems that affect South Africa in different seasons. This provides background to identify weather systems with the capacity to entrain DS, which is also discussed. Meteorological variables to be investigated in this study are also discussed in relation to what is known about how they behave during DS.

2.2. Dust storm cycle

The dust cycle forms an integral part of the Earth System, involving the processes of emission of dust particles from the ground surface, transport through the atmosphere, and deposition of the particles, all occurring at different time scales (Goudie and Middleton, 2006, Shao et al., 2011b, Shao et al., 2011a). The dust cycle, illustrated in figure 2.1, begins when strong winds blow over bare land surfaces or surfaces with low vegetation cover, which is called the entrainment of dust. Dust particles, depending on their sizes, are then released into the atmosphere, which is also referred to as the emission of dust into the atmosphere.

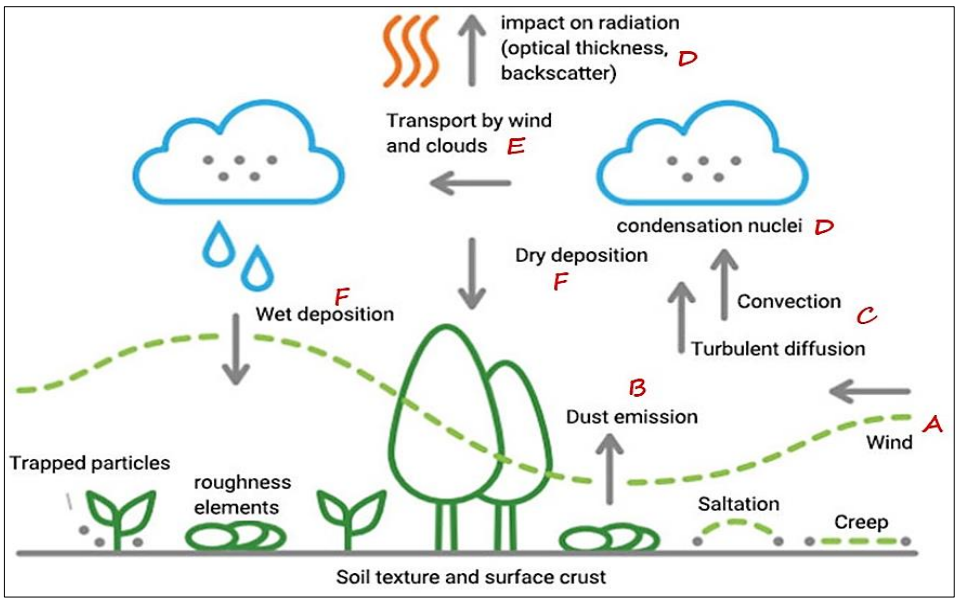

Figure 2.1: DS cycle, indicating key influences of wind erosion. A is entrainment of dust, B is where the dust is emitted into the atmosphere, C is the processes that carries the dust particles carried upward (convection and turbulent diffusion), D is the dust becoming condensation nuclei, as well as impacting radiation, E is transportation of dust particles by wind (often synoptic scale), F is dust particles deposited back on land, either through dry or wet depositions (Adapted from Goudie and Middleton, 2006).

Once airborne, how far up the dust is carried will depend on several factors such as wind speed and turbulence, dust grain characteristics, and their settling velocities (Goudie and Middleton, 2006). The dust particles will either fall back not too far from the dust source region or continue to be carried into the upper troposphere by turbulent diffusion and convection. Here, dust particles can travel thousands of kilometres through synoptic and global circulation, affecting a different country or continent than the source region. It is not uncommon for a major Saharan DS to travel over 6000 kilometres, reaching the Caribbean islands, North America, and South America (Francis et al., 2020, Middleton and Kang, 2017). There are major dust transport pathways that form a global pattern indicated in figure 2.2. Dust particles also react and mix with air pollutants, which intercept and reflect atmospheric radiation, as well as creating cloud condensation nuclei (CCN) (Shao et al., 2011b). Eventually, the dust is then deposited either through gravitational settling, known as dry deposition, or through precipitation (rain, hail, or snow), known as wet deposition (Goudie and Middleton, 2006).

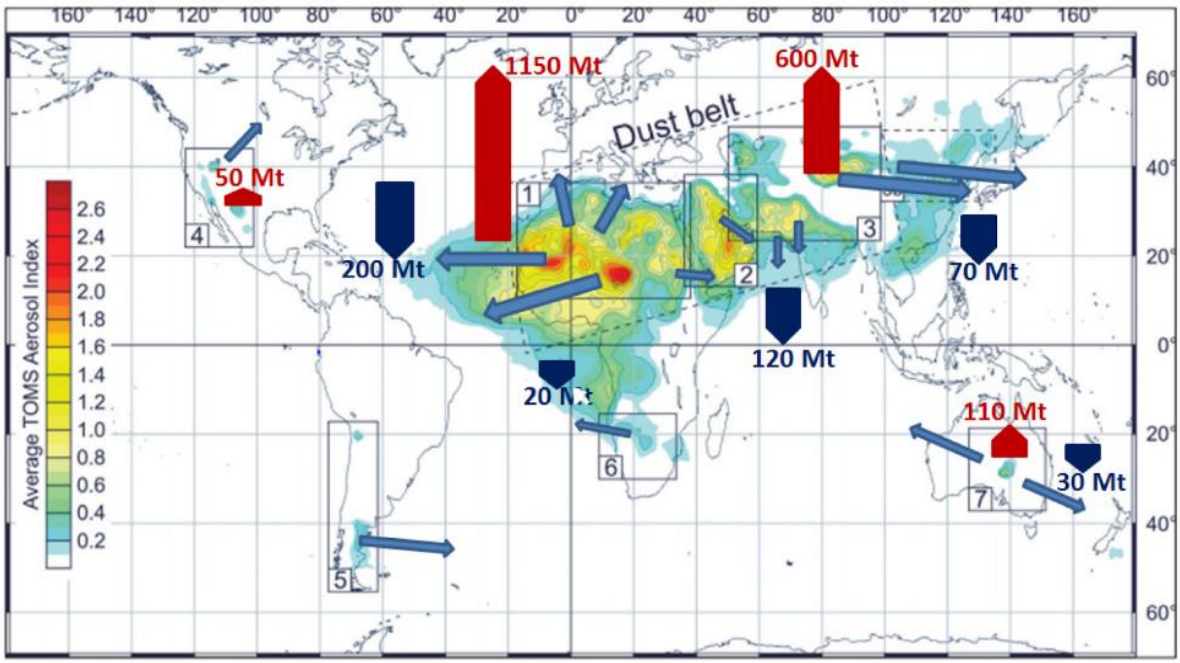

Figure 2.2: Main routes of desert dust transport (light blue arrows) and locations of the major dust sources: (1) Sahara; (2) Arabia; (3) Asia; (4) North America; (5) South America; (6) southern Africa; and (7) Australia, depicted using global means of the measured daily TOMS Aerosol Index values (1979–2011). Dust emissions from different regions in Mt are indicated by red arrows and deposition to the oceans in Metric ton (Mt) is indicated by dark blue arrows. (Adapted form Goudie and Middleton, 2017)

2.3. Dust source regions

2.3.1.Natural vs anthropogenic dust source regions

Natural dust source regions are characterised by barren or sparsely vegetated areas (such as savannas and open shrub lands), where there is little human habitation or activity, such as deserts,

flood plains (that would otherwise be wet during rainy reasons), and dry lake beds which occur not because of human influence (Chen et al., 2018, Ginoux et al., 2012). They account for roughly 75% of the global emissions, with North Africa accounting for approximately 55% of global dust emissions, mostly from the Sahel (Ginoux et al., 2012). Anthropogenic dust source regions are source regions that have their soil conditions altered by some sort of human activity, resulting in the loosening of topsoil (Chen et al., 2018). Examples of such human activities are overgrazing, agricultural activities, and overpopulation to name a few. Dried up ephemeral water bodies caused by human-induced hydrological changes (artificial lakes, paving, compacting soil, etc) can also act as anthropogenic dust source regions (Bryant et al., 2007, Chen et al., 2018). According to the Global Assessment of Sand and DS (UNEP et al., 2016) the contribution of anthropogenic dust source regions to the global dust emission has large uncertainty, ranging from less than 10% up to 50% of global emissions, but most likely about 25%. Furthermore, since anthropogenic dust sources are associated with land use and ephemeral water bodies, both in turn linked to the hydrological cycle, their emissions (and therefore their contribution to the global emissions) are affected by climate variability (Ginoux et al., 2012).

2.3.2.Global overview of dust source regions

The largest natural DS sources are located in the Northern Hemisphere, mainly in a broad "dust belt" that extends from the west coast of North Africa, across the Middle East, Central and South Asia, to China (Middleton and Kang, 2017). Figure 2.3 indicates global DS source regions, with the "dust belt" visible in the Northern Hemisphere. The Southern Hemisphere also has some significant source regions, although smaller in spatial extension, located in South America, southern Africa, and Australia. Major dust source regions identified in figure 2.3 are all located in the world's major deserts on all continents, except for Antarctica.

Apart from deserts, other dust source regions are dried-up flood plains (that would otherwise be wet during rainy reasons), and dry lake beds are also considered natural (hydrologic) dust source regions (Ginoux et al., 2012). A good example of this in southern Africa is the Makgadikgadi Salt Pans in northern Botswana and the Etosha Pans in northern Namibia which are also considered to be a (hydrologic) dust source region.

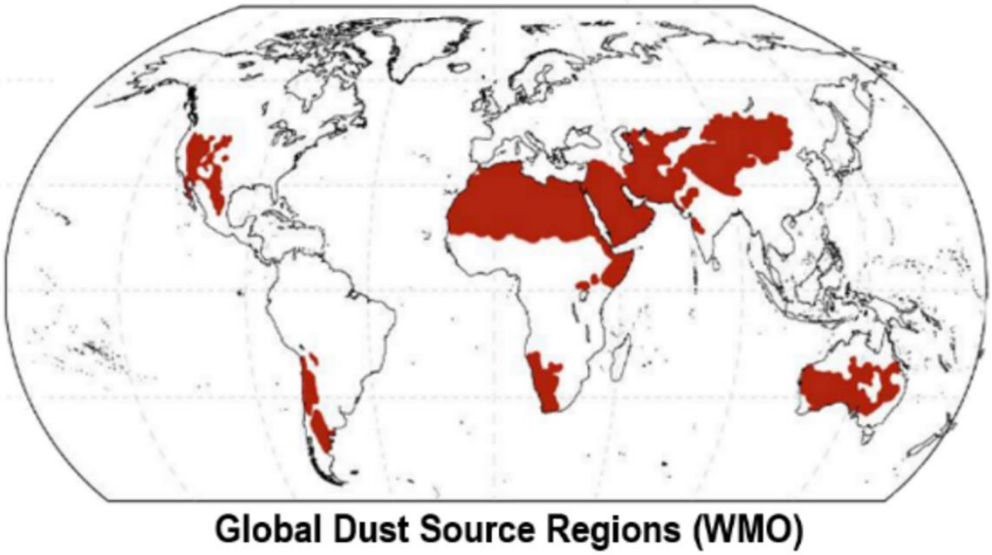

Figure 2.3 : Image of the global dust storm source regions. The "dust belt" can be seen over North Africa, spreading into the Middle East, Central and South Asia, to China. In southern Africa, major natural dust storm source regions are located both in the Namib Desert in western Namibia, as well as Kalahari Desert in Botswana, southern Namibia, and western South Africa (Source: COMET, 2010)

2.3.3.South African context

There are very few inventories of dust sources that exist outside of the dust belt in the Northern Hemisphere. Countries, such as South Africa, that are not significant contributors to global emissions, have no pressing motivation to focus on such inventories. However, reduction in vegetation cover due to poor land use or climate change provides the potential for new source areas (Bhattachan et al., 2012).

There have been a few studies conducted over the years to establish source regions over southern Africa. A study was done on the global scale attribution of natural and anthropogenic dust sources, which identified several source regions over the western parts of South Africa, as well as their seasonal variability, based on satellite data and the degree of land use and the presence of ephemeral or impermanent water bodies (Ginoux et al., 2012). Later, Vickery et al. (2013) established a dust plume source inventory from 2005 to 2008 for southern Africa. The results are presented in figure 2.4 (in triangles), where the main source region over South Africa was located in the southern Kalahari Desert (the location of the Kalahari Desert is shown in figure 1.1). Other minor source regions were located in the Free State. An expansion to this study was done by Bekiswa (2019) and Eckardt et al. (2020b), characterising major dust sources in South Africa by focusing on dust events between 2006 and 2016. The studies found that the Free State had the highest number of dust events with over 120 events (71%), with North West Province following with only 20 dust events (27%), and Northern Cape takes the third position with about 10 occurrences during this period (Bekiswa, 2019). The recent source regions are highlighted in figure 2.4 in black dots. It is important to note that approximately half of

these events occurred during the severe drought season of 2015 to 2016. The South African government declared the two provinces with the highest number of dust events (i.e. Free State and North west) drought disaster areas in the same season (Botai et al., 2016).

The Free State and North West provinces are dominated by grasslands and are well-known areas of agricultural commercial activities such as maize farming, and livestock farming. These cultivated areas often have varying degrees of bareness depending on the season, water availability, and agricultural activity in any given season. Therefore, given the activities associated with the major source regions, it can be concluded that South Africa's major dust source regions are anthropogenic. Other source regions are found in the northern parts of the Northern Cape, which form part of the south western part of the Kalahari Desert. It is an area that is dominated by savanna, sparsely vegetated, and consisting of mostly highly erodible soil type. Due to these characteristics, there is little influence by human activity (such as farming) and are therefore classified as natural dust source regions (Knippertz and Stuut, 2014).

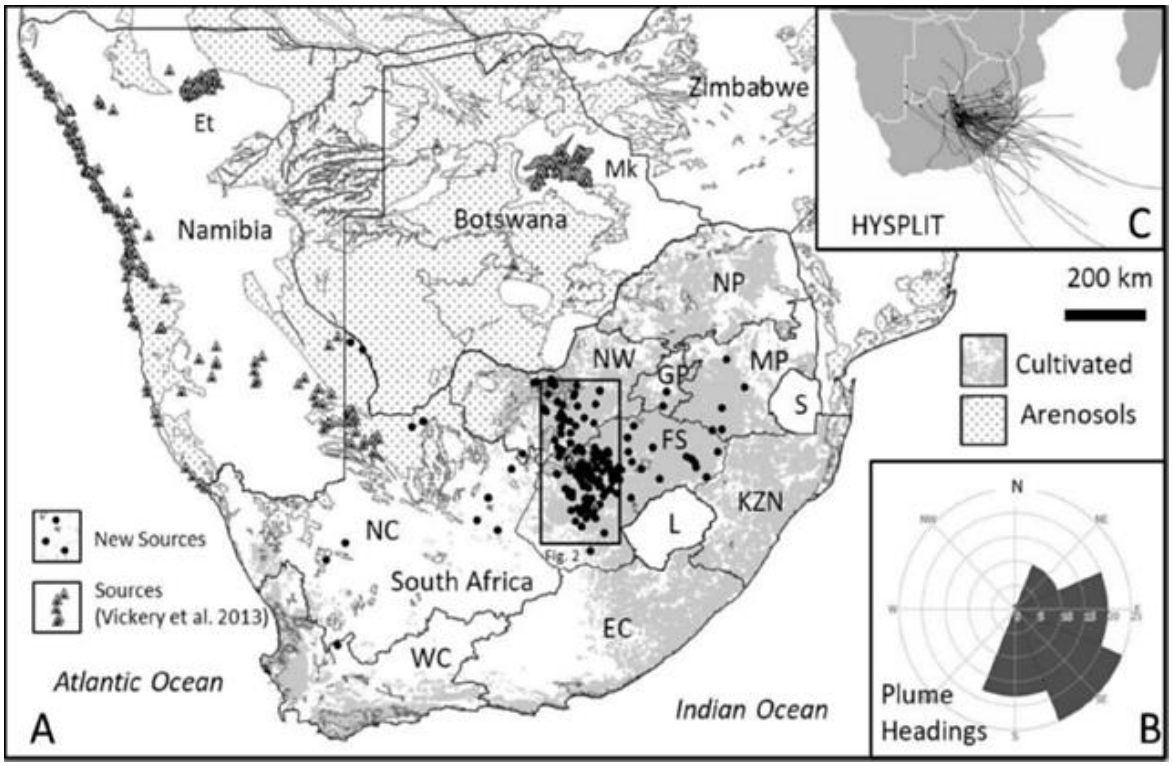

Figure 2.4 : Previous regional source record from 2005 to 2008 (Vickery et al. 2013) (triangles) established inland basins sources such as Etosha (Et), Makgadikgadi (Mk), coastal dust sources, and in the south western Kalahari Desert (Northern Cape). The study by Eckhardt (2020) expanded the source point record from 2006 to 2016 for South Africa only (circles) and identified a cluster of sources in the Free State on western edge of the summer rainfed cultivation area (light grey) and at the southern extend of the Kalahari Arenosols (dot pattern). (Adapted from Eckhardt et al, 2020).

2.4. Classification of dust producing weather systems

Each DS region or source region, whether local or global, has its own local characteristics that influence DS formation, transportation, and deposition as discussed in the DS cycle in section 2.2. However, what is common in each of these dust source regions is the meteorological conditions that prevail, resulting in the occurrence of DS. According to Shao (2008), the meteorological conditions necessary for DS to occur are as follows:

I. Strong near-surface wind to lift sand and dust particles from the surface.
II. Strong turbulence or convection to disperse particles to high levels (necessary for long-range transport).
III. Strong winds to transport particles horizontally.

Several studies (Knippertz and Stuut, 2014, Hyde et al., 2018, Brazel, 1989) identified the weather systems (both mesoscale and synoptic scale) that produce conditions necessary for DS. However, they focussed mainly on the Northern Hemisphere, as this is where the most significant dust source regions in the dust belt are located. Some examples of weather systems that are associated with intense DS in the Northern Hemisphere are large-scale monsoon-type flows (associated with a continental heat low), anticyclones, cyclones, and their cold fronts, upper troughs and cut-off lows, and convective storms that produce gust fronts (Knippertz and Stuut, 2014). This is not to say that the findings do not apply to South African DS. Rather, this highlights the importance of understanding what the dominant weather systems in South Africa are, specifically weather systems that generate strong near-surface wind speeds that can entrain and carry dust.

2.5. Mean circulation patterns over southern Africa

Before discussing the weather systems that can produce DS, South Africa's general circulation needs to be well understood. The mean circulation pattern over southern Africa, indicated by figure 2.5, is mostly anticyclonic throughout the year, while the anticyclone intensifies and moves northwards in winter. In January, the mean circulation at near surface level (850 hPa) consists of a heat low centred over the central interior, linked to the tropical low north of Botswana by a trough extending to the low.

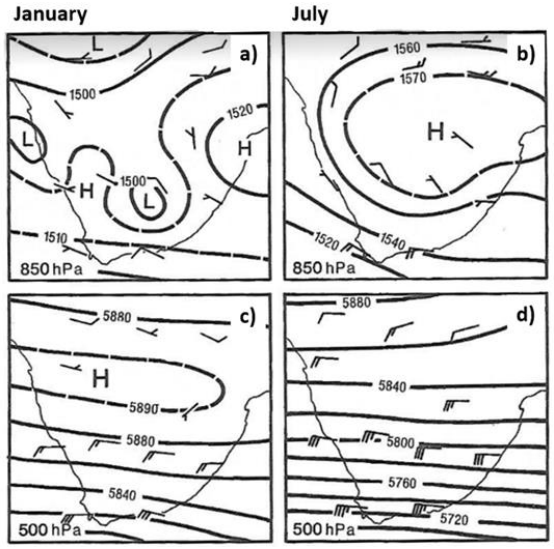

Figure 2.5: Monthly mean winds in knots of geopotential heights at 850 a for a) January and b) July, and 500 hPa for c) January and d) July. (Adapted from Tyson and Preston-Whyte, 2000)

Within the mean circulation, there are day-to-day weather patterns of South Africa shown in figure 2.6, that owe their origins to the subtropical, tropical, and temperate or mid-latitude controls or influences of the general circulation (Tyson and Preston-Whyte, 2000). The subtropical control is evident through the semi-permanent South Indian Anticyclone located east of South Africa, the continental high and the South Atlantic Anticyclone west of South Africa. The tropical control is evident through the tropical easterly flows, with the mid-latitude control evident through the westerly flow. Locally, the mid-latitude control is also evident through the west coast troughs, and coastal lows (usually ahead of a cold front), which are also responsible for berg winds.

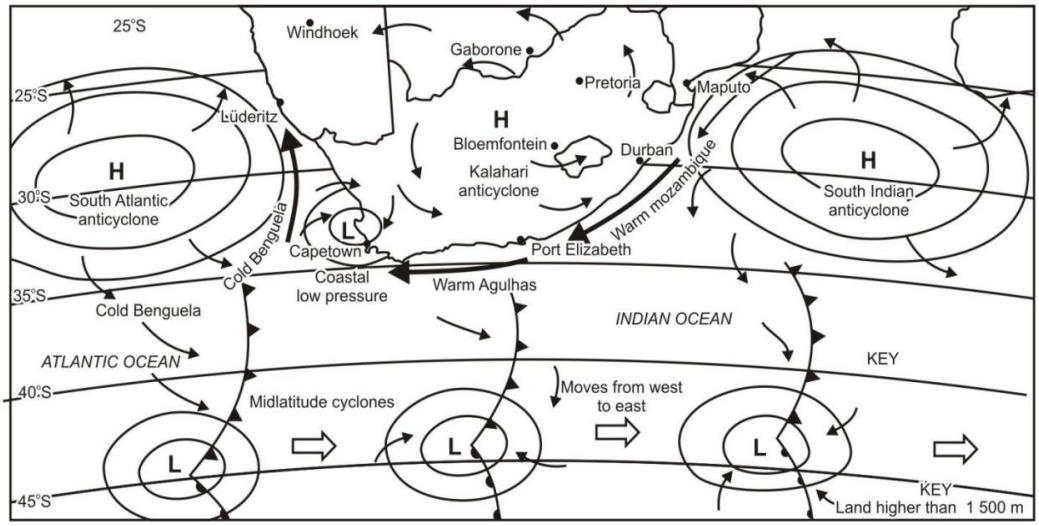

Figure 2.6 : Weather patterns over South Africa (adapted from Tyson and Preston-Whyte, 2000)

2.6. Weather systems that are likely associated with DS over South Africa

In this study, weather systems over South Africa that commonly produce strong winds are of special interest as wind is the main contributor to dust entrainment. There are previous studies that have highlighted weather systems associated with DS activity in other parts of the world (Brazel, 1989, Goudie and Middleton, 2006, Knippertz and Stuut, 2014, Lei and Wang, 2014, Hyde et al., 2018, Gherboudj et al., 2017). Examining these studies on weather systems associated with DS activity with studies that focus on weather systems associated with maximum wind gusts over South Africa (Kruger et al., 2010, Goliger and Retief, 2002) the following weather systems that are likely to induce DS can be proposed:

I. Cold fronts (prefrontal and post-frontal conditions) common in winter months, upper troughs and cut-off lows (but less likely) frequent in spring and autumn months;
II. Gust fronts generated by the outflow from convective storms such as mesoscale convective complexes, squall lines, etc. (DS generated from these systems are referred to as 'haboobs' in the Northern Hemisphere);
III. A combination of two systems, namely i) deep surface trough which is situated to the west, and ii) ridging of the Atlantic or Indian Ocean high pressure systems from the east causing strong winds in the central interior;
IV. A coastal low that develops along the west coast (sometimes extending from a deep surface trough) and adjacent interior ahead of the passage of a cold front (this can often produce berg winds).

2.6.1.Cold fronts

In other regions (e.g. the Gobi desert in China, Iraq) a large number of their dust events, especially those in spring, are driven by cold fronts (often associated with steep upper air troughs), extending from mid-latitude cyclones (Knippertz and Stuut, 2014, Goudie and Middleton, 2006). Although cold fronts occur throughout the year, they are known to affect South Africa during autumn, winter and spring months (Eumetrain, 2021). The wind shift across a cold front is usually associated with a pronounced reversal of direction and changes in wind speed gustiness as seen in figure 2.7 (Tyson and Preston-Whyte, 2000). Cold fronts are accompanied by an invasion of cold air from the south and southwest, and preceded by a strong, hot, and dry north westerly wind ahead of it. The intrusion of cold air from the south behind the cold front can lead to a rapid pressure increase, leading to dust being lifted at the leading edge of the front (Shao, 2008). This may not be the case with every cold front, but oftentimes strong south-westerly winds (12–15 m/s) prevail behind the cold front, causing

wide-spread dust emission in a south-westerly direction, which is characteristic of front-induced DS (Shao et al., 2011b, Lei and Wang, 2014). The dust emission in a south-westerly direction is associated with cold fronts in the Southern Hemisphere, in line with the wind shift associated with a cold front in the southern Hemisphere. The strength of the cold front determines the strength of the winds associated with it, which ultimately determines the possibility of dust emission.

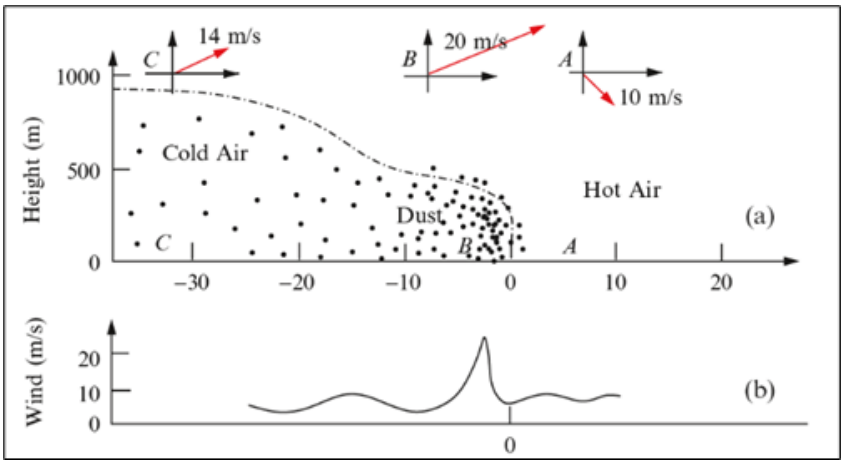

Figure 2.7: Cross section through the leading edge of the front, showing the height of the advancing wedge of cold air and the wind vectors at three sites: ahead of the front (site A), immediately behind the front (site B) and about 30 km behind the front (site C); (b) is the wind speed along the area of the cross section. (Adapted from Shao, 2008).

2.6.2.Convective development from mesoscale systems

Convective development can be classified as mesoscale weather systems. The major difference between synoptic-scale and mesoscale weather systems is the size and duration, highlighted in figure 2.8a. Outflow boundaries from thunderstorm activity can be strong enough to entrain dust, which is often referred to as haboobs in the Northern Hemisphere. They occur when cold air from convective development reaches the ground and spreads out in the direction of the storm's outflow boundary as indicated in figure 2.8b, the turbulent gust leading edge is referred to as a gust front and can reach

wind speeds of between 50 to 70 km/h. The DS can develop into a towering wall with a height of over 1 km.

Figure 2.8 : (a) Space and time scales of dynamical processes in the atmospheres, where the time scale and size of the weather systems are highlighted. (b) Cross-section schematic of a haboob/dust storm caused by the cool outflow from a thunderstorm, with the leading edge that is propagating ahead of the storm called an outflow boundary. The strong, gusty winds that prevail at the boundary are defined as a gust front. The rapidly moving cool air and the gustiness at the gust front raise dust (shaded) high into the atmosphere. (Adapted from Goudie and Middleton, 2006)

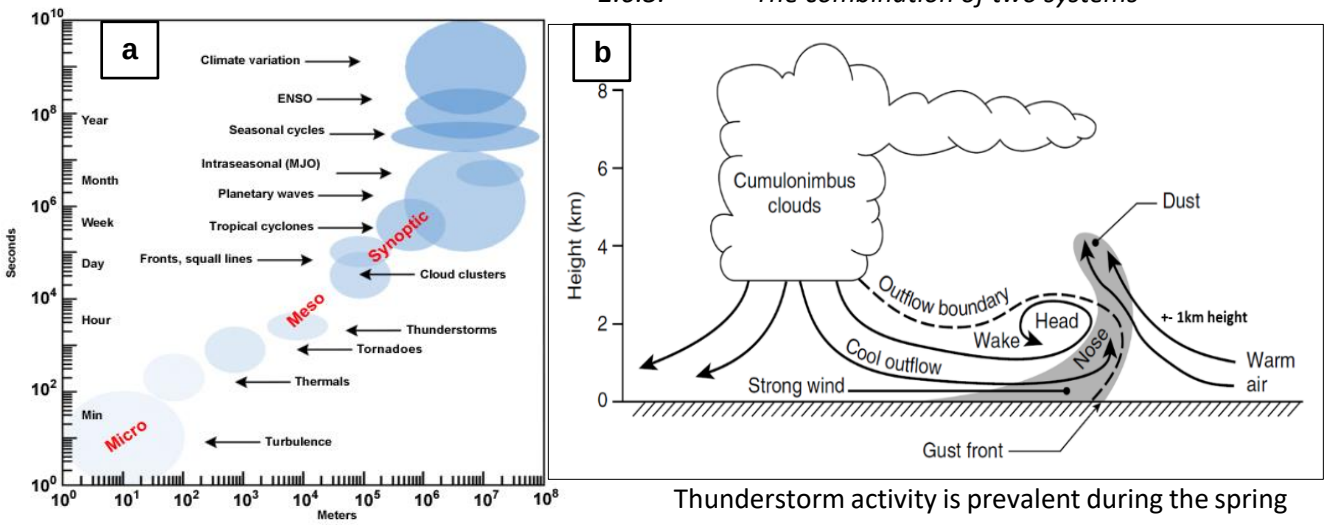

2.6.3. The combination of two systems

Thunderstorm activity is prevalent during the spring and summer months, mainly over the interior of the country. Although they are a mesoscale phenomenon, they can be generated from synoptic-scale systems. For example, a deep surface trough over the central parts of the country with a surface high pressure to the east can result in surface convergence over the interior (Kruger et al., 2010). With enough moisture, thunderstorms can develop east of the trough. However, these two synoptic systems can still produce strong gusty winds with no moisture to trigger convective development.

2.6.4.Coastal lows and berg winds

Coastal lows are shallow coastal systems that develop to the height of the escarpment (850 hPa). They develop along the entire coast of South Africa, usually ahead of the approaching cold front. The leading edge of the low is characterised by an offshore flow which causes dynamic warming of subsiding air (Tyson and Preston-Whyte, 2000). The warm offshore winds are called berg winds and are common in the late winter into early spring. Along the west coast, these strong offshore winds are known to produce visible dust plumes extending into the sea. The development of berg winds is not just limited to coastal lows, but deep surface troughs along the west coast can also play a role in the development of berg winds.

2.7. Soil moisture

Soil moisture, according to the American Meteorology Society (AMS) Glossary of Meteorology, can be defined as the total amount of water, including water vapour, in unsaturated soil (soil that is partially saturated with water). The near-surface (0 –10 cm) layer responds quickly to heavy precipitation and rapidly drying events (NIDIS, n.d.). Deeper layers are not considered for this study as they would not influence dust emission at the surface.

To understand the relationship between soil moisture and dust emissions, the factors that influence soil moisture itself should not be ignored. Surface soil moisture content is influenced by a variety of meteorological factors such as incoming solar radiation, wind, humidity, and, most importantly, precipitation as indicated in figure 2.9 (Petropoulos, 2013). For example, the amount of incoming solar radiation and wind speed can influence the rate of evaporation and transpiration from soils, which will in turn increase or decrease soil moisture content. The vegetation, primarily the cover, density, and type, influences soil moisture in the surface layer by adding organic matter to the soil surface layer and extracting water from the soil to be used for vegetation transpiration (Petropoulos, 2013). Apart from meteorological factors and vegetation, there are also other factors that contribute to soil moisture as shown in figure 2.9, such as soil properties and the topography of an area.

When considering a DS outbreak, processes that are responsible for the mobilisation of dust occur when the threshold value of the wind velocity or the threshold wind velocity (TWV) is reached (Wang, 2006). This threshold is governed by several conditions and factors of which soil moisture is considered to be one of the most significant among the other factors. This is because soil moisture contributes to the binding or viscous force that keeps the soil particles together, as well as the capacity of a surface that is susceptible to wind to resist wind erosion (Wang, 2006, Li et al., 2010).

Regarding the relationship between soil moisture and DS, the less soil moisture there is, the lower the viscous force between soil particles. The opposite is also true, where higher soil moisture means that the viscous force between soil particles will likely be higher. Furthermore, the change in soil moisture also affects the TWV needed to lift the soil particles (Li et al., 2005, Yang et al., 2019). Studies have shown that the minimum TWV needed to initiate a DS is higher with high soil moisture content (Yang et al., 2019, Kim and Choi, 2015). It is important to note that the threshold for soil moisture in several studies (Yang et al., 2019, Li et al., 2005, Kim and Choi, 2015) differs from area to area, due to a number of factors such as soil particle size and vegetation cover and seasonal climate common in the said area. Even with the variation in soil moisture threshold, the conclusion that higher soil moisture reduces the possibility of a dust outbreak still remains consistent.

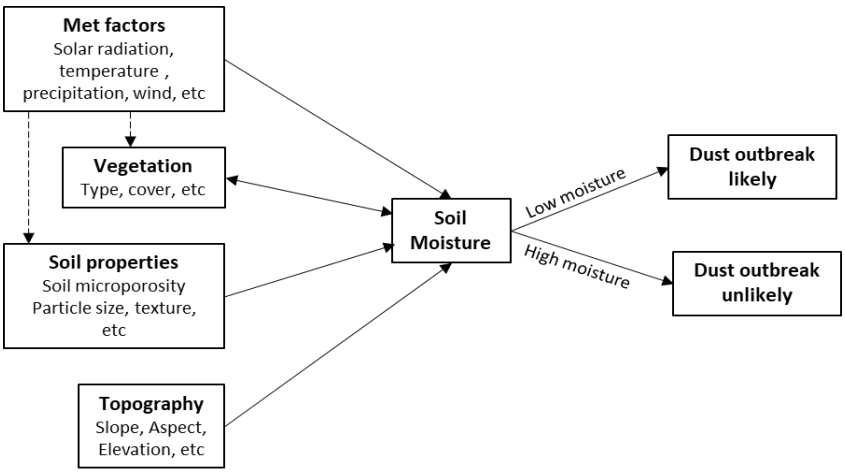

Figure 2.9: This is a simplified diagram of factors influencing soil moisture, and how soil moisture influences the possibility of a dust outbreak.

2.8. Relationship between meteorological variables and Dust Storms

In this section, the relationship between meteorological variables and DS is explained. The variables that are focussed on are temperature, mainly looking at the maximum temperature (T_{max}) and the diurnal temperature range (ΔT) as well as the which are RH and T_d. Precipitation is discussed in two aspects, namely rainfall over South Africa, and precipitation in the dust cycle. The last variable discussed in this section is wind, which is also discussed in two aspects. The first aspect focuses on the South African wind climate to get an overall picture of the seasons in which stronger winds occur when considering all four seasons of the year, as well as the areas where the stronger winds prevail more often in South Africa. The second aspect is the TWV, to understand what impacts the TWV, and how it differs from area to area.

2.8.1. Temperature

The relationship between temperature and dust emissions is complex. Temperature can indirectly affect dust emissions, and dust emitted into the atmosphere can directly affect temperature. An example of the former is that increasing temperatures, coupled with a decrease in rainfall, can result in an increased evaporation rate. This will result in decreased soil moisture, and ultimately the TWV will be lower, meaning that it will be relatively easier to lift dust particles. This corresponds to a study done by Yang et al. (2019) in the Taklimakan Desert in China, where findings indicated that as temperature increased, the corresponding soil moisture level decreased and TWV for dust emission was lower. Another example is where relative humidity decreases with an increase in temperature, which also leads to a decrease in the threshold wind velocity (Namdari et al., 2018). Higher temperatures can also assist in vegetation growth which then acts as a mechanical barrier that

effectively increases the threshold friction velocity (Aili et al., 2016). Figure 2.10 shows how temperature changes, coupled with other factors, can contribute positively or negatively to dust outbreaks.

A more direct part of the relationship between temperature and dust emission is where temperature is directly impacted by dust particles which is illustrated in figure 2.11. During DS, two possible scenarios can occur that will affect both surface temperature and atmospheric temperature aloft. Solar radiation is scattered and reflected by a layer of dust aerosol to a considerable degree, reducing the downward shortwave radiation during the day, leading to a daytime cooling in the boundary layer (Helmert et al., 2007, Nazarov et al., 2010). However, at night, the heat absorbed by dust particles is reradiated back into the atmosphere, thereby warming it.

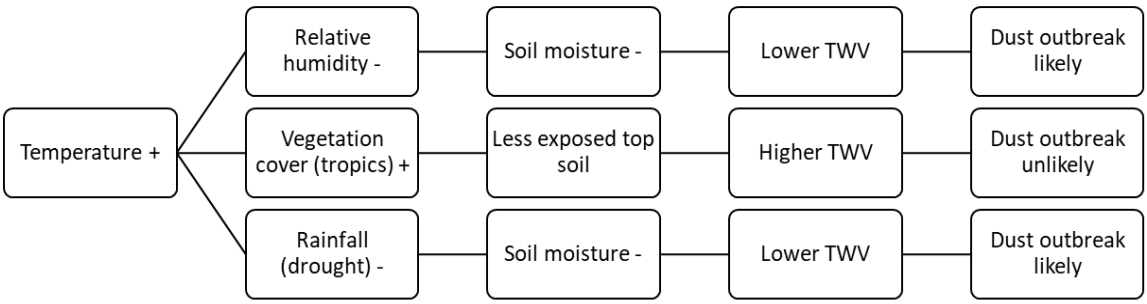

Figure 2.10: The relationship between temperature and dust outbreaks further investigated. Negative sign (-) indicates a decrease in the factor, and a positive sign (+) indicates an increase in the factor. An increase in temperature can have both a positive and negative effect on the development of DS.

In a study done by Abdullaev and Sokolik (2019) in Tajikistan, daytime surface temperature decreases caused by DS were up to 16 ˚C, while night-time surface temperature increases were up to 7 ˚C in comparison to a clear or non-dust day. The daytime cooling and the night-time warming will therefore lower the diurnal temperature range, leading to weaker turbulence in the boundary layer. Above the boundary layer, absorbing (dust) aerosols will warm up the air of the free troposphere, inducing and prolonging a temperature inversion in the upper boundary layer (Li et al., 2017). This will reduce the entrainment of dry air in the boundary layer from the free troposphere, leading to more moisture in the boundary layer. The temperature inversion also limits the diffusion of the dust plume, which often leads to deadly air pollution episodes lasting for several days (Li et al., 2015). If this occurs, long-range transport of dust particles is unlikely to occur, as particles would need to be lifted into the free troposphere for long-range transportation (see figure 2.6).

This interaction relies heavily on the optical (absorption and scattering of radiation by particles) and microphysical properties of dust particles (Nazarov et al., 2010, Abdullaev and Sokolik,

2019). Huang et al. (2014) further indicated that when a dust layer touches the ground and lasts several days, an increase in temperature can occur. However, when the dust layer is elevated, there is a decrease in surface temperature. The vertical range and duration of the dust layer can also determine the effect that dust particles will have on surface temperature. Some studies have linked the decrease in the horizontal visibility range with a decrease in ΔT. However, due to limited observations of horizontal visibility, the evolution of visibility range and ΔT will not be investigated.

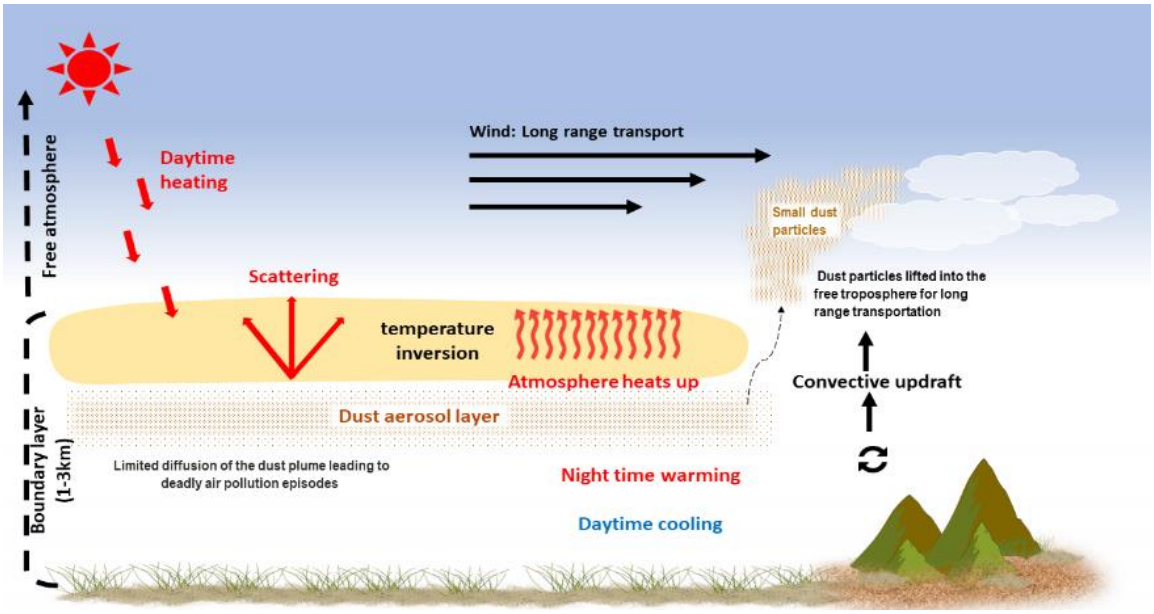

Figure 2.11: A schematic diagram showing how dust aerosol influences temperature. Incoming solar (red short arrows) is reflected back into the atmosphere, cooling the boundary layer, but causing an inversion (indicated in

orange) at the top of the boundary layer. The inversion results in limited diffusion, causing possible pollution episodes, where particles are trapped under the inversion layer. If convective updraft breaks the inversion, dust particles can be lifted into the free atmosphere, where they can be subjected to long range transport.

2.8.2.Relative Humidity (RH)

Humidity contributes to the variability in soil moisture which is a key factor in the TWV of an area. Furthermore, the effect of the humidity variation upon particle entrainment appears to be constrained to inter-particle cohesion (McKenna Neuman, 2003). For studies conducted (Ravi et al., 2004, Csavina et al., 2014) the conclusion was that the TWV positively correlated with RH. In other words, an increase in RH results in an increase in TWV, which would often result in a lower likelihood of a DS occurring. A study was done by McKenna Neuman and Sanderson (2008) on the effects of RH on emissions of aeolian systems in different environments (i.e. warm desert environments, polar regions, and coastal regions). In warmer environments and at a constant temperature, an increase in RH resulted in an increase in the TWV necessary to induce particle transportation. The threshold for RH that induces a change in the TWV differs from region to region. For arid regions in North America (Mojave Desert and Canyonlands), Ravi and D'Odorico (2005) found that the TWV increased with relative humidity values higher than 35%, while for semi-arid regions in Mexico (Juarez) and the United States of America (Green Valley in Arizona), RH over 25% promoted interparticle cohesion, which increased TWV (Csavina et al., 2014).

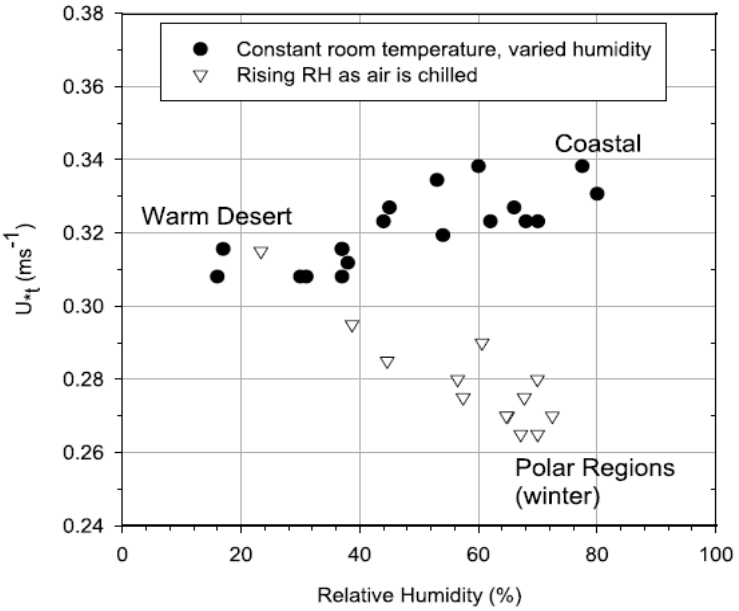

Figure 2.12: Effect of RH upon the TWV (U_{*t}) for the entertainment of 210 mm sand particles. The data represent the wide range of earth's environments in which aeolian transport occurs. (Adapted from Neuman and Sanderson, 2008).

An important factor contributing to the amount of RH present in the atmosphere is temperature. Figure 2.12 simplifies this relationship: warmer temperatures mean that the evaporation rate increases, which lowers the RH in the atmosphere.

Dust emission during a DS can indirectly impact RH values. Since RH is dependent on temperature, the onset of a DS can cause radiative cooling which decreases temperature. The cooler conditions will slow down the evaporation rate, causing an increase in RH during or right after a DS event. This was evident several in studies on DS in Saudi Arabia and India (Maghrabi, 2011, Maghrabi, 2017, Chakravarty et al., 2021, Maghrabi and Al-Dosari, 2016). In the study conducted in Riyadh, central Saudi Arabia, these conditions persisted for two days following the storm in comparison with conditions before the storm (Maghrabi, 2011). The range of RH increases varied for different studies, ranging from 1% to 70% but can be up to 100% (Maghrabi and Al-Dosari, 2016, Chakravarty et al., 2021). These changes are not only dependent on temperature changes, but due to the characteristics of the dry air mass that brought the DS (Maghrabi, 2011).

2.8.3.Dew point Temperature (T_d)

Dew point temperature (T_d) is the temperature to which air at a constant pressure and water vapour content must be cooled in order to become saturated and for dew to precipitate (Tyson and Preston-Whyte, 2000). In simple terms, it is the temperature at which the atmosphere becomes saturated with water vapor, causing condensation to occur. Both T_d and RH are used in the prognosis of weather and are also indications of moisture in the atmosphere (Elemo et al., 2021). The relationship between RH and T_d cannot be explained without including the influence of temperature. The difference between the temperature and T_d can indicate whether the RH is low or high. When the difference between air temperature and T_d is substantial, the RH is low, but when the difference is small, the relative humidity is high (Ahrens and Henson, 2019).

There are certain situations, however, where the RH is high, or the atmosphere is even saturated (i.e. RH is 100%), but the air is said to be dry. Consider polar air mass, which is cold, to have a temperature of 5 ˚C, and T_d of the same value. The RH will be 100%, meaning the atmosphere is saturated. On the other hand, desert air mass, with a temperature of 30 ˚C and a T_d of 15 ˚C will have a lower RH value. However, the desert air will still have a higher vapor content compared to the polar air as the T_d value is higher. If one can increase temperature, at a constant T_d value, the air will become drier as the dew point depression decreases. Therefore, RH helps identify how saturated the atmosphere is, but T_d helps confirm how dry or moist the atmosphere is. Understanding the relationship between RH, T_d, and temperature, it can be assumed that if the difference between the

temperature and T_d decreased, the RH would increase, which would subsequently increase the TWV required to lift dust particles into the atmosphere. The opposite would also be true, where if the difference between the temperature and T_d increases, RH is likely to decrease, which would result in a lower TWV.

2.8.4.Precipitation

Precipitation affects one of the significant controls of DS activity which is soil moisture. Rainfall patterns influence soil moisture content, which influences the viscous force between soil particles, which then influences the TWV. Studies have shown that areas that receive higher rainfall generally have a lower frequency of DS, and areas that receive lower rainfall have a higher frequency of DS. Therefore, seasonal variability of rainfall patterns can also be linked to the seasonal variability of DS in an area. This cannot be discussed without including the El Niño Southern Oscillation (ENSO) which is linked to the South African temperature and rainfall variations, and affects weather and climate patterns globally (Landman et al., 2017).

a) Rainfall over South Africa

El Niño is associated with above-normal rainfall over South Africa, while El Niño is associated with below-normal rainfall that may lead to drought conditions. Eckardt et al. (2020b) attributed the increased DS events over South Africa to the recent drought of 2015 to 2016 (as a result of the 2014-2016 El Niño), stating that half of all DS event days in their study (conducted between 2006 and 2016) occurred during the drought of 2015 and 2016. Prolonged drought periods have also been linked to increased dust emissions in some of the major dust source regions such as the Sahel (Goudie and Middleton, 2006).

Figure 2.13 indicates South Africa's rainfall according to its seasons. South Africa is a relatively dry country, with an average annual rainfall of approximately 450-500 millimetres (mm) (GCIS, 2021). It is also mostly a summer rainfall region indicated by figure 2.13 (December to February), except for the Western Cape, which receives most of its rainfall during winter, as shown in figure 2.13. For the rest of the country, winter months (June, July, and August) are relatively dry, which plays a part in the increased likelihood of dust emissions. During summer months, the wetter regions of the eastern half of the country are likely to have less dust emissions. However, it is also important to note in figure 2.13 that the Northern Cape and the interior of the Western Cape receive little rain

throughout the year (less than 50 mm annually), subsequently contributing to a higher likelihood of dust emissions throughout the year, and not just in a specific season.

Figure 2.13: Seasonal rainfall in South Africa (from Van Zyl et al., 2015)

b) Precipitation in the dust cycle

As part of the dust cycle, precipitation is responsible for the wet deposition of the particles, effectively removing dust particles from the air. Wet deposition can occur either below a cloud when raindrops, snowflakes, or hailstones scavenge dust as they fall, often referred to as washout, or within a cloud when dust particles are captured by water droplets and descend to earth when the precipitation falls, often referred to as rainout (Goudie and Middleton, 2006, Knippertz and Stuut, 2014). Furthermore,

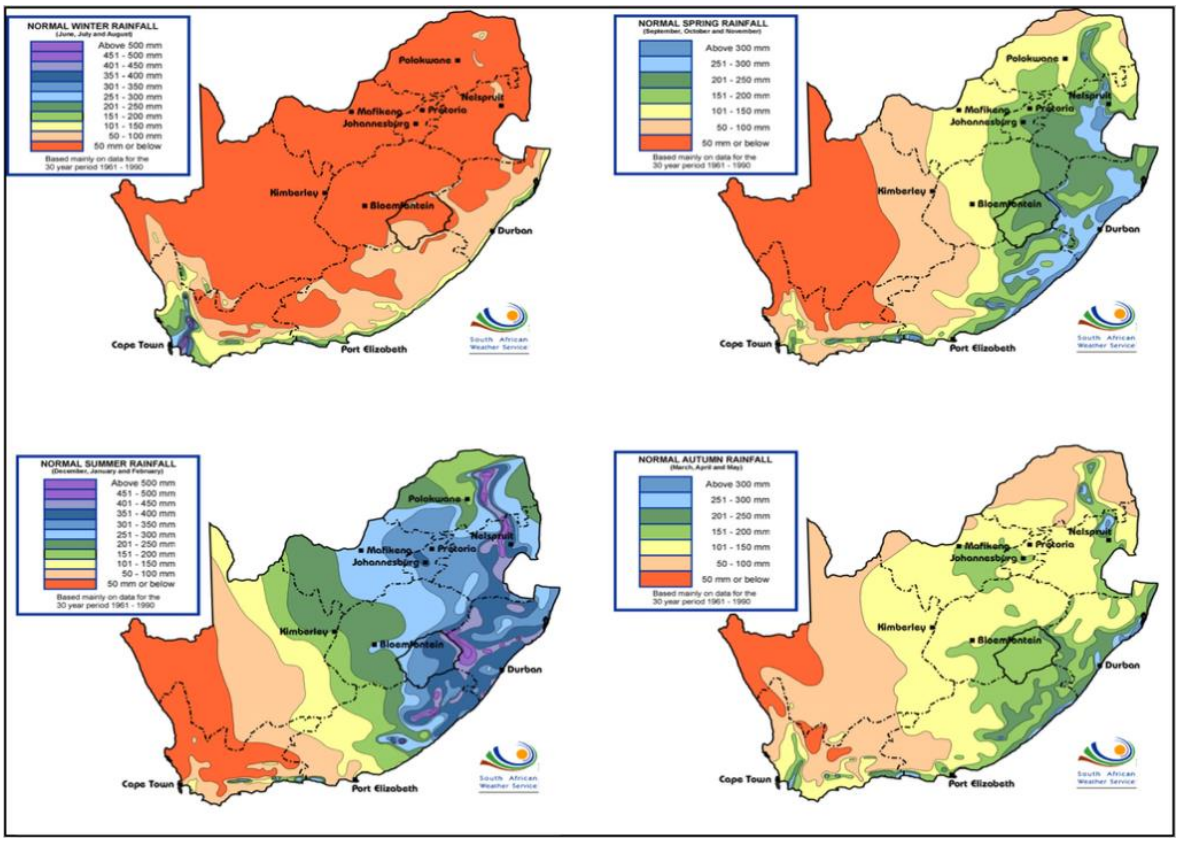

dust aerosols can also reduce the acidity of precipitation, which has long been regarded as an environmental concern. This is because dust can often be rich in calcium and other bases that are alkaline (Goudie and Middleton, 2006). The washout process (below-cloud) is more effective in removing larger or more coarse particles, while the rainout process (in-cloud) is more effective in removing smaller particles.

Dust particles can also act as CCN for liquid cloud droplets, as well as ice nuclei for ice crystals. This means that they have a substantial influence on the microphysical properties of water and ice clouds, which in turn affect the processes that lead to precipitation (Andreae and Rosenfeld,

2008). The presence of aerosols can either act as a precipitation suppressor, or as a precipitation enhancer, depending on several factors. When clouds develop in an atmosphere with higher concentrations of dust aerosols (which can act as CCN), they will result in a higher concentration of smaller cloud droplets. The reduction in cloud droplets leads to a deceleration of the merging of cloud droplets, which further leads to a suppression of precipitation in shallow (and at times short-lived) clouds such as stratocumulus, small cumulus, and orographically formed clouds (Andreae and Rosenfeld, 2008, Huang et al., 2014). The suppression of precipitation will result in a decrease in soil moisture. This can lead to drought enhancement and more dust emissions, ultimately providing a possible desertification feedback loop (Goudie and Middleton, 2006). Higher concentrations of aerosols can also increase precipitation in the case of deep convective clouds. Warm rain formation mechanisms are suppressed due to smaller dropletsizes (deceleration of coalescence of droplets), causing a delay in precipitation. This can cause droplets to ascend to supercooled levels, which form ice hydrometeors that release latent heat from freezing aloft and reabsorb heat at lower levels when they melt, resulting in greater upward heat transport for the same amount of surface precipitation (Andreae and Rosenfeld, 2008). This will therefore mean more instability will be available, invigorating the growth of convective clouds and possible additional rainfall as seen in figure 2.14. In summary, a change in CCN, which is determined by, amongst other factors, dust emissions, can be a major factor that influences precipitation amount (Khain and Pokrovsky, 2004, Huang et al., 2014). Furthermore, it is not uncommon for South Africa to experience severe thunderstorms during the summer months. Therefore, there could be a possibility of increased severity in thunderstorm activity over South Africa, with increased DS activity.

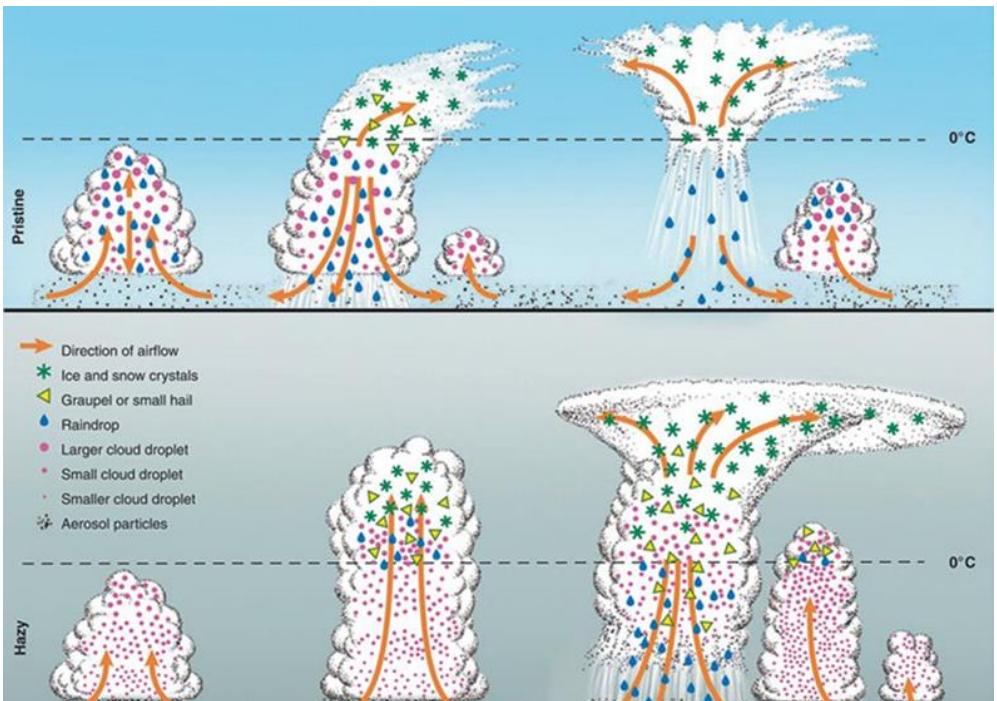

Figure 2.14: Evolution of deep convective clouds developing in the pristine or clear (top) and polluted (bottom) atmosphere. Cloud droplets coalesce into raindrops that rain out from clouds not affected by aerosols. In a polluted atmosphere, smaller drops in the polluted air do not precipitate before reaching the supercooled levels, where they freeze into ice precipitation that falls and melts at lower levels (growing and mature stages). The additional release of latent heat of freezing aloft and reabsorbed heat at lower levels by the melting ice. The consumption of more instability for the same amount of rainfall will result in invigoration of the convective clouds and additional rainfall (Adapted from Rosenfeld et al., 2008).

2.8.5.Wind

Before discussing the relationship between wind and DS exclusively, wind is first considered in the context of seasons. This creates a better picture of the seasons likely to be affected by DS.

a) South African wind climate

There are synoptic scale conditions or weather systems that are conducive to the development of strong winds over the county. Due to the seasonality of these systems, some seasons are likely to experience wind gusts more than others. In South Africa, the strong winds can be categorised into two types based mainly on their origins.

Kruger et al. (2016) investigated the wind hazard profile for South Africa where the overall wind hazard and the wind hazard per season were determined. There are strong winds generated from synoptic scale systems (cold fronts, cut-off lows, etc) more prevalent in the autumn and winter seasons, and those generated from mesoscale origin, mainly convective development such as thunderstorms which are more prevalent in the spring and summer seasons. A study was done by Kruger et al. (2016) to determine a wind hazard profile per season for South Africa. The results of the studies are shown in figure 2.15. Focussing on the DS sources regions in the country, the earlier source regions previously identified by Vickery et al. (2013) in the Northern Cape, as well as the more recently identified cluster of source regions in the North West and Free State provinces (Eckardt et al., 2020b), are all subjected to strong winds during spring and summer. The strong winds can also prevail into the autumn season for the Free State and the eastern parts of the Northern Cape.

Overall, the highest relative wind hazard (pertaining to dust emission) is found in the Central Karoo of the Western Cape, further north eastwards from Worcester, Beaufort West, south eastern

parts of the Northern Cape, parts of the Free State and the eastern parts of the Eastern Cape (see figure 2.15e).

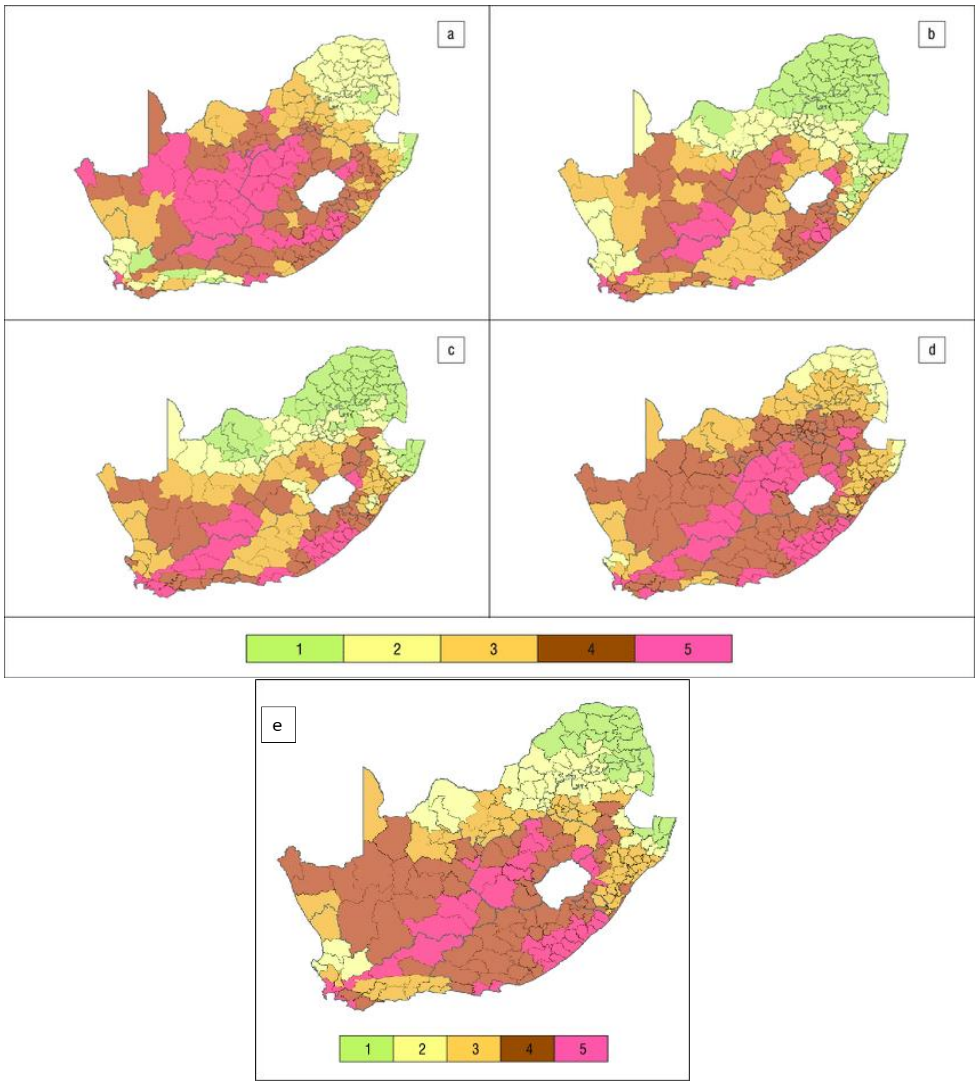

Figure 2.15: Relative wind hazard per season on a scale of 1 (low wind hazard risk) to 5 (highest risk): (a) summer (DJF), (b) autumn (MAM), (c) winter (JJA) and (d) spring (SON), (e) is the relative wind hazard for all seasons combined. (adapted from Kruger, Pillay and van Staden, 2016)

b) Threshold wind velocity

There are several factors that contribute to the generation of dust, but wind is the main driver and a primary contributor to the initiation of dust emission. For soil particles to be lifted into the atmosphere, a minimum wind speed, the TWV, is required to initiate the process. The susceptibility of soil surfaces to degradation through wind erosion differs from place to place, which also means that the TWV is also variable. It is important to note that there are several factors that contribute to the variability of the TWV. These include soil surface conditions such as soil moisture, vegetation cover, and surface roughness, as well as climatic factors such as precipitation, air temperature, and humidity (de Oro and Buschiazzo, 2009, Goudie and Middleton, 2006). Of the factors mentioned, some studies

(Selah and Fryrear, 1995, Yang et al., 2019, Ravi et al., 2004) have further suggested that the contribution of soil moisture, humidity and temperature to the TWV is more significant than other factors.

The relationship between soil surface conditions and the TWV is a direct relationship. High soil moisture content will result in a higher viscous force between particles (Yang et al., 2019), which means the TWV of the area will increase. Larger soil particle size as well as more vegetation cover will increase the threshold wind velocity of an area. The opposite remains true as well, where low soil moisture content, as well as less vegetation cover will result in a decrease in the TWV.

However, the relationship between climatic conditions and the TWV is a more complicated one. For example, higher temperatures would be helpful for vegetation growth, which will act as a barrier, and ultimately increase the TWV (Aili et al., 2016). However, higher temperatures during conditions with lower precipitation can induce drought, which will result in lower soil moisture and possibly a reduction in vegetation cover, ultimately decreasing TWV for that area. Substantial temperature differences can also initial strong winds in an area. This was evident in a study conducted by Aili et al. (2016) over the Taklimakan desert in China, where temperature differences between the mountain and the desert caused strong winds that frequently resulted in DS in the area. Studies (Ravi and D'Odorico, 2005, Yang et al., 2019) have also indicated that the TWV increases with an increase in humidity, as higher humidity values have a positive effect on the surface soil moisture content. Figure 2.16 simply indicates the factors that influence the TWV that have been discussed. The lowering of the factors in the right contributes to the lowering of the TWV.

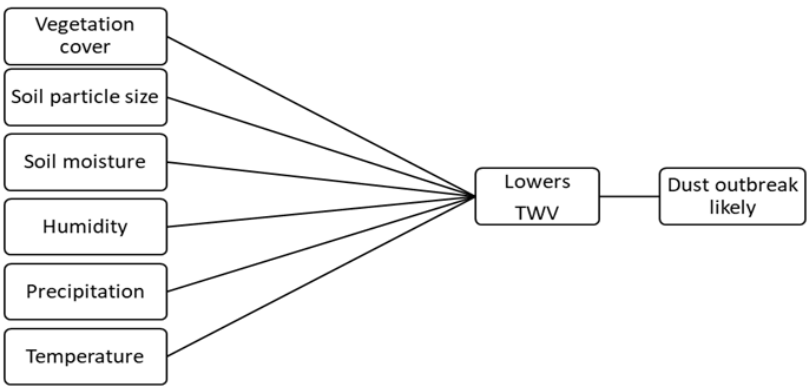

Figure 2.16: A simplified diagram of factors that can lower the threshold wind velocity (TWV). A decrease in the factors on the left contributes to lowering the TWV.

There have been several estimates done for TWV given the number of variables it is dependent on. Table 2.1 indicates the TWV for different desert environments in the Northern Hemisphere. This was an estimate done primarily depending on soil particle size in different desert areas. Globally, the lack of in situ data coupled with the uncertainties of the dependencies, several dust and climate models have stipulated a spatially and temporally constant threshold of wind erosion for surface 10m wind over dry surfaces at around 6 to 6.5 m/s for simplicity (Pu et al., 2020).

Table 2.1: Threshold wind velocity for different desert environments. (Adapted from Comet,2010)

Environment	**Threshold wind speed**
Fine to medium sand in dune covered areas	4 to 7 m/s
Sandy areas with poorly developed desert pavements	9 m/s
Fine material, desert flats	9 to 11 m/s
Alluvial fans and crushed salt flats (dry lake beds)	13 to 16 m/s
Well developed pavement	18 m/s

However, there are several models that parameterize the constant dry threshold friction velocity (usually a function of soil particle size, soil, and air density) or threshold wind velocity with dependencies on soil moisture, surface roughness length, and vegetation coverage (Pu et al., 2020). Some of these models are the Hamburg version of the European Centre for Medium-Range Weather Forecasts (ECMWF) model Hamburg Aerosol Module (ECHAM-HAM), and the Hadley Centre Global Environmental Model, version 2, Earth System (HadGEM2-ES). The study done by Pu et al. (2020) on retrieving the global distribution of the threshold of wind erosion indicated the threshold for wind erosion globally for the dusty months for both the Northern and Southern hemispheres, focussing on the main dust source regions for each hemisphere. The thresholds are shown in figure 2.17.

Consideration was also made for the sensitivity of wind erosion threshold to the different retrieval criteria of soil moisture, vegetation cover, snow cover (for places in the Northern Hemisphere), and dust optical depth (DOD). For southern Africa, the wind erosion threshold ranged from 5,41 m/s to 6,72 m/s, while other studies (Eckardt et al., 2020a) used 6 m/s as the threshold wind velocity. For this study, the threshold wind velocity will also be taken at 6 m/s in line with Eckardt et al. (2020) study, and it was the median of the southern African range from Pu et al. (2020).

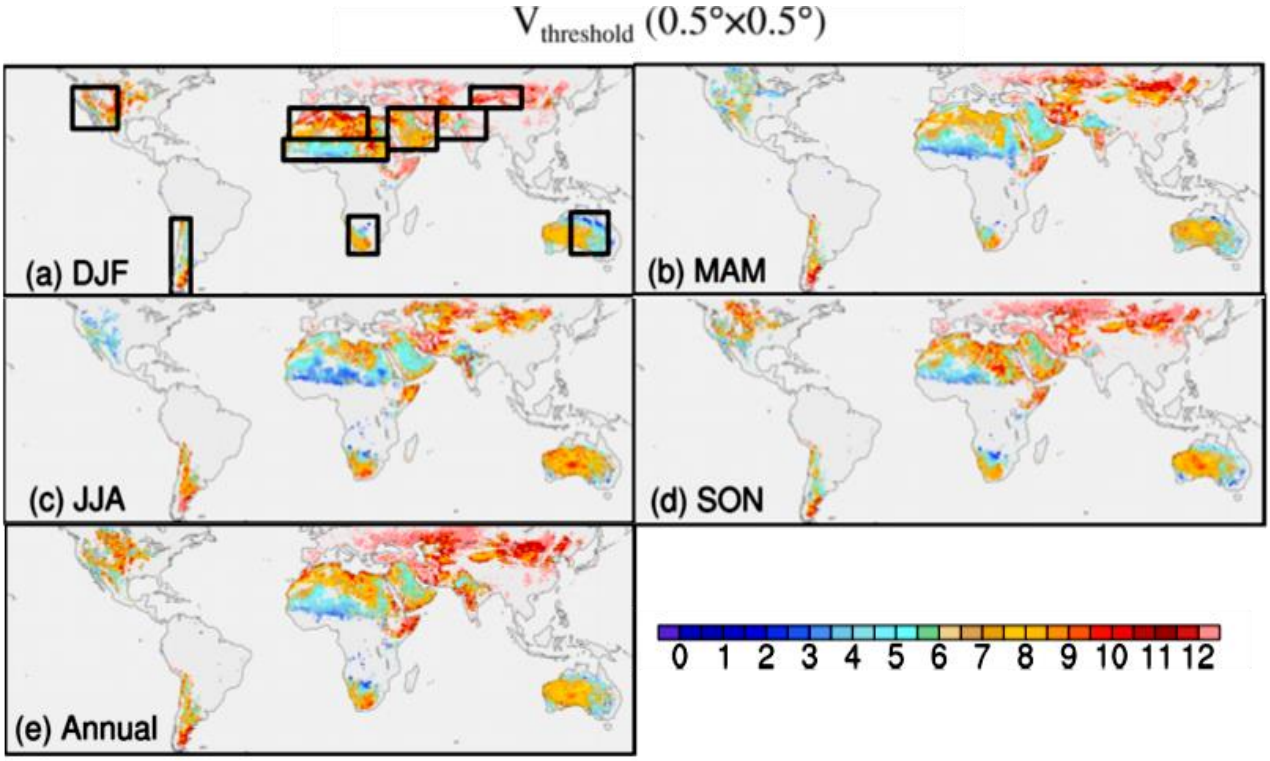

Figure 2.17: Threshold of wind erosion ($V_{threshold}$; unit: m/s) derived from satellite products and reanalyses for each season and the annual mean using DOD_{thresh}=0.5 (or 0.05 for less dusty regions). Black boxes in (a) denote nine main dust source regions used in the study (from Pu et al., 2020).

2.9. Summary

This chapter provides a background on the meteorological factors that contribute to the occurrence of DS, in line with the objectives of this thesis. The source regions of DS are discussed, focussing on the difference between natural and anthropogenic source regions. The major source regions are located in the Northern Hemisphere, with the more minor source regions located in the Southern Hemisphere. South African source regions are also highlighted, including the natural source regions, and the newly identified anthropogenic source regions.

One of the main aims of the study is to identify weather systems associated with DS events. These included synoptic weather systems such as cold fronts, cut-off lows, upper air troughs, combination of a surface trough in the west and the ridging of the Atlantic or Indian High, and a surface trough along the west coast often resulting in a coastal low. Mesoscale weather systems that can induce DS are gust fronts produced by thunderstorm activity. Finally, a summary is given for each meteorological variable selected for the study, highlighting the unique relationship each variable has with dust. This gives a basis for understanding how the meteorological variables evolve before, during, and after the occurrence of the DS.

3. Chapter 3: Data and Methodology

3.1. Introduction

In this chapter, the data used, and the processes followed to achieve the aims of the study are detailed. Firstly, the study area is shown and discussed to give a background for the area of study. The next sections explain the methodology used to identify the DS events, as well as the different sources of data used in identifying the DS events. The process of classification of the DS events is detailed for both interior and coastal DS, as well as how the stations are selected for analysis of the meteorological variables. The data used and the process followed to identify the weather systems associated with DS are explained. The methodology and data highlighted above explain how the first aim, which is to identify the synoptic systems associated with different coastal and interior DS events, is achieved. The last section lists the meteorological variables selected for the study, which are wind speed and direction, temperature, humidity, dewpoint temperature (T_d), and rainfall, as well as soil moisture. The process of how each variable is analysed is also included. The last section highlights how the

second aim of the study, which is to determine how meteorological variables evolved before, during, and after the DS events, is achieved.

3.2. Study area

South Africa is a semi-arid to arid country, characterised by summer rainfall over most of the country, excluding the Western Cape, and the south coast and adjacent interior. It is located between 22°S to 35°S latitudinally and between 17°E to 33°E longitudinally. The diverse climate of South Africa, which is also influenced by the topography, is classified into different climate regions according to the rainfall and temperature of an area. These regions are indicated in the Köppen-Geiger map and are shown in figure 3.1a. These climate regions are important to mention as they play a factor in the seasonality and frequency of DS in the area. The general areas of focus are the central and western parts of the country, which are made up of the Grassland, Savanna, Nama-Karoo, Succulent Karoo, and the Desert biomes. The climate regions or biomes in the western parts, namely the Nama-Karoo and Succulent Karoo (southern part of the Kalahari Desert), are barren or sparsely vegetated, and receive 100 to 150 rainfall per annum and are also characterized by high temperatures. These regions are considered to be natural dust source regions.

Grassland and croplands, which are mostly over the central parts of the country, are characterized by varying bareness depending on the season as well as water availability. These areas can serve as

anthropogenic dust sources as they are influenced by human activities such as agriculture and industrial activities (Chen et al., 2018).

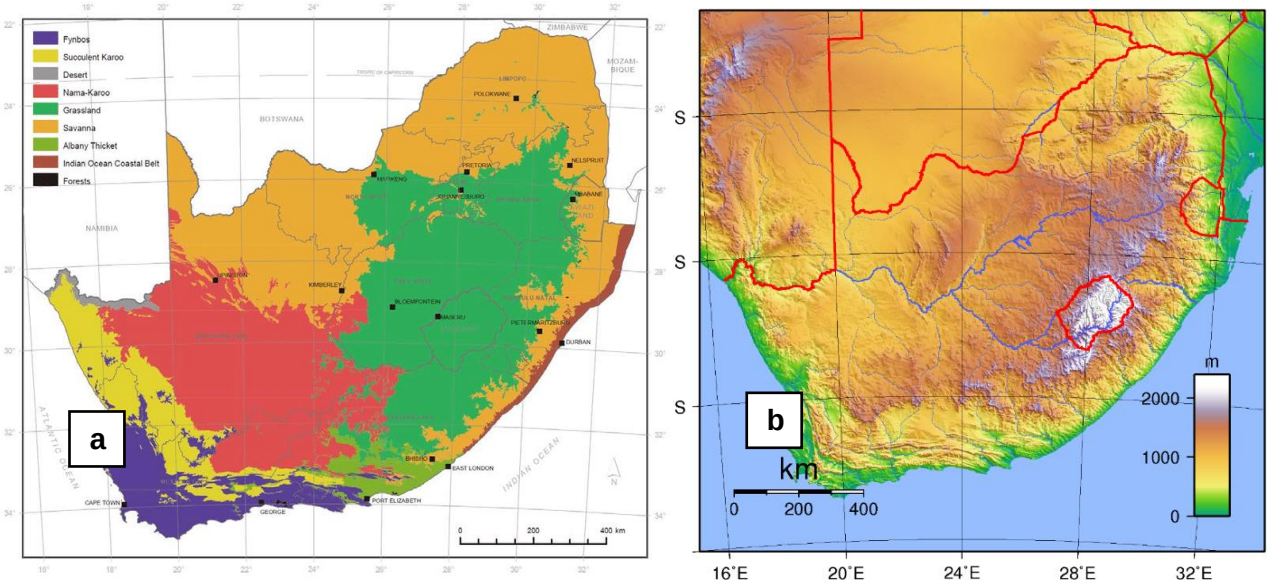

Figure 3.1: Image showing the a) different biomes of South Africa (from Rutherford et al, 2006) and b) the topography of South Africa.

South Africa is also characterised by a steep horseshoe-shaped escarpment separating the coastal plain from a high-lying interior plateau, which stands at more than 1000m above sea level as shown in figure 3.1b. The eastern escarpment is more susceptible to deep convection and high rainfall amounts due to orographic uplift along the escarpment (Muofhe et al., 2020). In the west, the topography plays a significant role in the occurrence of specific weather systems and phenomena such as coastal lows and berg winds which are important in the possible development of DS along the coast.

3.3. Identifying dust storm events

There is a lack of consistent recording of DS over South Africa as is the case for many severe weather phenomena. Therefore, other methods had to be employed to find and collect DS cases. The DS events that were therefore considered for this study were selected using a simple 4 step process:

i. If the DS can be clearly identified on satellite imagery (all five coastal DS and three interior DS were primarily identified).
ii. Media and social media reports and images of the DS event and possible impacts. Previously identified case studies (one interior DS was primarily identified)
iii. Meteorological observations (one interior DS was primarily identified)

Initially, 11 case studies were identified using the 3-step process mentioned. The case studies identified were not all the dust storms that occurred, but only those that were identified. The extra case that was not included in the research occurred over the northern Cape. However, there was only

one weather station found within the vicinity of the dust storm area of initialization, whereas all other case studies had at least three weather stations within their area of initialization. The Northern Cape dust storm was therefore not included. The final decision was ten DS cases, where five represented the coast and five represented the interior.

3.3.1.Satellite imagery

Satellite imagery that was used was the European Organisation for Exploitation of Meteorological Satellites (EUMETSAT) Spinning Enhanced Visual and InfraRed Imager (SEVIRI) which has a 15-minute temporal resolution and a field of view covering South Africa. The Dust Red, Green, Blue (RGB) product makes use of a combination of the infrared (IR) 12.0 µm, IR 10.8 µm, and IR 8.7 µm channels of Meteosat Second Generation (MSG) which are in the infrared region of the spectrum. The combination of the different channels is highlighted in table 3.1. The channel difference in the red band is between IR12.0 and IR10.8, which helps to identify thickness of the cloud where dust will increase the red contribution. The IR10.8 and IR8.7 channel difference is assigned to the green band and dust will have a small contribution. IR10.8 in the blue band identifies the cloud top temperatures and dust cloud will have warmer temperatures. The combination of this results that dust will appear magenta of pink in the day but have a purple colour at night. This satellite product is also known as the Dust RGB and is designed to identify and monitor dust day and night. Therefore, during the day dust appears as magenta or pink, but in the evening, it appears as purple. Identifying DS using the Dust RGB is a common method used in several studies relating to DS (Romano et al., 2013, Miller et al., 2019, Eckardt et al., 2020b). However, there are limitations to the use of this product. It is not possible to determine the height or concentration of the cloud from this product alone. Although Dust RGB can detect dust plumes at night, it is not always simple. The thermal contrast between the land and the elevated dust is smaller at night, but larger during the day (COMET, 2012). At night, animating the Dust RGB assisted in identifying the dust plume, as the reduced thermal contrast may have resulted in the land appearing similar in colour to the elevated dust.

Another satellite product that was also used in this study was the Day Natural Colour (DNC) RGB. It makes use of the VIS 0.8 µm, VIS 0.6 µm, and the Near IR 1.6 µm channel which is highlighted in table 3.2. The DNC RGB is easy to use and interpret as most of the colours are very similar to a True Colour image of the Earth.

Table 3.1 : Table indicating the channel combinations that make up the Dust RGB as well as the purpose of each channel combination. (adapted from https://www-cdn.eumetsat.int/files/2020-04/pdf_rgb_quick_guide_dust.pdf)

SEVIRI Dust RGB

Colour	Channel [µm]	Physically relates to	Smaller contribution to the signal of	Larger contribution to the signal of
Red	IR12.0–IR10.8	Cloud optical thickness Thin dust	Thin ice clouds	Dust
Green	IR10.8–IR8.7	Cloud phase	Thin ice clouds Dust	Water clouds Deserts
Blue	IR10.8	Temperature	Cold clouds	Warm surface Warm clouds

This RGB is sensitive to photosynthetically active vegetation and appears green while deserts, bare soils, and dry vegetation show different shades of brown (Eumetrain, n.d.). The oceans appear black as almost all solar radiation is absorbed by water molecules in the ocean. This product is ideal for identifying coastal DS because of the contrast between the dust being blown off the coast and the ocean. There is one major limitation to this satellite product. Since it utilises the visible region of the spectrum, it can only be used during the day. Therefore, the combined use of both the DNC RGB and the Dust RGB proved effective in identifying dust over the interior and along the coast for both day and night.

Table 3.2: Table indicating the channel combinations that make up the Day Natural Colour (DNC) RGB as well as the information. (Adapted from

SEVIRI Natural Colour RGB

Colour	Channel [µm]	Physically relates to	Smaller contribution to the signal of	Larger contribution to the signal of
Red	NIR1.6	Cloud phase Snow cover	Ice clouds Snow covered land/sea ice	Water clouds
Green	VIS0.8	Cloud optical thickness Green vegetation	Thin clouds	Thick clouds Snow covered land Vegetation
Blue	VIS0.6	Cloud optical thickness Green vegetation	Thin clouds Vegetation	Thick clouds Snow covered land Sea ice

3.3.2.Media reports and images or impacts

If the visibility of the DS was hidden under clouds, media reports and images were considered. The main sources of media used to find events were online newspapers such as News24 (https://www.news24.com/), eNCA (https://www.enca.com/weather), as well as reputable weather social media pages such as Storm Report SA, Reenval SA, and South African Weather Service (SAWS). In the case of media reports, more than two sources were acquired to avoid the possibility of using information that was false. There have been previous mini case studies done internally for forecasting training purposes as well as externally that were published in journals and different websites.

3.3.3.Meteorological observations

Meteorological observations will be considered for DS that were hidden under clouds. The observations were reported in the form of Meteorological Terminal Aerodrome Reports (METARs) which were freely obtained from the South African Weather Services' aviation website (https://aviation.weathersa.co.za/#showMetars).

METARs are routine aerodrome weather reports issued at hourly or half-hourly intervals (WMO, 2022). These METARs contain information such as wind speed and direction, temperature, atmospheric pressure, dew point, present weather (thunderstorm, rain, haze, dust, fog, etc), and clouds of operational importance to aviation as well as the height of the cloud base. An example is shown in figure 3.2. A trend forecast can sometimes be included in the observations. According to the (WMO, 2022), a trend forecast is included when a change, required to be indicated in accordance with the governing criteria for significant changes, is expected for one or several of the observed elements – wind, horizontal visibility, present weather, clouds, or vertical visibility. One of the following change indicators shall be used for a trend forecast: BECMG or TEMPO. An example of this is indicated in figure 3.2, where dust temporarily reduced visibility to 5000m. The coding of the weather on these reports is based on the international standard of coding of weather by the WMO. Table 3.3 indicates the different weather phenomena and their codes that can be used in METARs, with a focus on the 'weather phenomena' columns.

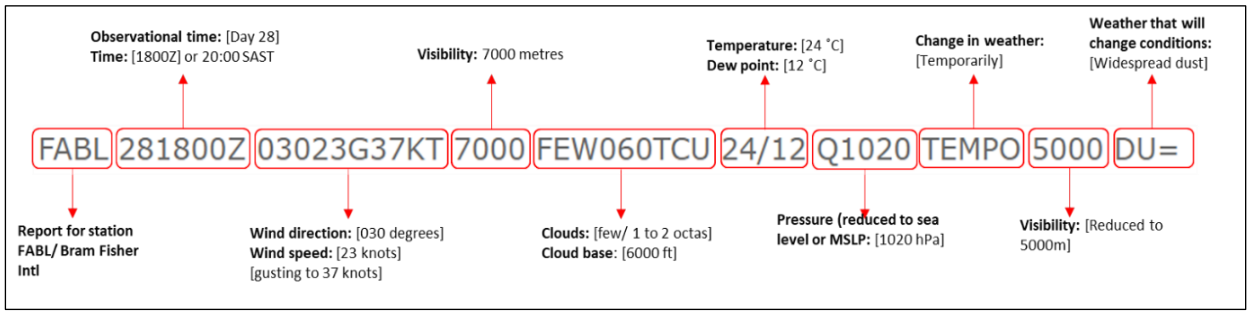

Figure 3.2: An example of a METAR that has been decoded. This METAR is for Bram Fischer International Airport in Bloemfontein, Free State on 28 December 2018 at 1800Z.

A major limitation of METARs is that these observations are only done at airports. This data is attainable from SAWS. Therefore, if a DS was not observed at an airport where visual observations are done in line with the International Civil Aviation Organization (ICAO) standards, it becomes difficult to gather more information about the event. DS are also classified according to their visibility range,

detailed in section 1.2. Due to the limited observations, the classification or categorization of the DS according to McTainsh and Pitblado (1987) was not possible for this study.

Table 3.3: codes of weather found on METARs. columns 1 to 5 in the table above in sequence, that is, intensity, followed by description, followed by weather phenomena. An example could be: +SHRA (heavy shower(s) of rain).

QUALIFIER		WEATHER PHENOMENA		
INTENSITY OR PROXIMITY	DESCRIPTOR	PRECIPITATION	OBSCURATION	OTHER
1	2	3	4	5
– Light	MI Shallow	DZ Drizzle	BR Mist	PO Dust/sand whirls (dust devils)
Moderate (no qualifier)	BC Patches	RA Rain	FG Fog	SQ Squalls
+ Heavy (well developed in the case of dust/sand whirls (dust devils) and funnel clouds)	PR Partial (covering part of the aerodrome)	SN Snow	FU Smoke	FC Funnel cloud(s) (tornado or waterspout)
VC In the vicinity	DR Low drifting	SG Snow grains	VA Volcanic ash	SS Sandstorm
	BL Blowing	PL Ice pellets	DU Widespread dust	DS Duststorm
	SH Shower(s)	GR Hail	SA Sand	
	TS Thunderstorm	GS Small hail and/or snow pellets	HZ Haze	
	FZ Freezing (supercooled)	UP Unknown precipitation		

3.4. Classifying dust storm events

Since there is no extensive visual observation network that focuses on identifying DS across the country, these DS events are not an accurate representation of all DS that have occurred. After the dates of DS were selected, they were separated according to their location (interior DS or coastal DS). The DS were also classified according to their source regions, focussing on whether it was natural or anthropogenic source regions, which was further elaborated in section 3.2.

The interior DS were further classified as induced by synoptic weather systems or induced by mesoscale weather systems. Figure 3.3. shows a simplified process of classification of the DS cases. This method of classifying DS is similar to that applied by Novlan et al. (2007) in a study to identify the synoptic climatology of blowing dust events in El Paso, Texas. The major difference between synoptic-scale and mesoscale weather systems is the size and duration. Although synoptic-scale weather systems (such as a cut-off low) can produce mesoscale systems, the main identifier of whether it was a mesoscale-induced DS or not is the presence of thunderstorms. If thunderstorms were present in the vicinity of the DS, and the DS was triggered by the gust front of the thunderstorm, the DS is classified as a mesoscale-induced DS. If there were no thunderstorms present in the vicinity of the DS,

it was assumed that the DS was triggered by winds produced primarily from the strong winds associated with the synoptic scale weather system. The DS is classified as a synoptic scale-induced DS.

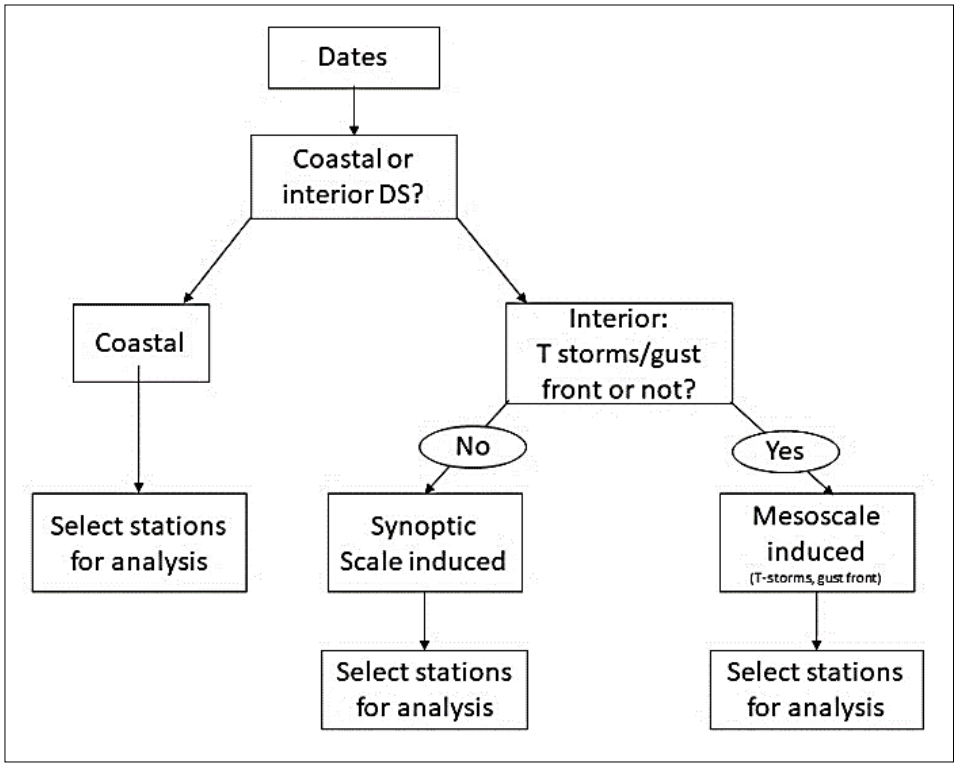

Figure 3.3: Simplified process of classification of DS cases.

3.5. Selection of weather stations for analysis

To analyse the evolution of meteorological variables, the weather stations collecting the data needed for analysis were identified. The SAWS has an automatic weather station (AWS) network across the country that provides surface meteorological observation such as wind speed, wind direction, temperature, humidity, etc. The SAWS AWS network is shown in figure 3.4, where the green indicates all the current AWSs, while the blue indicates AWSs with visual observations done at the station. For the selection of the stations to be used for analysis, the approximate area of initialisation of the DS was identified. The method used in section 1 to identify the DS was also used to identify the approximate area of initialization of the DS. This included both satellite imagery and media sources. The stations from the SAWS AWS network within the approximate area were then selected. If there was more than one station in a specific point within a few kilometres of each other, only one station was selected. The station selected was depended on data availability, and the station with visual observations done were considered first. Apart from that, any of the two stations are considered. For coastal DS, the area of initialisation was similar for all DS, therefore the same stations were selected

for all DS cases. However, for the interior DS cases, the area of initialization was different for most of the cases. Therefore, different stations were considered for analysis.

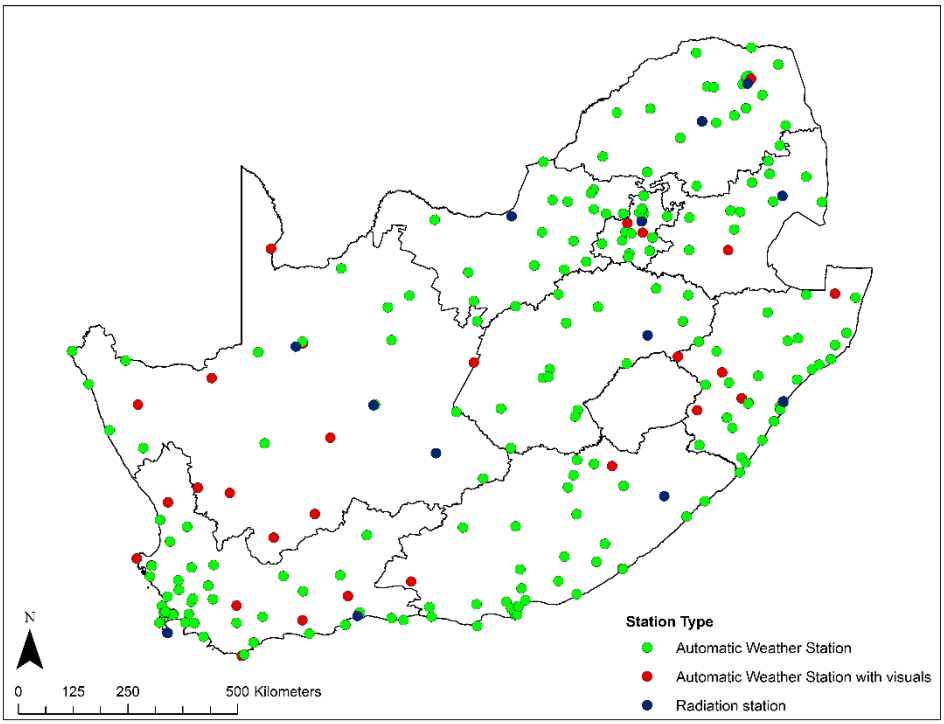

Figure 3.4: Automatic weather stations (AWS), automatic weather stations (AWS) with visuals and radiation stations across South Africa that SAWS is responsible for (from SAWS).

3.6. Identification of dust producing weather systems

To identify the synoptic scale weather systems, two sources of data were used. The first was obtained from the National Centre for Environmental Prediction Reanalysis ll (NCEP Reanalysis 2) which is freely accessed from https://psl.noaa.gov/data/gridded/data.ncep.reanalysis2.html). The variables are the mean sea level pressure (MSLP) to identify the surface circulation and the 500 hPa geopotential height to identify the mid-level circulation at a temporal resolution of four times daily and daily averages. This was done together with the surface synoptic charts from SAWS, which are freely accessible on the SAWS website (https://www.weathersa.co.za/home/historicalsynoptic), which are analysed at 1200Z daily. They also contain actual observations of wind and temperature for the same validity time as the charts (i.e. 1200Z), as well as placements of any frontal systems.

3.7. Meteorological variables

The meteorological variables selected for analysis were wind speed and direction, temperature, relative humidity (RH), and dew point temperature (T_d). The focus was 2 to 3 days before, during the DS, and 1 to 2 days after the DS. Other studies have focused on the day before, during, and the day

after the DS. However, taking into consideration the average lifespan of weather systems, the period for analysis was extended for this study to 2 to 3 days before for this study. This was helpful in identifying not just the evolution of the meteorological variables, but also understanding how the changes are linked to the prevailing weather system.

3.7.1. Wind speed and direction

The windspeed data was acquired from SAWS in m/s for the stations selected. For the coastal DS, wind speed was analysed hourly, with the highest wind gusts compared against each other. To estimate the average windspeed at the start of the DS, the windspeed of each station selected for a DS at the start of the DS was averaged. The same was done for the interior DS. Wind direction was analysed by generating wind roses using WRPlot by Lakes Environmental Software (https://www.weblakes.com/software/freeware/wrplot-view/) to simulate the wind direction frequency and wind speed (m/s) at the selected stations. As indicated in figure 3.5, wind roses display the dominant direction from which the wind is blowing, as well as the wind speed (m/s). This was done to identify the dominant wind direction on the day of the DS. The legend with the different colours represents the classes of wind speeds. For example, the wind rose in figure 3.5 indicates that winds blew mostly from an easterly and south easterly direction, with wind speeds of between 8 and 12 m/s dominating with south-easterly winds occurring approximately 10% of the time. Hourly wind speed and direction were analysed for each station used in the study. This was done before, during, and after the DS, with a special focus on the day of the DS event.

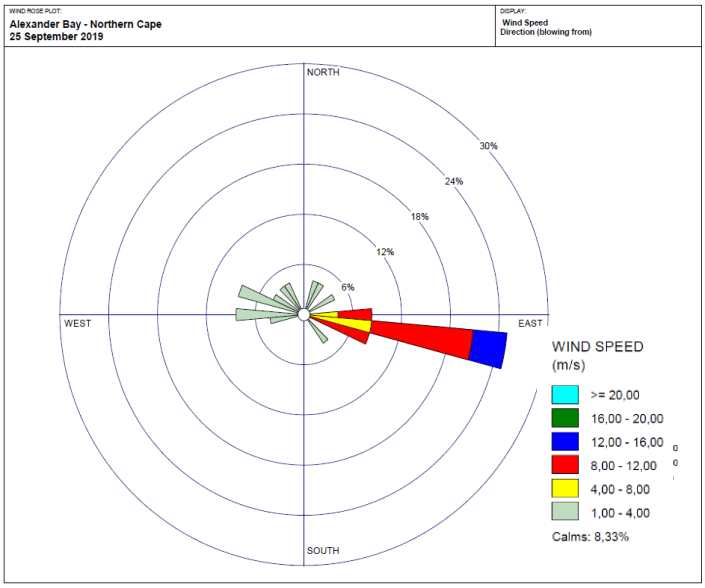

Figure 3.5: Wind rose for Alexander Bay on 25 September 2019.

*3.7.2.Temperature (T_{max}) and Diurnal Temperature Range (*ΔT*)*

Temperature can either indirectly affect dust emissions, or dust emitted into the atmosphere directly affects temperature. Increased temperatures have been shown to decrease relative humidity, which influences the evaporation rate. Soil moisture content is determined by the evaporation rate. In other words, a high evaporation rate can lower soil moisture. Decreased soil moisture will cause particles to be lifted much more easily (i.e. lower TWV). In order to analyse this effect, the temperature was analysed, with a focus on the daily maximum temperature T_{max} two days before, during, and after the DS event. This will also be compared against the average maximum temperature for that month.

During DS, dust particles that linger in the atmosphere, more specifically in the boundary layer, can cause a cooling of daytime temperatures but also a warming of evening temperatures. To identify this effect, the diurnal temperature range was analysed. A similar method was applied in other studies (Desouza et al., 2011, Nazarov et al., 2010, Abdullaev and Sokolik, 2019) to identify how temperature is impacted by the presence of dust aerosols. This was done by calculating the difference between the minimum and maximum temperatures as follows:

$$\Delta T = T_{max} - T_{min}$$

where T_{max} is the maximum temperature and T_{min} is the minimum temperature of the day. This was calculated before, during and after the DS to identify any changes to ΔT.

3.7.3.Moisture indicators: Relative humidity (RH) and dew point temperature (T_d)

High RH levels can contribute to the reduction of DS over an area, whereas low RH levels can contribute to an increase in DS occurrences in an area. Studies have shown that the threshold velocity increases with increasing air humidity for low values of relative humidity (RH < 35%) (Ravi et al., 2006), while other studies indicated an average ranging between 20 to 40% was linked to an increase in the frequency of DS in the middle East (Namdari et al., 2018). For this study, 40% was considered as the threshold. RH contributes to the variability in soil moisture which is a key factor in the TWV of an area. RH was acquired from SAWS and was analysed using daily averages. The analysis was done before, during and after the DS events. Another indicator for moisture in the atmosphere is dew point temperature or T_d and is expressed in degrees Celsius (˚C). T_d was analysed hourly, focusing on three days before the DS and during the DS event.

3.7.4.Soil moisture and rainfall

Rainfall patterns influence soil moisture content, which influences the viscous force between soil particles, which then influences the threshold velocity. Generally, areas that receive high amounts of rainfall are associated with lower frequencies of DS events (Ghalib et al., 2021). The rainfall amounts (mm) were attained from the SAWS AWS network and daily total rainfall was analysed.

Soil moisture (%) for the day of the DS event was also investigated focussing on daily averages. This is because dust emission occurs from arid or semi-arid areas, where changes in soil moisture due to evaporation occur slowly, as these soils are already very dry (Ma et al., 2023). For this study, only daily soil moisture maps were generated from the Geospatial Interactive Online Visualization and Analysis Infrastructure (Giovanni) website (https://giovanni.gsfc.nasa.gov/giovanni/) which is maintained and developed by the NASA Goddard Earth Sciences Data and Information Services Centre (GES-DISC). Giovanni is a tool that allows users to rapidly visualize, interact, and analyse vast amounts of Earth science remote sensing data without having to download the data, although data downloads are also supported. The product used for the soil moisture analysis was the AMSR2/GCOM-W1 surface soil moisture from the that is derived from passive microwave remote sensing data from the Advanced Microwave Scanning Radiometer 2 (AMSR2), using the Land Parameter Retrieval Model (LPRM). The product also has a spatial resolution of 10km x 10km, producing two files per day, one ascending (daytime) and the other descending (night-time) as shown in figure 3.6. The volumetric soil moisture was derived from the C- band (at 6.7 GHz) and expressed in percentage (%).

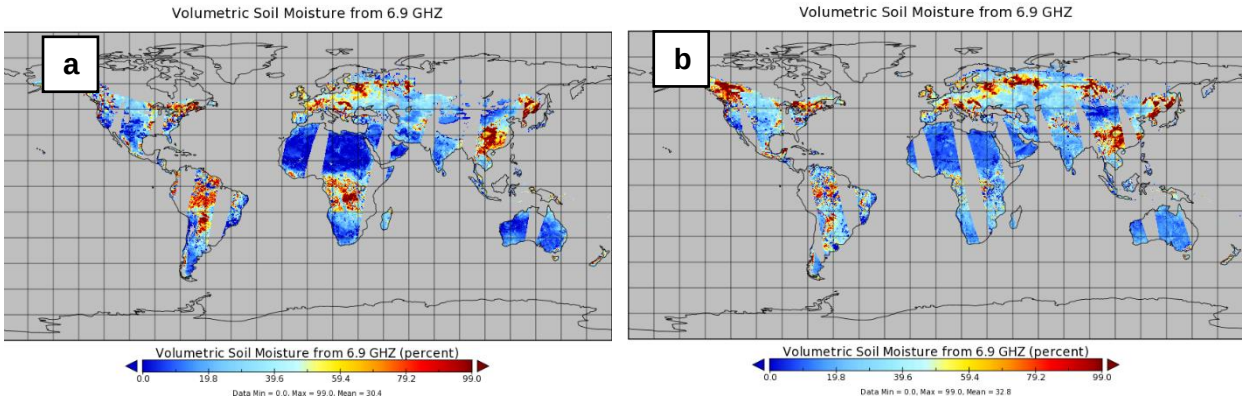

Figure 3.6: A sample map of LPRM-AMSR2 soil moisture generated by NASA Giovanni where a) ascending product or the daytime product and b) the descending or the night time product.

3.8. Summary

This chapter gives an overview of the data and methodology applied to achieve the aims and objectives of this research. The process of identification and classification of the DS is described, as

well as the selection process of the meteorological stations used in the analysis of the meteorological variables.

The section also summarises how each meteorological variable is analysed. Wind speed and direction are analysed before, and during the DS, focussing mainly on the day the DS started. The moisture indicators, RH and T_d, were analysed before, and during the DS, where RH was averaged daily, and T_d was analysed hourly. RH was also analysed after the DS. Soil moisture was analysed before and during the DS, looking at averages over the two days. Rainfall was analysed before and during the DS, looking at daily averages. These meteorological variables were analysed to see how they evolved during the occurrence of the

4. Chapter 4: Results

4.1. Introduction

In this chapter, the weather systems that produced DS selected for this study are analysed. They were then classified according to the meteorological scale of the responsible weather system (i.e. synoptic or mesoscale weather systems) for both coastal and interior DS. Sections 4.2 and 4.3 discussed the characteristics of the identified DS cases, as well as the weather systems that produced them. The two sections addressed the first objective of the study. From sections 4.4 to 4.7, the discussion mainly focused on the different meteorological variables and their characteristics associated with the DS events, which addressed the second objective of the study. The results were then summarised in section 4.8.

4.2. Selected DS cases

The DS selected for this study were ten in total and are summarised in table 4.1. To address the first objective of Aim 1, the selected DS were classified using the process highlighted in section 3.4. They were first classified according to their origin (coastal or interior DS). Five DS were identified along the coast, and five were identified over the interior. The interior DS were then further classified into

DS originating from mesoscale or synoptic scale weather systems. Out of the five DS, two originated from synoptic-scale weather systems. The other three were caused by mesoscale systems, or as a result of thunderstorm activity in the vicinity of the source region.

4.2.1.Spatial distribution and duration of DS cases

The spatial distribution of each DS was determined using satellite imagery. This could only be done DS that could be clearly identified on satellite imagery. METAR observations were also analysed to identify the stations that were used in the analysis of the meteorological variables. The coastal DS were located over a similar area along the west coast, shown in figure 4.1. Therefore, the stations selected for analysis are similar for all the cases and are listed in Table 4.1. There was more variation in the prevailing weather systems when it came to interior DS, which contributed to the significant difference in spatial distribution.

Table 4.1: DS events over South Africa selected for this study, including the duration of the DS, the season the DS occurred in, whether it originated from mesoscale or synoptic scale weather systems, as well as the stations selected for analysis.

	Date	Season	Interior	Coastal	Mesoscale (M)/ Synoptic scale (S)	Stations selected for analysis	Duration
1	2014/10/16	Spring	x		*M*: Gust front visible	Bloemfontein Stad, Glen College AWS, Bloemhof, Welkom	3 days
2	2016/01/13	Summer	X		*M*: thunderstorms visible; DS hidden under clouds	Kimberly AWS, Fauresmith	a few hours
3	2017/08/22	Winter	X		*S*: Post frontal	JHB Bot Tuine, JHB intl. WO Ermelo, Wonderboom	1 day (from 11:30)
4	2018/12/28	Summer	x		*M*: Gust front visible	Bloemfontein Stad, Glen College AWS, Bloemhof	3 hours (19:30 - 22:00)
5	2021/07/08	winter	X		*S*: Pre-frontal	Beaufort Wes, Graaf Reinet, Fraserburg, Calvinia WO, Brandvlei	6 hours (13:30 - 19:30)
6	2018/10/20	Spring		X	*S*: surface trough western interior	Alexanderbaai, Port Nolloth, Springbok WO, Vioolsdrif AWS	6 hours (8.30 - 15:00)
7	2019/09/25	Spring		X	*S*: Surface trough extending into a coastal low	Alexanderbaai, Port Nolloth,Springbok WO, Vioolsdrif AWS	15 hours (05.30 - 20:00)
8	2020/07/15	Winter		X	*S*: Surface trough along the west coast	Alexanderbaai, Port Nolloth, Springbok WO, Vioolsdrif AWS	3 days (10:00 15th - 18:00 17th)
9	2021/07/14	Winter		x	*S*:surface trough along the west coast	Alexanderbaai, Port Nolloth, Springbok WO, Vioolsdrif AWS	3 hours (13:30 - 17:30)
10	2021/07/23	Winter		X	*S*: trough exending alongthe west coast	Alexanderbaai, Port Nolloth, Springbok WO, Vioolsdrif AWS	2 days (09:30 23rd - 19:00 24th)

The DS cases originating from thunderstorm activity had a smaller spatial distribution, which meant that the stations selected for analysis for each DS were distributed over a smaller area. The DS associated with synoptic-scale weather systems had a larger spatial distribution, which also meant that the distribution of the stations selected for analysis was over a larger area.

In the last column of table 4, the duration for each dust storm event is included. The duration for the coastal DS, and the DS originating from synoptic scale weather systems, was determined mainly using satellite imagery. There was little to no cloud cover, which allowed for a more specific duration to be confirmed. However, determining the duration of interior DS originating from mesoscale weather systems was not as straightforward due to cloud cover from the thunderstorm activity, which obscured the DS. In conjunction with satellite imagery, visual observations from a METAR, were also used to identify the DS start time and the approximate location. This is why the duration for the DS on 13 January 2016 was mostly an estimation (a few hours) in table 4.1.

4.2.2.Source Regions

The coastal DS selected for this study were over the same area (i.e. along the west coast), while the interior DS were more distributed over the country. Figure 4.1 indicates the general distribution of all DS for this study as well as their general direction. The coastal DS were all confined to the west coast of the country, in the succulent Biome (refer to figure 3.1). Such areas are arid regions dominated by loose soil and little to no vegetation, often characterized by hash conditions such as high temperatures and low rainfall. The source region of the coastal DS is considered as natural as it forms part of the Namib Desert.

The source regions of the selected interior DS are similar to the recently identified source regions by Eckardt et al. (2020b), which were mainly in the North West, Free State, Gauteng and Mpumalanga Provinces. These newly identified source regions were classified as anthropogenic as they were over cultivated land. An interesting find with the case study of 8 July 2021 was that it extended over the western parts of the Eastern Cape, which was not previously identified as a source region by Vickery

et al (2013) and Eckhart et al (2020), but in an earlier different study by (Ginoux et al., 2012) as an anthropogenic source region.

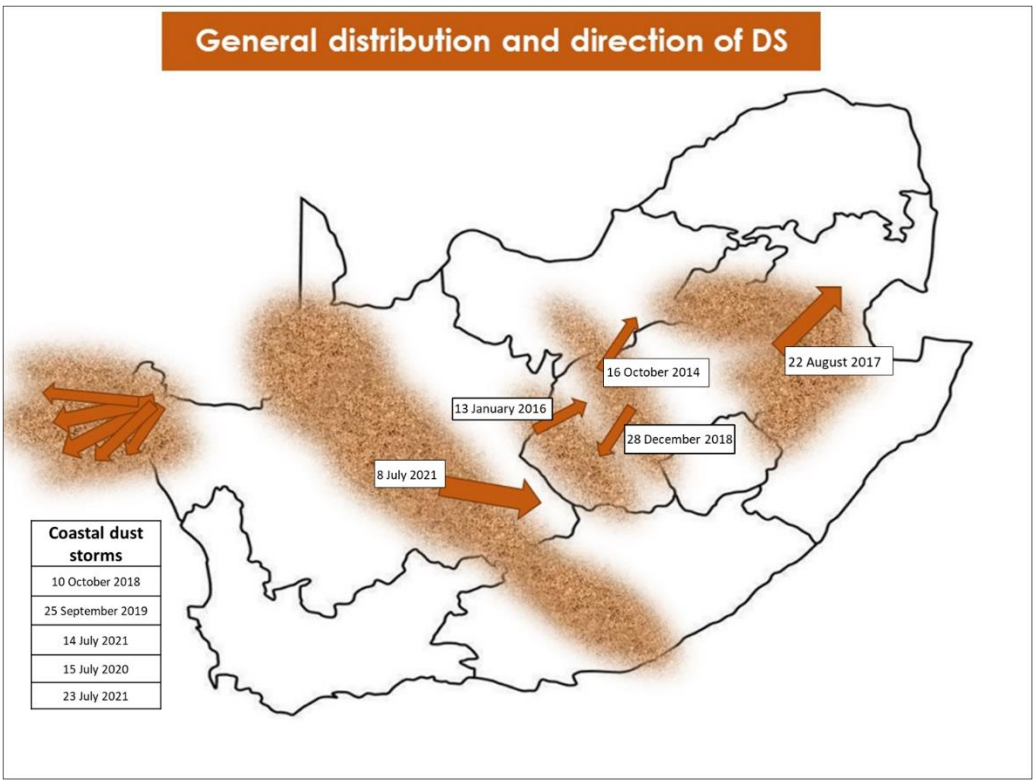

Figure 4.1: General spatial distribution of DS for this study as well as the general direction of the DS. The brown shaded areas indicate the general distribution of the DS. The arrows show the general direction of each DS, with each arrow representing a DS. The thicker arrows over the interior are indication of the DS resulting from synoptic scale weather systems, while the smaller arrows indicate the DS originating from mesoscale systems (thunderstorm activity).

4.3. Overview of DS producing weather systems

This section addresses objective 2 of Aim 1, which is to identify the weather systems associated with interior and coastal DS.

4.3.1.Coastal DS

The list of coastal DS selected is indicated in table 4.1 from numbers 6 to 10. The main weather systems that were responsible for coastal DS was the combination of a surface trough over the western interior or along the west coast, with a high pressure situated south, south-east, or over the interior of the country. The weather systems and the general circulation associated with coastal DS were similar,

although differing in their central pressures (which denotes their intensity), as well as minor variations in the location of the weather systems. Figure 4.2 shows the synoptic circulation of the coastal DS events. In all the cases, the frontal systems were associated with upper air troughs that were leaning slightly westward of the surface cold front (i.e. baroclinic system).

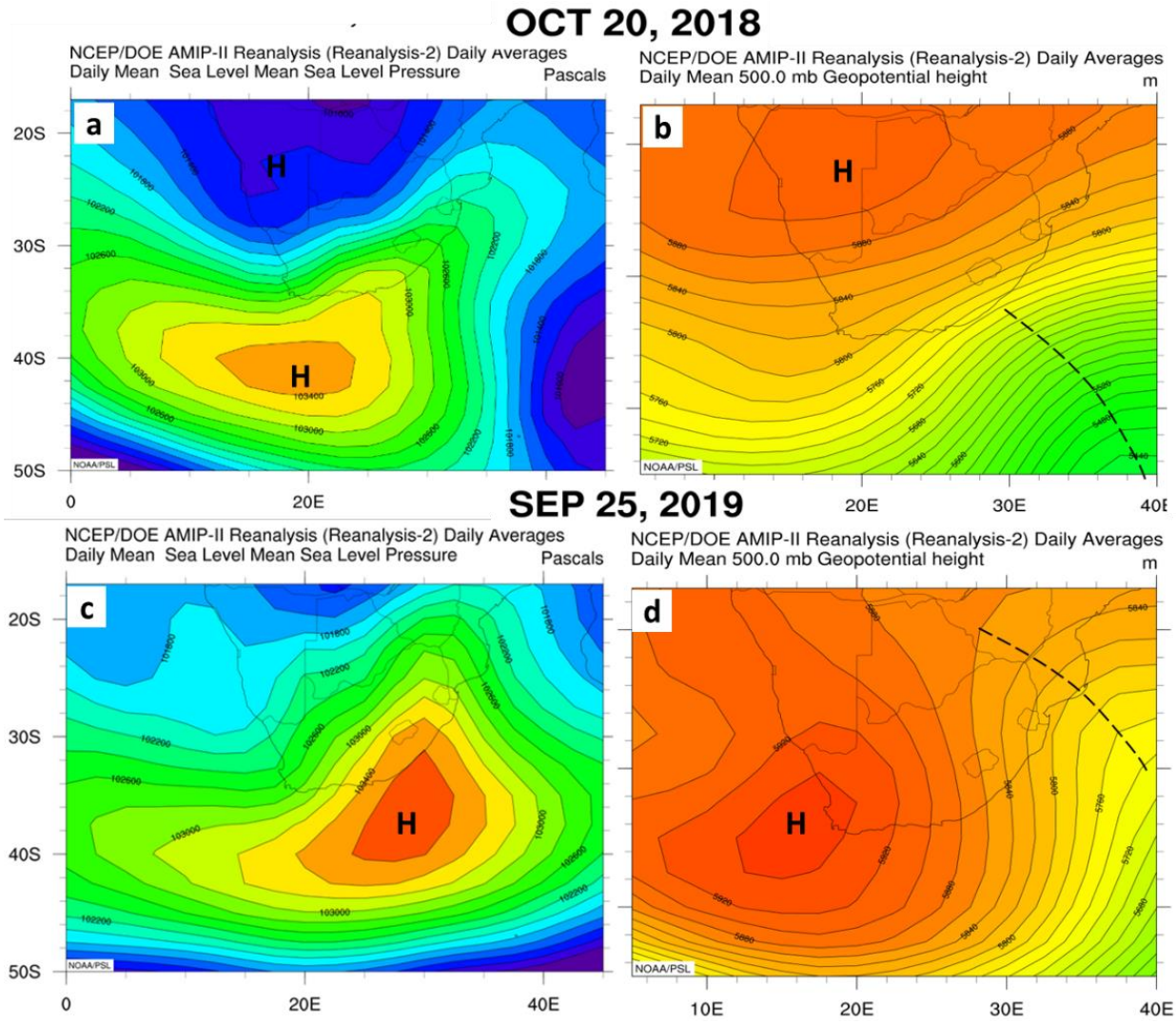

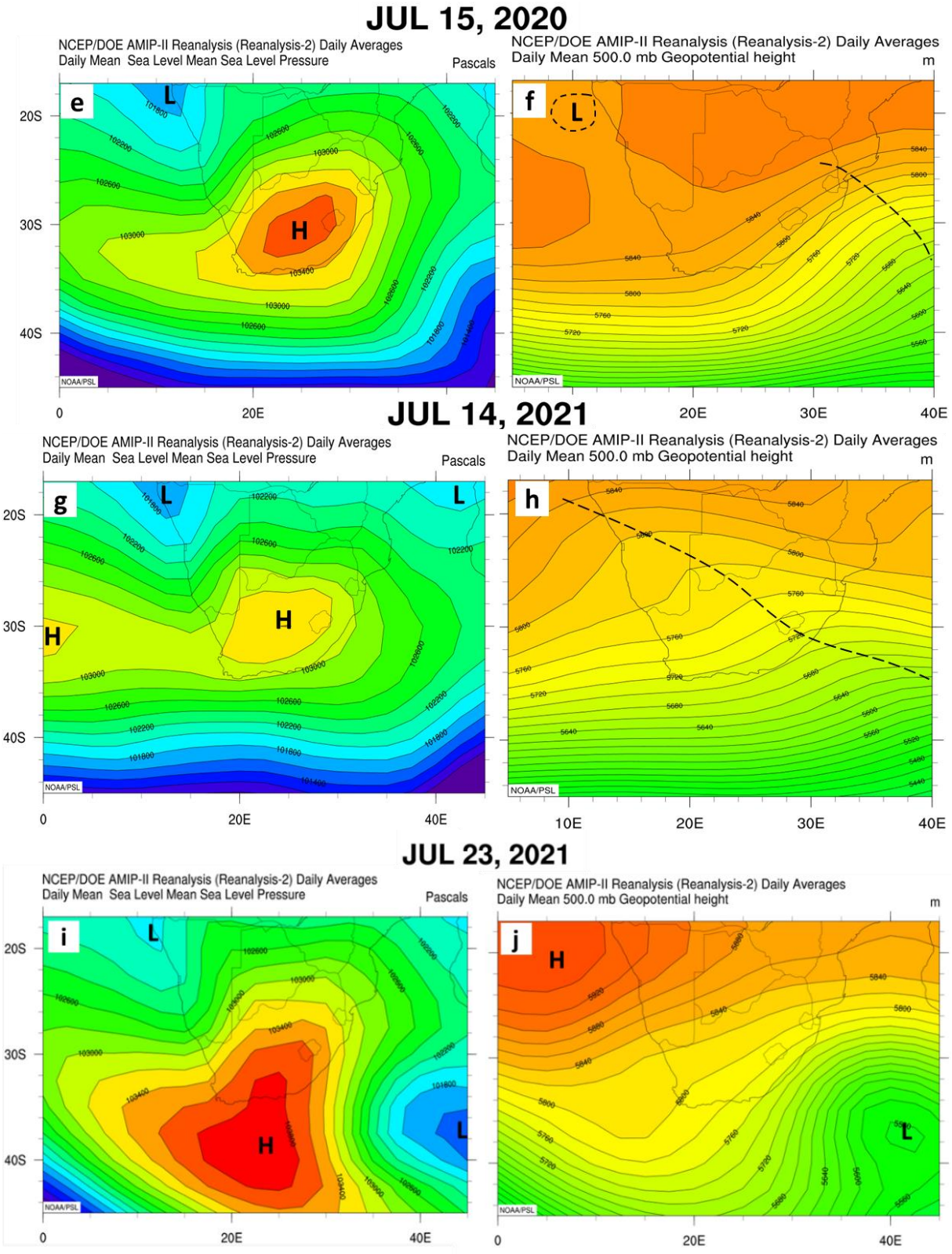

Figure 4.2: Mean sea level pressure in Pascals (Pa) for a) 20 October 2018, c) 25 September 2019, e)15 July 2020, g)14 July 2021, i) 23 July 2021. 500 hPa geopotential height for b) 20 October 2018, d) 25 September 2019, f)15 July 2020, h)14 July 2021, j) 23 July 2021, with the dotted line indicating the position of the upper air trough.

There were two DS cases that lasted longer than a day. The first occurred on 15 July 2020, lasting three days, and the second occurred on 23 July 2021, lasting two days. Both these DS were associated with strong high-pressure systems with central pressures of 1036 hPa and 1038 hPa respectively (see figures 4.2e and 4.2i). They also developed between a series of fronts moving over the country or after the passage of a frontal system. The DS with the shortest life span occurred on 14 July 2021 and only lasted only three hours. It was also associated with the weakest high-pressure system of all the DS, with a central pressure of 1032 hPa (see figure 4.2g).

4.3.2.Interior DS

The cases selected for this study are shown in table 4.1 from numbers 1 to 5, also specifying those that were synoptic scale-induced DS and mesoscale-induced DS. The DS resulting from synoptic scale weather systems were associated with cold fronts, being both prefrontal (ahead of the cold front) and post-frontal (after the cold front) DS. They were both associated with upper air troughs. The upper air trough can enhance uplift and intensify the cold front, and can also result in thunderstorm development associated with the cold front, as well contribute to increased surface winds (Eumetrain, 2021).

Figure 4.3 indicates the surface and mid-level circulation associated with the prefrontal and post-frontal DS events. The DS that occurred on 22 August 2017 was triggered with the passage of the cold front and was further transmitted as the high-pressure system (1028 hPa) ridged from the west (see figure 4.3a). The DS that occurred on 8 July 2021, shown in figure 4c, was prefrontal and was triggered by the strong winds ahead of the cold front. Although both cold fronts were associated with an upper air trough, there were no thunderstorms present.

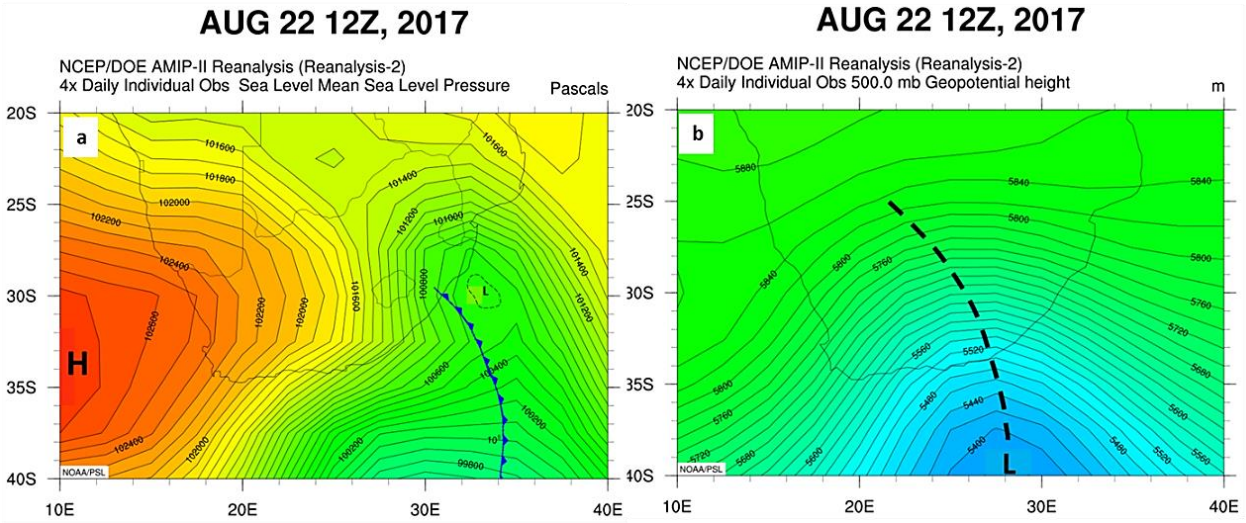

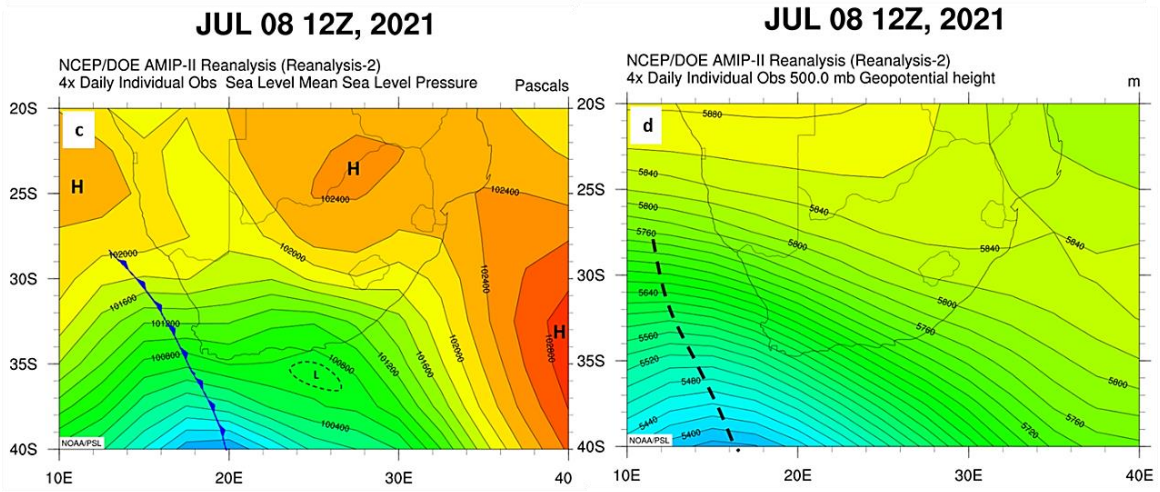

Figure 4.3 : Mean Sea level pressure (Pa) for a) 22 August 2017 and c) 08 July 2021; 500 hPa geopotential height for b) 22 August 2017 and d) 08 July 2021, with the dotted line indicating the position of the upper air trough.

Figure 4.4 shows the surface and mid-level circulation of the DS originating from mesoscale weather systems. The DS originating from mesoscale weather systems had thunderstorms, even though there were synoptic weather systems at play. The surface circulation of the DS that occurred on 13 January 2016, illustrated by figures 4.4c and 4.4d, and 28 December 2018, illustrated by figures 4.4e and 4.4f, was a trough extending over the interior combined with a high-pressure system to the east or southeast of the country. The combination of these two surface systems created an area of convergence that contributed to the development of thunderstorms. Both cases were also associated with upper troughs that enhanced the intensity of the thunderstorms.

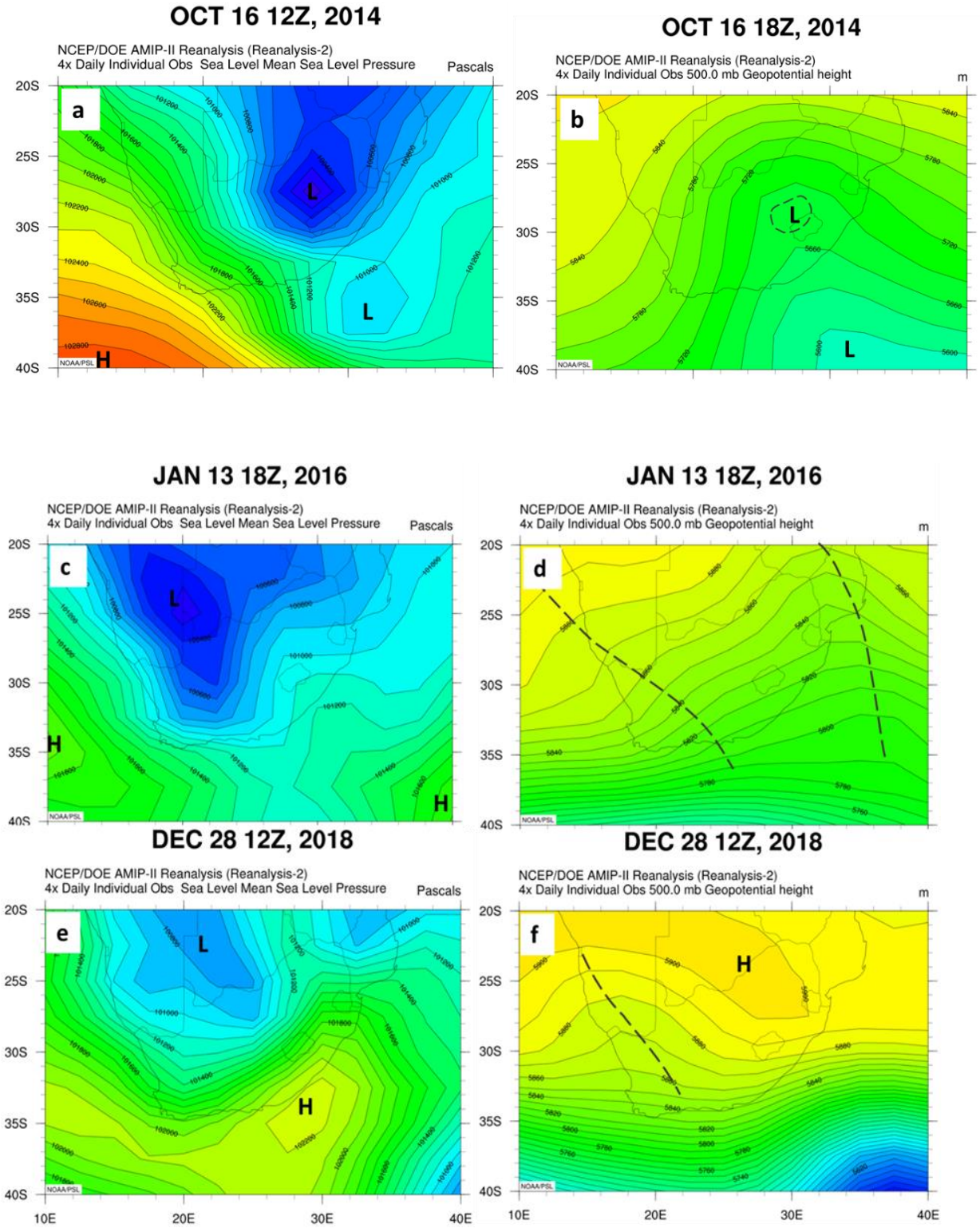

Figure 4.4: Mean Sea level pressure (Pa) for a) 16 October 2014, c)13 January 2016, and e) 28 December 2018; 500 hPa geopotential height for b) 16 October 2014 (cut-off low), and d)13 January 2016 and f) 28 December 2018, with the dotted line indicating the position of the upper air trough.

DS originating from thunderstorm activity are often hidden under clouds, which was the case for the DS on 13 January 2016 shown in figure 4. The METAR observation, indicated on figure 4.5, was

helpful in identifying the DS, as well as the approximate timing of the DS. The DS that occurred on 16 October 2014 was associated with a cut off low that extended into a surface low over the eastern half of the country as illustrated on figure 4.4a and 4.4b. The DS that occurred on 16 October 2014 and 28 December 2018 followed the trail of the gust front produced by the thunderstorms which was visible on satellite imagery. Appendices 1 and 2 show the DS triggered by the gust front on satellite imagery, indicated by the red arrow.

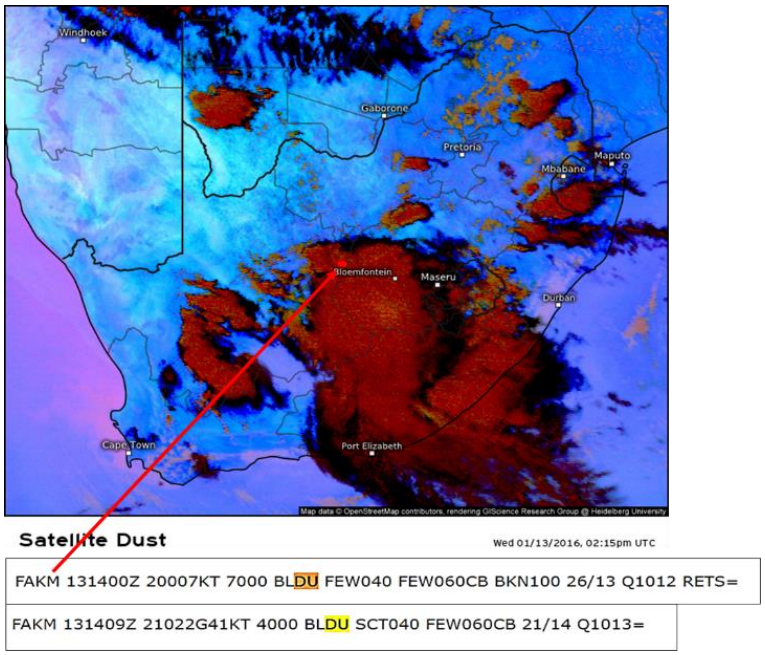

Figure 4.5: A dust RGB satellite imagery for 13 January 2016 at 15:15 SAST. The red dot is the approximate location for Kimberley Airport (FAKM), with the METAR for FAKM at 1400Z, and SPECI for the same airport at 1409Z. BLDU is the abbreviation for Blowing Dust. (© EUMETSAT, 2022)

4.4. Analysis of changes in temperature (T)

4.4.1.T_{max}: Coastal

The coastal DS selected ranged from mid-winter into late spring, with figure 4.6 zooming in on the location of the stations selected for analysis. This is important to note, as the season and location do have an impact on the maximum temperature. The coastal DS selected spanned from mid-winter to late spring, with Figure 4.6 highlighting the specific locations of the stations chosen for analysis. It is crucial to highlight that both the season and location significantly influence the maximum temperature. The stations closer to the coast (Port Nolloth and Alexander Bay) were generally warmer than the interior stations (Springbok and Vioolsdrif) due to the influence of the maritime air mass.

Even with this, the general observation was a gradual increase in maximum temperature leading up to the day of the DS event.

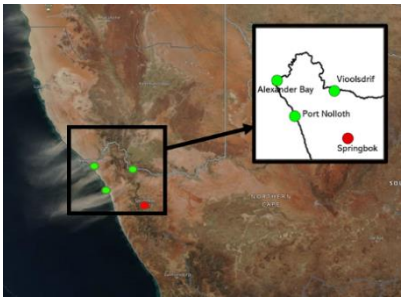

Figure 4.6: The location of the coastal DS, as well as the stations selected for analysis. The interior stations are approximately 100 km inland. NASA Worldview (2020). Retrieved from https://worldview.earthdata.nasa.gov/

Figure 4.7 indicates the maximum temperature for the selected coastal DS events against the average maximum temperature for that month for the different stations. The DS that occurred in spring generally had higher temperatures, with the coastal stations peeking over 35°C. The most notable temperatures are those of 20 October 2018 and 25 September 2019, where all stations were between 37°C and 39°C except for Springbok, which is more inland. More specifically, Port Nolloth reached 38°C on 25 September 2019, which was 17°C warmer than the average for that month, while Alexander Bay reached 39°C, which was 14°C warmer than the average for that month. For the winter cases (i.e. the July cases), the maximum temperature did not exceed 27°C, even for the DS that lasted longer than a day. The 14 July 2021 DS event that lasted only 3 hours had the lowest range of maximum temperatures ranging from 11˚C (Vioolsdrif) to 21˚C (Port Nolloth).

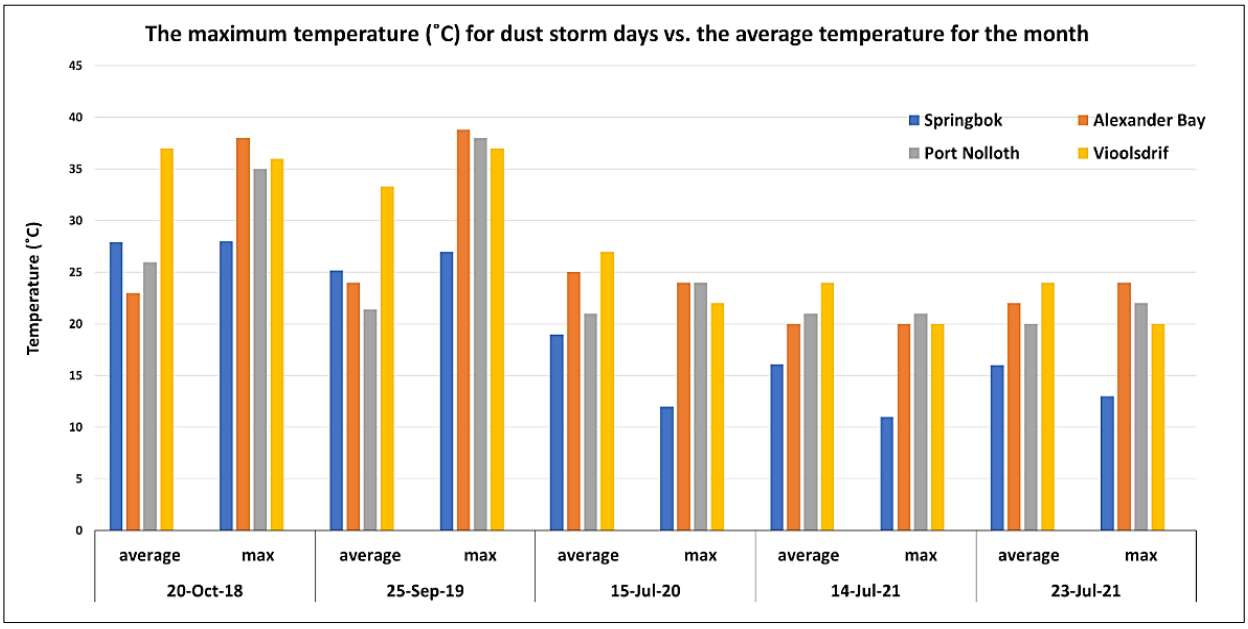

4.4.2.Figure 4.7: The maximum temperature for the selected DS cases (on the day of the DS) against the average maximum temperature for that month. This was done for the four stations selected for analysis. T_{max}*: Interior*

The behaviour of the maximum temperature leading up to the day of the event was different for mesoscale and synoptic scale-induced DS. For DS induced by synoptic scale systems, there was a gradual increase in the maximum temperature, with the highest temperature occurring on the day of the DS. The maximum temperature for all stations was higher than the averages for that month for both synoptic scale-induced DS, as indicated by figures 4.8a and 4.8b. Temperatures also decreased the day after the DS. For the DS that occurred during the passage of a cold front on 22 August 2017 (figure 4.8a), the decrease ranged between 4˚C and 6˚C across all the stations, whereas the decrease associated with the prefrontal DS on 8 July 2021 (figure 4.8b) ranged between 5˚C and 10˚C across all the stations. A reason for this can be linked to the synoptic scale system, which was a cold front. Cold fronts are associated with the invasion of cold air from the south and southwest, producing cold snaps with their passage (Tyson and Preston-Whyte, 2000) .Therefore, the drop in temperature observed after the DS had occurred can be attributed to post-frontal conditions where the air mass behind the cold front is cooler.

For the thunderstorm-induced DS, the opposite was observed. Temperatures cooled on the day of the DS and were only 1˚C to 2˚C less or more than the averages of the selected stations for that month. However, the DS of 16 October 2014 was cooler than the monthly averages by 3˚C to 5˚C. This could likely be a consequence of the synoptic scale system, a cut-off low, which is a cold-cored synoptic-scale mid-tropospheric low-pressure system, that can produce heavy rainfalls, as well as lower the surface temperatures (Xulu et al., 2023).

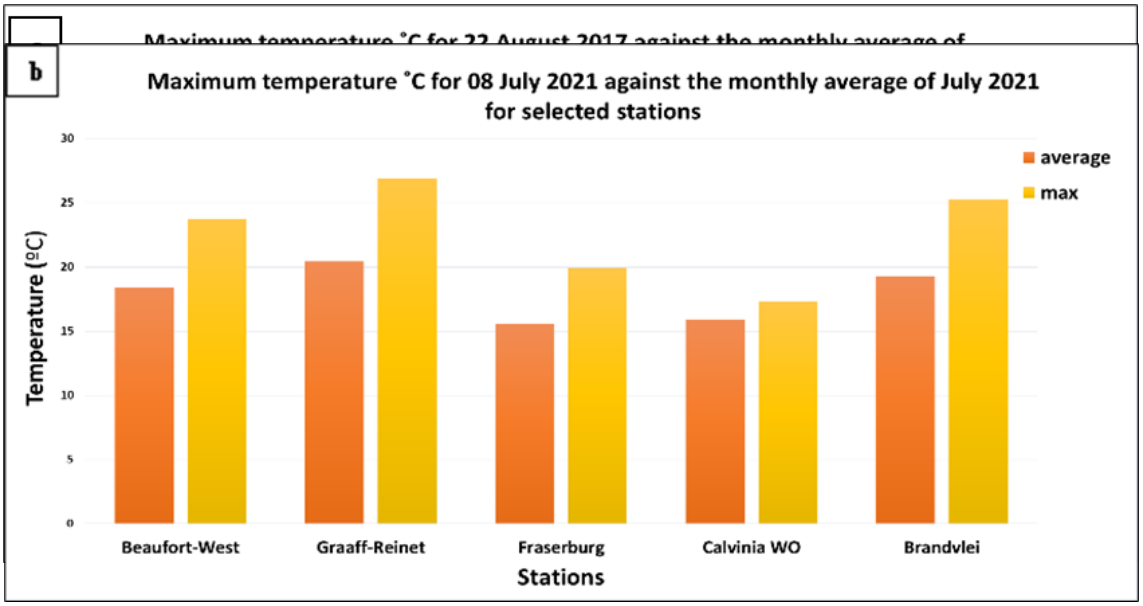

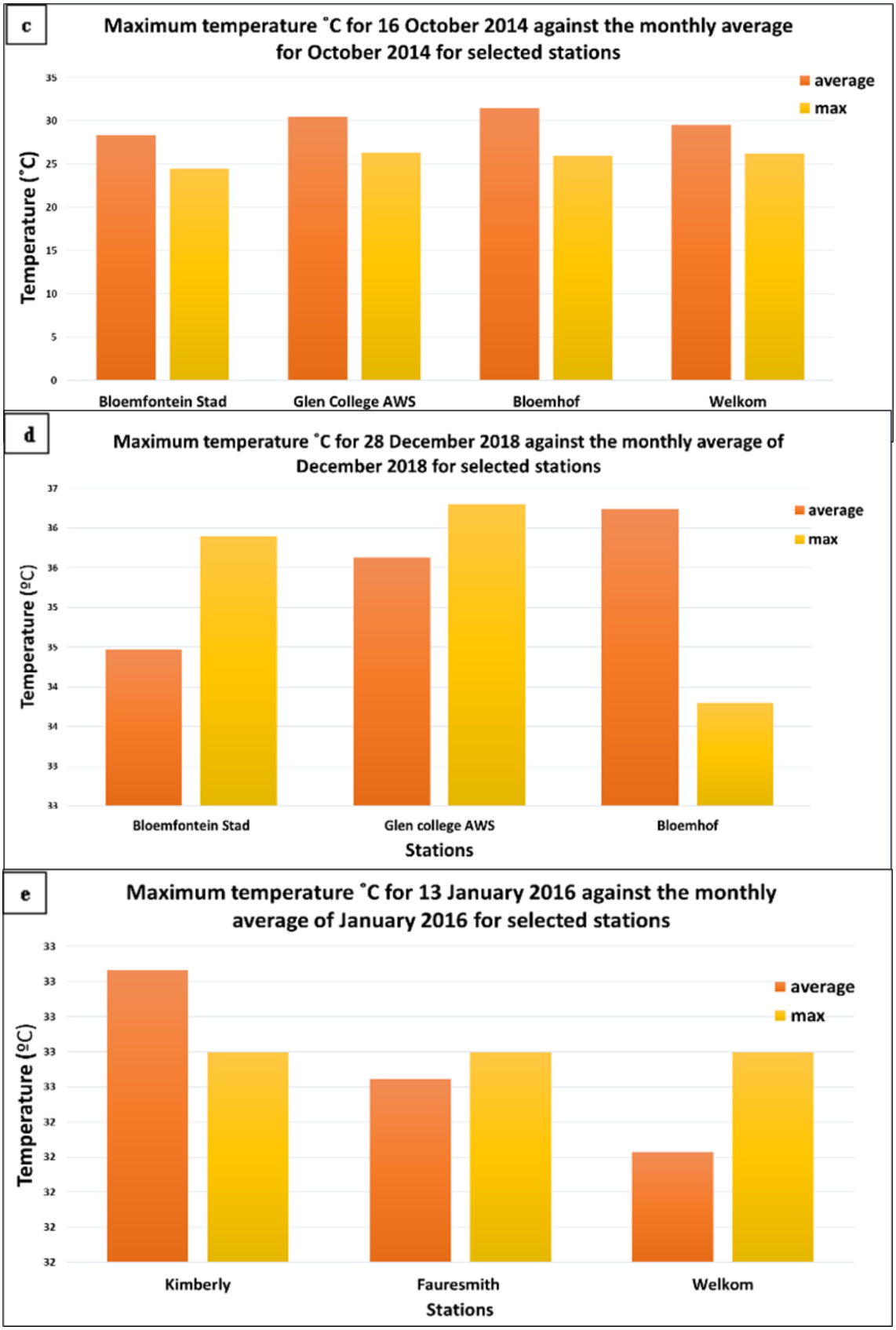

Figure 4.8: A graph indicating the maximum temperature of the selected stations against the monthly average for the two synoptic scale DS a) 22 August 2017 and b) 08 July 2021, and the mesoscale induced DS c)16 October 2014, d) 28 December 2018 and e) 13 January 2016 .

4.4.3.ΔT: Coastal DS

Tables 4.2 indicates the behaviour of ΔT before, during, and after the episodes of dust events, where the values shaded in blue show where there was a decrease from the day before. The values indicate the ΔT two days before, 1 day before, during and the day after the DS. All values highlighted in red are values that were the highest during the period of analysis on the day of the DS. In other words, the ΔT was the highest on the day of the DS for all the values highlighted in red. The values highlighted in blue indicate where there was a decrease in ΔT values the day after. For the coastal DS, ΔT for most of the stations was highest during the DS, with the spring DS (i.e. 20 October 2018 and 25 September 2019) having the highest ΔT. There was also a decline in the ΔT observed the day after the DS, with the highest decline observed during the spring DS events. Each case showed a drop in ΔT the day after, as indicated by one or both of the coastal stations, although not all four stations in each case demonstrated this change.

Table 4.2: Behaviour of diurnal temperature range before, during and after a DS for coastal regions. Since the source region for the coastal DS is similar, the same stations were used for all cases. Stations highlighted in brown are the stations right by the coast

Diurnal Temperature Change ΔT - Coastal					
Date of dust event	Station name	2 days before	1 day before	During	Day after
20-Oct-18	Springbok WO	11	8	25	17
	Port Nolloth	9	7	28	23
	Alexanderbay	14	14	14	16
	Vioolsdrif - AWS	18	19	14	16
25-Sep-19	Springbok WO	14	11	12	9
	Port Nolloth	14	12	27	25
	Alexanderbay	17	24	27	22
	Vioolsdrif - AWS	13	13	14	16
15-Jul-20	Springbok WO	4	5	7	9
	Port Nolloth	2	4	8	7
	Alexanderbay	7	8	16	12
	Vioolsdrif - AWS	3	3	6	9
14-Jul-21	Springbok WO	10	5	8	9
	Port Nolloth	8	9	17	15
	Alexanderbay	8	9	15	16
	Vioolsdrif - AWS	3	2	3	2
23-Jul-21	Springbok WO	8	7	8	8
	Port Nolloth	13	13	16	19
	Alexanderbay	12	11	20	14
	Vioolsdrif - AWS	13	13	10	15

The highest ΔT values also occurred on the day of the DS for most of the coastal stations. As highlighted in section 4.4.1., the general observation was a gradual increase in maximum temperature leading up to the day of the DS event, with not much change in the minimum temperatures leading to the day of the DS. This resulted in high ΔT values on the day of the DS. However, the minimum temperatures increased the day after the DS (see addendum 7). Altogether, this resulted in an overall

decrease in ΔT values the day after the DS. A possible reason for this decrease for both coastal and interior DS is that solar radiation is reflected by a layer of dust aerosol to a considerable degree, reducing the downward shortwave radiation during the day, leading to a daytime cooling in the boundary layer (Helmert et al., 2007, Nazarov et al., 2010). However, at night, the heat absorbed by dust particles is reradiated back into the atmosphere, thereby warming it. This will reduce the diurnal variation of temperature in the area where the DS has occurred.

4.4.4.ΔT: Interior DS

Table 4.3 indicates the ΔT before, during, and after the episodes of dust events for the interior DS. In general, ΔT was highest for most of the stations the day before the DS, unlike the coastal DS cases where the highest ΔT was observed on the day of the DS. The day after the DS case, ΔT was lower than the day before, similar to some of the coastal DS cases. A possible reason for this is mentioned in section 4.4.3.

There was one exception that did not follow this trend of decline in ΔT the day after. This was the DS that occurred on 13 January 2016, which was also hidden under clouds due to thunderstorm development (see figure 4.4). However, the increase was not significant, with the ΔT remaining the same or increased by 1˚C for the selected stations the following day.

Table 4.3: Behaviour of diurnal temperature range before, during and after a DS for interior regions. The values indicate the T two days before, 1 day before, during and the day after the DS. All values highlighted in red are values that were the highest during the period of analysis. The values highlighted in blue indicate where there was a decrease in ΔT values the day after.

Diurnal Temperature Change ΔT - Interior					
Date of dust	**Station name**	**2 days before**	**1 day before**	**During**	**Day after**
16-Oct-14	Bloemfontein Stad	21,2	16,8	15,7	12,2
	Glen College AWS	25	19,6	17,2	13,4
	Bloemhof	22	16,9	16,8	15,2
	Welkom	19,7	13,5	15,8	14,7
13-Jan-16	Kimberly	20	15,1	15,2	15,8
	Fauresmith	18,4	15,7	17	18,2
	Welkom	18,1	19	13,9	15,4
22-Aug-17	JHB Bot Tuine	15,6	19,2	17,7	16,5
	JHB int WO	14,4	12,1	16,6	15,3
	Ermelo	16,2	17,4	18,3	19,4
	Wonderboom	15,5	21,1	24,8	19,2
08-Jul-21	Beaufort West	19,8	18,6	15,6	11,8
	Graaff-Reinet	26,4	26,3	11,8	19
	Fraserburg	21,8	21	19,8	13
	Calvinia WO	15,9	20,2	12	11,3
	Brandvlei	23,8	23,7	16,7	12,9
28-Dec-18	Bloemfontein Stad	17,4	19,6	17,1	13,8
	Glen College AWS	23,6	25	21	16,1
	Bloemhof	11,5	11,1	7,8	7,7

4.5. Analysis of changes in RH

4.5.1.Coastal DS

Figure 4.9 illustrates the daily RH for each of the coastal DS events. In general, RH decreased gradually leading up to the day of the DS. The coastal stations had considerably higher RH values as compared to the inland stations. RH was also at the lowest the day after the DS, which was a similar trend for all coastal DS. This could be influenced by berg wind conditions which are associated with hot and dry winds blown offshore. The station with the lowest RH in every DS event is Vioolsdrif, which is over 100 km inland. This can be expected, as the coastal stations will have influence from the ocean.

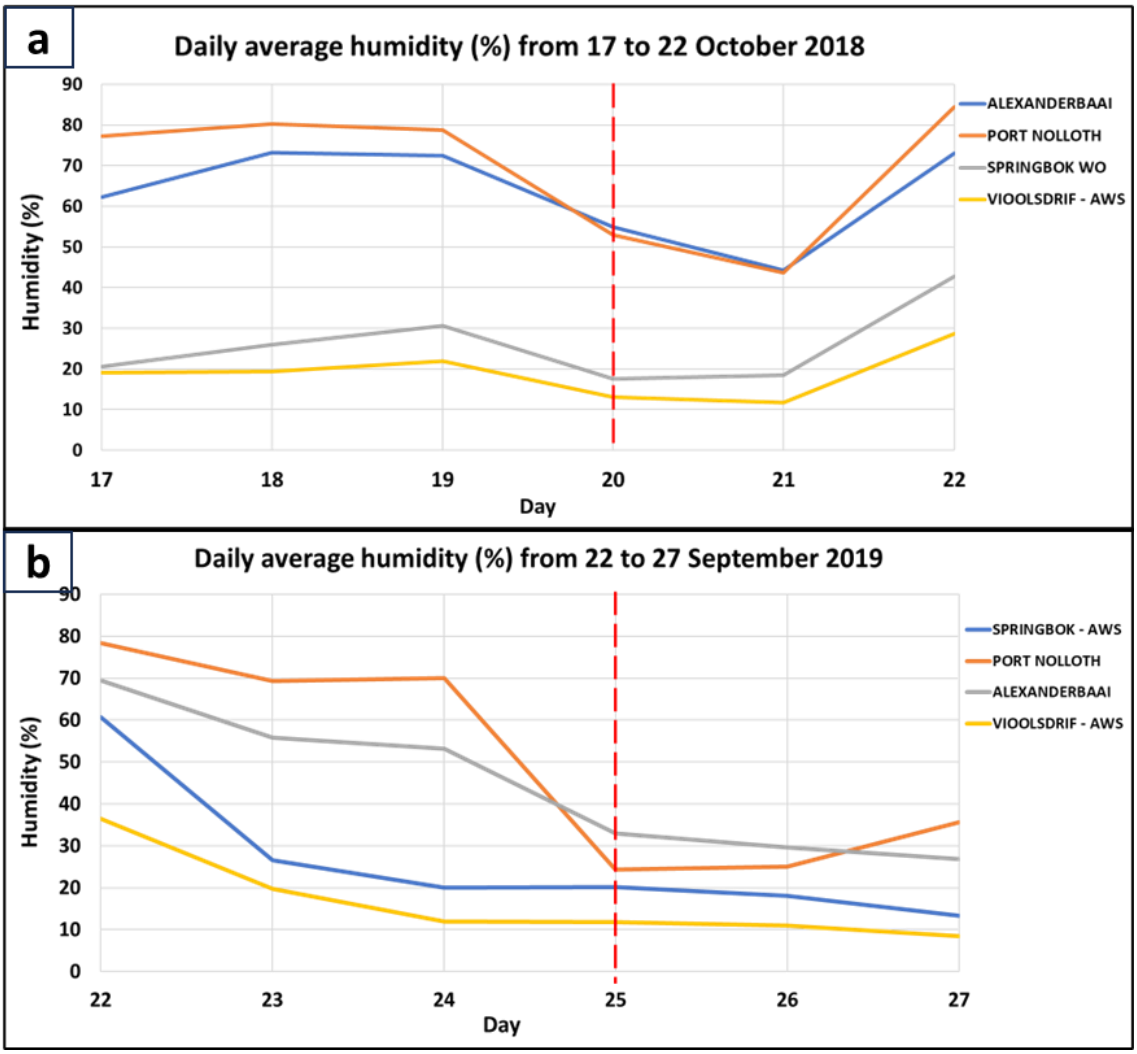

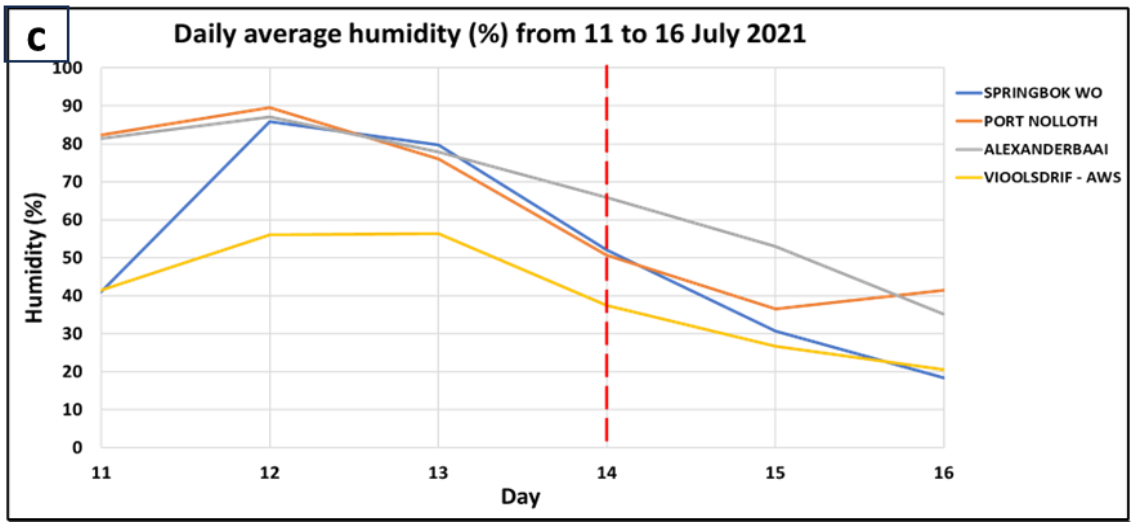
C
Daily average humidity (%) from 11 to 16 July 2021
Humidity (%)
100
90
80
70
60
50
40
30
20
10
0
11
12
13
14
15
16
Day
SPRINGBOK WO
PORT NOLLOTH
ALEXANDERBAAI
VIOOLSDRIF - AWS

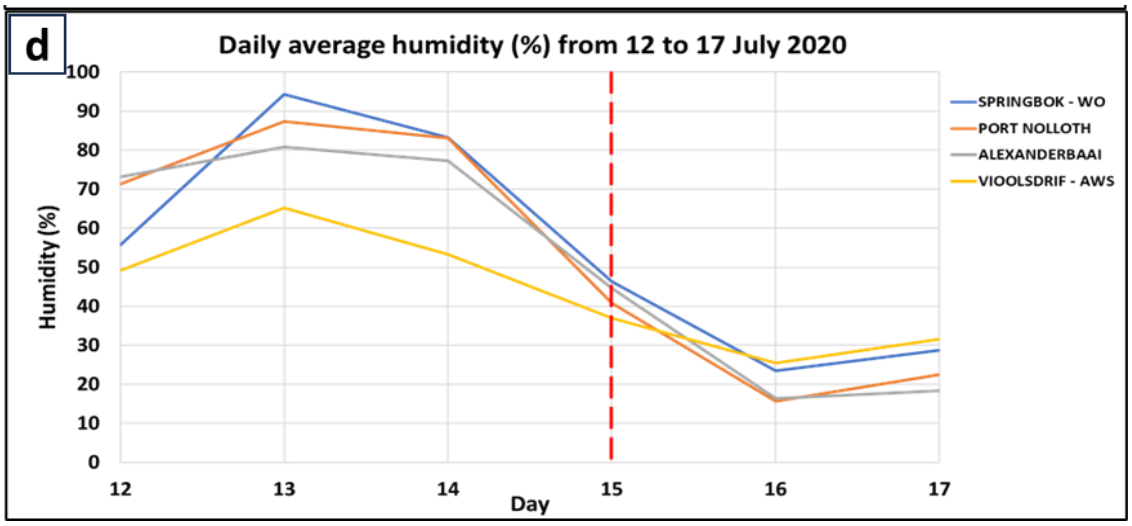
d
Daily average humidity (%) from 12 to 17 July 2020
Humidity (%)
100
90
80
70
60
50
40
30
20
10
0
12
13
14
15
16
17
Day
SPRINGBOK - WO
PORT NOLLOTH
ALEXANDERBAAI
VIOOLSDRIF - AWS

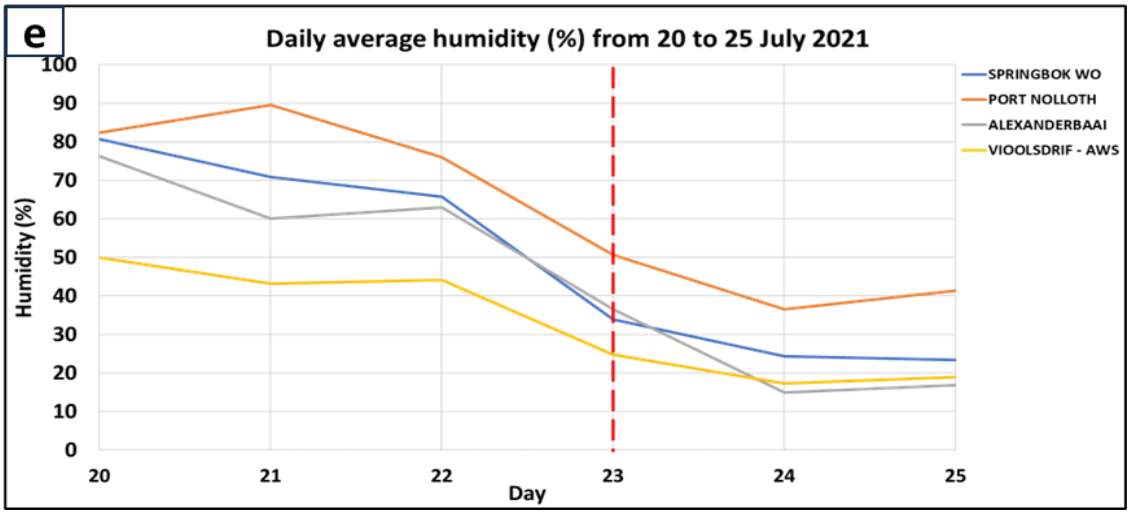
e
Daily average humidity (%) from 20 to 25 July 2021
Humidity (%)
100
90
80
70
60
50
40
30
20
10
0
20
21
22
23
24
25
Day
SPRINGBOK WO
PORT NOLLOTH
ALEXANDERBAAI
VIOOLSDRIF - AWS

Figure 4.9: Daily average humidity (%) for coastal DS events a) 17 to 22 October 2018, b) 22 to 27 September 2019 c) 11 to 16 July 2021, d)12 to 17 July 2020, e) 20 to 25 July 2021, where the red line indicates the day of the DS event.

4.5.2.Interior DS

The RH trend was different for interior and coastal DS. Table 4.4 shows the behaviour of RH before, during, and after a DS. For the DS on 22 August 2017, RH gradually decreased leading to the day of the DS and continued to decrease after the day of the DS, ranging from 23% to 32%. The lowest values were observed the day after the DS. This is because behind the cold front is dry and colder air which has less moisture. For the prefrontal DS on 08 July 2021, the RH values were between 21% and 53% and had been decreasing leading up to the day of the DS. The values increased after the DS, which could have been a result of the passage of the frontal cloud band, often associated with precipitation. Therefore, the synoptic weather system also plays a role in the RH values.

Table 4.4: Behaviour of RH before, during and after a DS for DS resulting from synoptic scale weather systems. All values highlighted in red indicate RH values that decreased after the DS, while the values in blue indicate RH values that increased the day after the DS.

Relative humidity (%) - interior (synoptic scale)					
Date of dust event	Station name	2 days before	1 day before	During	Day after
22-Aug-17	JHB Bot Tuine	52	48	33	23
	JHB int WO	55	47	33	25
	Ermelo	70	55	40	32
	Wonderboom	50	51	37	24
08-Jul-21	Beaufort West	29	21	28	53
	Graaff-Reinet	41	32	21	40
	Fraserburg	37	34	46	69
	Calvinia WO	44	41	53	79
	Brandvlei	30	29	42	63

Table 4.5 shows RH before, during and after of the mesoscale induced DS. Two of the interior DS were associated with low RH before the day of the DS, which ranged between 23% and 33%. The RH values then increased on the day of the DS for all but one station (Welkom on 13 January 2016). A

possible reason is that the onset of a DS can cause radiative cooling, which decreases temperature, which can cause an increase in RH during or right after a DS event due to a slower evaporation rate. For thunderstorm-induced DS, RH was generally between 45% and 65%. The presence of thunderstorms could have influenced the higher RH values.

Table 4.5: Behaviour of RH before, during and after a DS for DS resulting from mesoscale weather systems. All values highlighted in red indicate RH values that decreased before the DS, while the values in blue indicate RH values that were over 50% and were associated with thunderstorms during the DS.

Relative humidity (%) - interior (mesoscale)					
Date of dust event	Station name	2 days before	1 day before	During	Day after
16-Oct-14	Bloemfontein Stad	42	25	49	49
	Glen College AWS	42	26	47	45
	Bloemhof	33	33	34	41
	Welkom	39	22	47	41
13-Jan-16	Kimberly	55	58	63	52
	Fauresmith	55	54	65	54
	Welkom	58	60	58	59
28-Dec-18	Bloemfontein Stad	17	22	38	58
	Glen College AWS	18	29	45	58
	Bloemhof	17	27	56	66

4.6. Analysis of changes in T_d

4.6.1.Coastal DS

In general, there was a gradual decrease in T_d leading up to the day of the event, with Port Nolloth and Alexander Bay having higher T_d values of the stations throughout the entire period of analysis. Figure 4.10 shows the hourly T_d for the coastal DS events. T_d was less than 15˚C for all DS events three days before the DS occurred, but less than 11˚C on the day of the DS for all DS events. The DS event of 25 September 2019, shown in figure 4.10b, had T_d values that were below 0˚C for Springbok and Vioolsdrif the day before the DS, while the DS event of 20 October 2018, shown in figure 4.10a, had T_d values that were 0˚C three days before the event. The lowest T_d values for the coastal stations were between -2.8 and -3.4˚C for the events of 25 September and 15 July 2020. Between the DS events of 25 September and 20 October 2018, the more interior stations (Vioolsdsrif and Springbok) experienced their lowest temperatures, ranging from -12˚C to -13˚C.

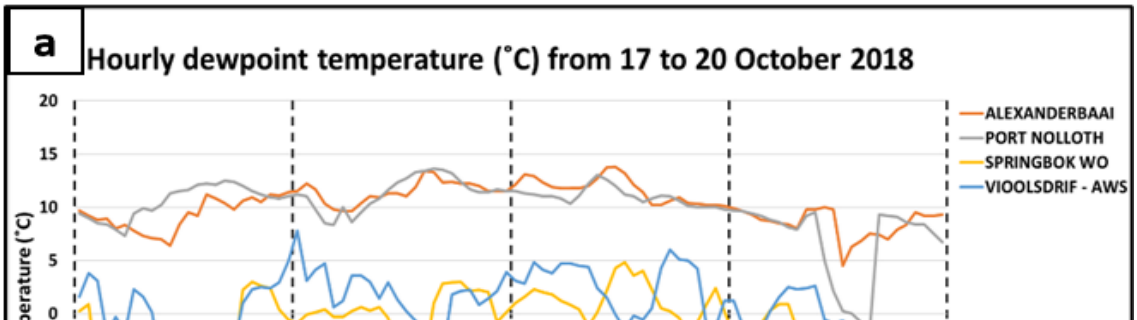

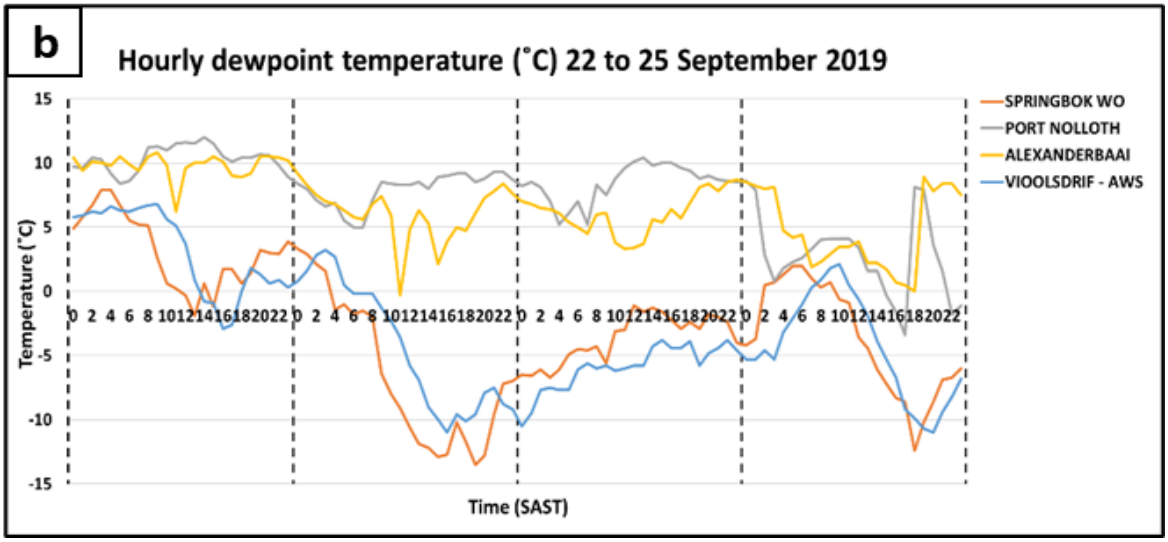
b
Hourly dewpoint temperature (˚C) 22 to 25 September 2019
SPRINGBOK WO
PORT NOLLOTH
ALEXANDERBAAI
VIOOLSDRIF - AWS
Temperature (˚C)
Time (SAST)

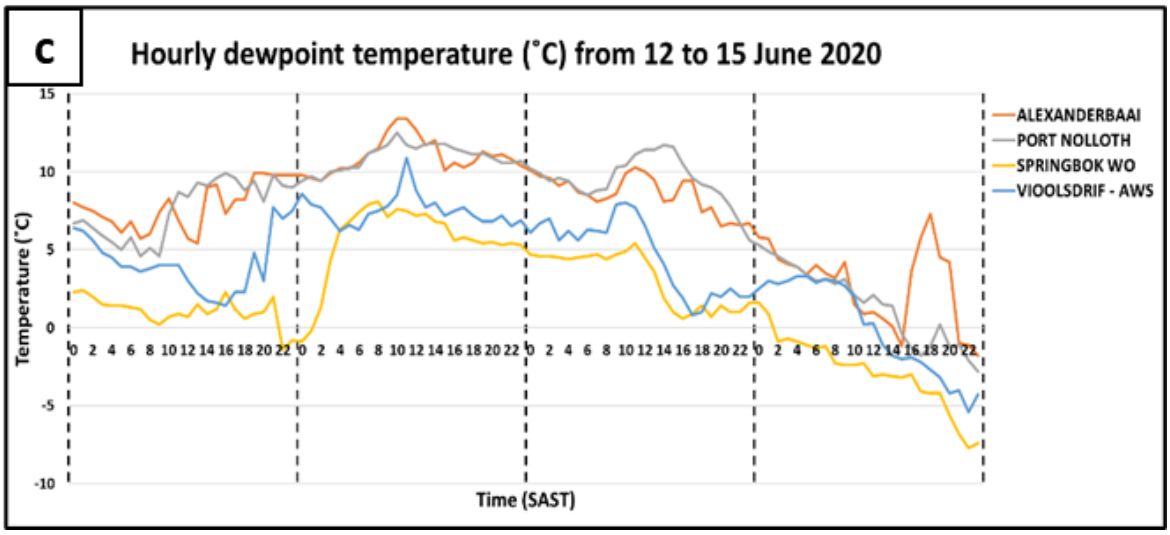
c
Hourly dewpoint temperature (˚C) from 12 to 15 June 2020
ALEXANDERBAAI
PORT NOLLOTH
SPRINGBOK WO
VIOOLSDRIF - AWS
Temperature (˚C)
Time (SAST)

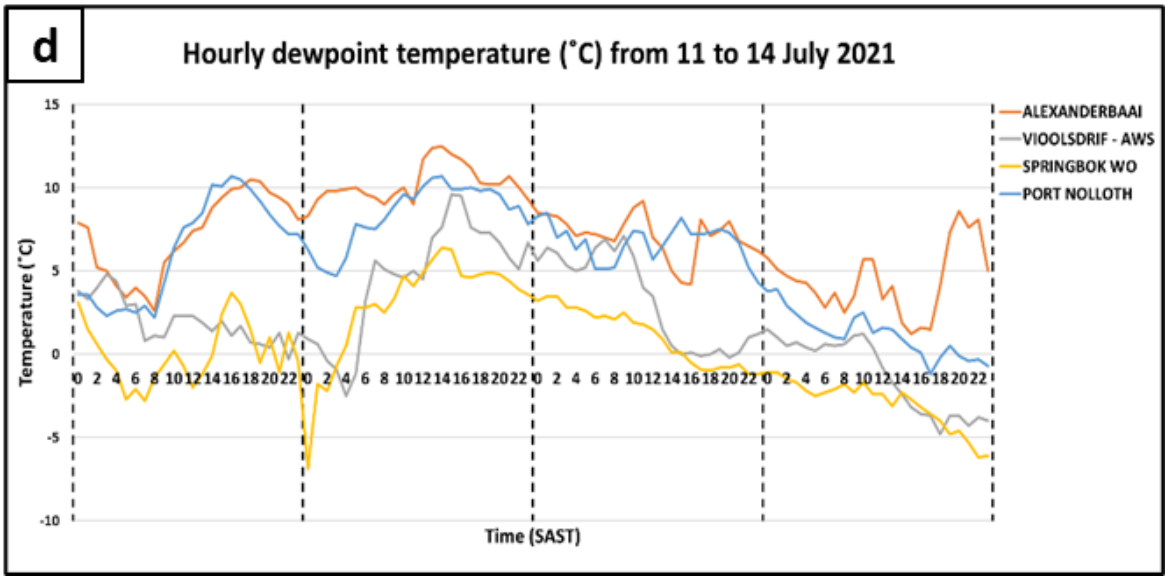
d
Hourly dewpoint temperature (˚C) from 11 to 14 July 2021
ALEXANDERBAAI
VIOOLSDRIF - AWS
SPRINGBOK WO
PORT NOLLOTH
Temperature (˚C)
Time (SAST)

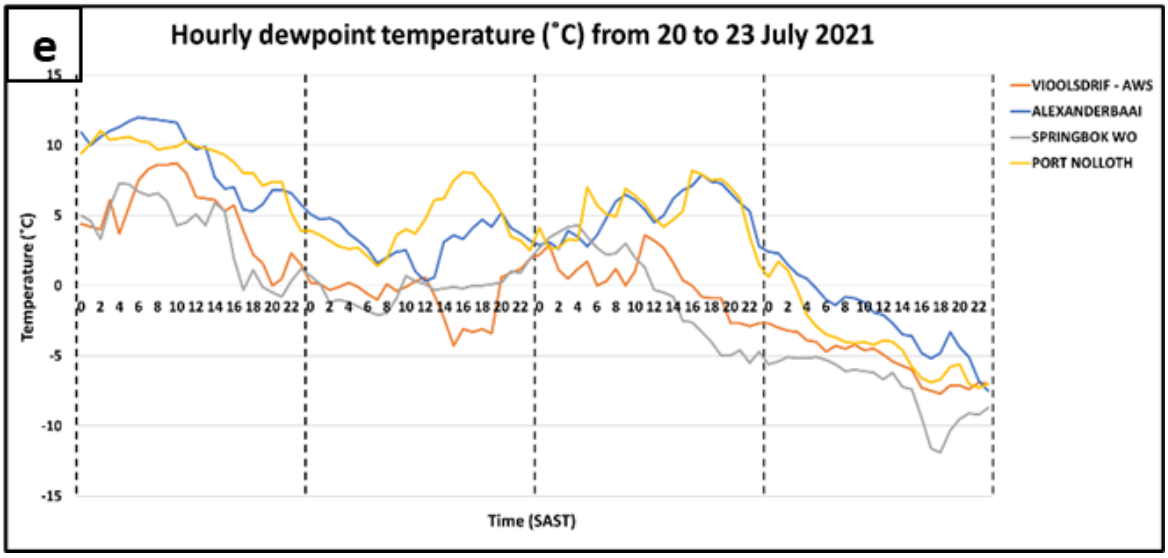

Figure 4.10:Hourly dew point temperature (Td) for a) 17 to 20 October 2018, b) 22 to 25 September 2019 c)12 to 15 July 2020, d) 11 to 14 July 2021, e) 20 to 23 July 2021 for the coastal stations. The dotted black lines indicate separate days.

4.6.2.Interior DS

The synoptically induced DS had far lower T_d values than the thunderstorm-induced DS. The DS that occurred on 22 August 2017, shown in figure 4.11a, had low T_d before the DS event, ranging from 4 to -3˚C for all stations two days before the DS occurred. However, on the day of the DS event, the T_d values dropped even further. The DS began at approximately 11:30, with the sharp decrease in T_d observed within 3 to 4 hours after the starting time for all stations, reaching between -8˚C and -14˚C by the evening. However, for the DS event on 8 July 2021, shown in figure 4.11b, an opposite trend was observed. Before the DS, the T_d was between 1˚C and -15˚C. The DS started at 13:30, lasting until approximately 19:30. Of the four stations selected for analysis, the T_d of three stations increased to a range of between 4˚C and 7˚C from 18:00, with one station, Calvinia WO, increasing earlier on at 10:00. This could be a result of the frontal band moving over the area in the afternoon, increasing the T_d as it moves over the area.

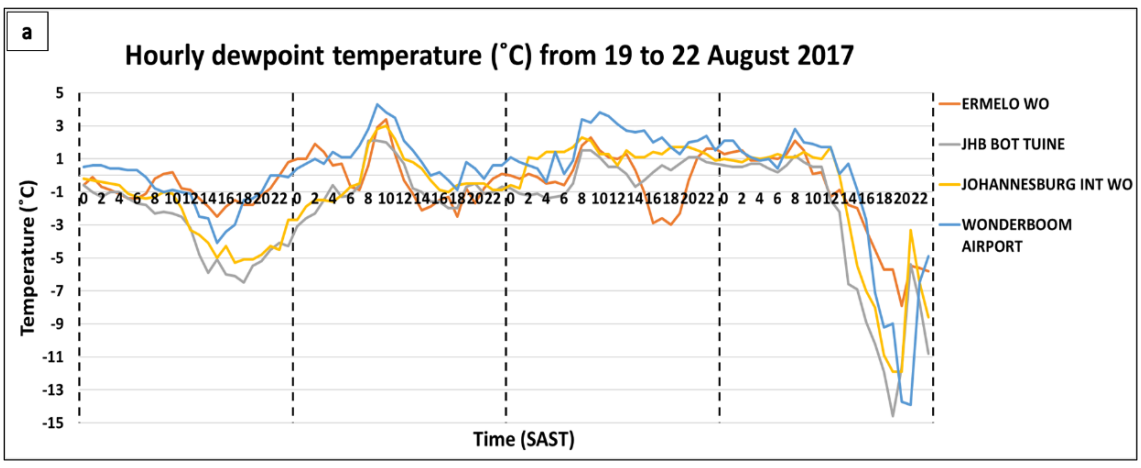

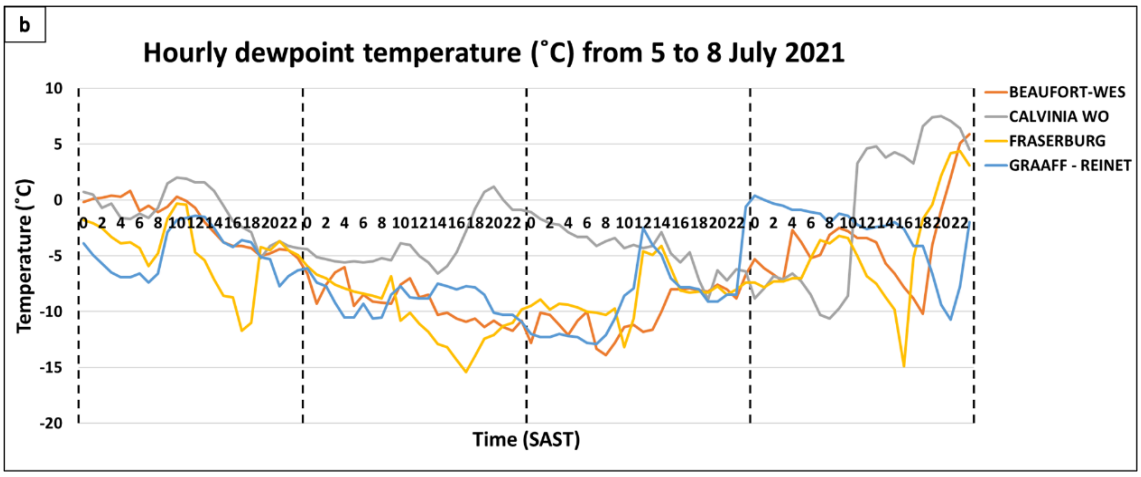

Figure 4.11: Hourly dew point temperature (Td) for a) 19 to 22 August 2017 and b) 5 to 8 July 2021 which are two interior DS cases that were caused by synoptic scale weather systems.

Except for the DS on 16 October 2014, the thunderstorm-induced DS had higher T_d on the day of the DS compared to the synoptically induced DS, with the maximum T_d of the stations ranging from 11 to 16˚C. The T_d of the thunderstorm-induced DS on 13 January 2016, shown in figure 4.12a, was between 10 ˚C and 16 ˚C the day before the DS. On the day, the T_d decreased during the period of the DS for two of the three stations. This pattern was also observed with the DS on 28 December 2018, shown in figure 4.12b. The T_d of two of the three stations decreased during the DS, with Glen College AWS reaching -1˚C at 19:00 but a sudden increase to 13˚C the next hour.

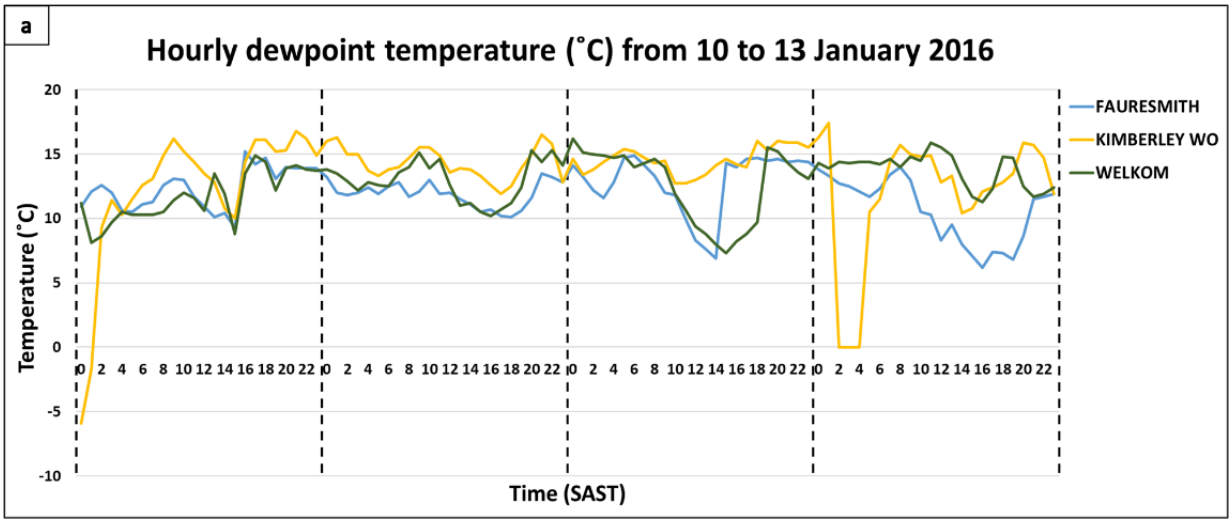

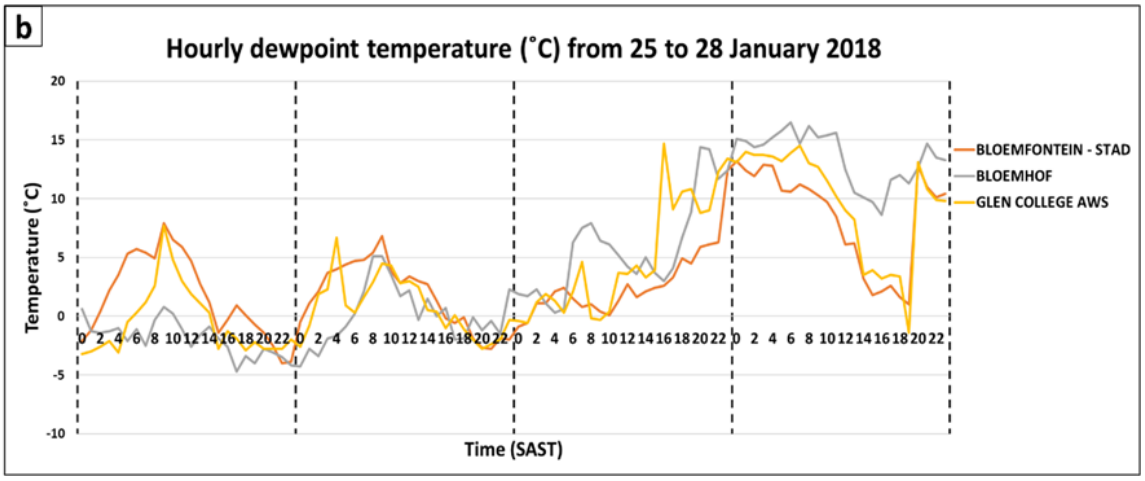

Figure 4.12: Hourly dew point temperature (Td) for a) 13 to 16 October 2014 and b) 25 to 28 January 2018 which are the two thunderstorm-induced DS cases.

The overall T_d for the DS event of 16 October 2014, shown in figure 4.13, was lowest of all the thunderstorm-induced DS. While the highest T_d values for the other DS ranged from 11 ˚C to 16 ˚C, maximum T_d on 16 October 2014 was 2014 was 9.3 ˚C for Welkom. A possible reason is that, although it was a thunderstorm-induced DS, the large-scale system is a cut-off low, which is part of the family of cyclones. They are often associated with dry air intrusion or a 'dry slot' on the western or south western side of the cut-off low (Catto, 2016). This is an area where colder, drier air descends behind the low, which is often visible on satellite image as a clear cloudless area (Catto, 2016).

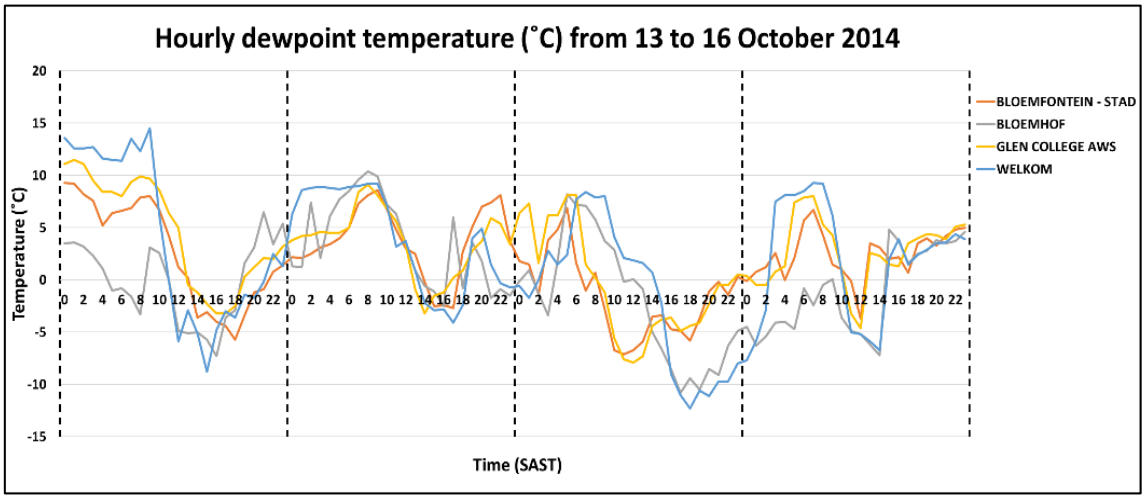

Figure 4.13: Hourly dew point temperature (T_d) for 13 to 16 October 2014.

4.7. Analysis of changes in wind speed and direction

4.7.1.Coastal DS

All cases selected had similar weather systems, though differing in strength. The strength of the weather systems plays a role in the wind speed. Coastal DS that lasted the longest were associated with winds peaking at 12-15 m/s, which were also associated with the stronger high-pressure systems. Table 4.6 shows what the wind speed at each station was at the time the DS started. Springbok, which is a more interior station at an elevation of 1006m above sea level (asl), had the highest wind speed at the start of the DS for all cases ranging between 10 and 14 m/s. Alexander Bay, which is right at the coast at an elevation of 24m asl, had the lowest wind speed for 4 out of the 5 cases, ranging between 1 and 2 m/s. The average wind speed between all four stations ranged from 5 to 8 m/s at the start of the DS. The stronger winds observed at the stations situated more interior can be attributed to the topography of the area, as they are situated at a higher altitude.

Table 4.6*: The wind speed (m/s) reported at each station at the approximate start of the DS. The last row is the average wind speed (m/s) of the 4 stations at the start of each DS.*

Date of DS Start of DS	**20-Oct-18** **08h00**	**25-Sep-19** **05h00**	**15-Jul-20** **10h00**	**14-Jul-21** **13h00**	**23-Jul-21** **09h00**
Springbok	12	14	10	10	11
Alexander Bay	1	2	5	1	2
Port Nolloth	3	9	6	4	7
Vioolsdrif	5	7	3	3	5
Average	5	8	6	5	6

Figure 4.14 indicates the highest gust winds on the day the DS started for all four stations. Apart from one event, all DS events had at least one station reaching a gust of 20 m/s on the day. On 14 July 2021, which is also the shortest DS event, there were wind gusts ranging from 8 to 11 m/s, except for Springbok which peaked at 18 m/s. The DS with the longest duration (15 July 2020) had strong wind gusts for all stations, ranging from 18 to 24 m/s.

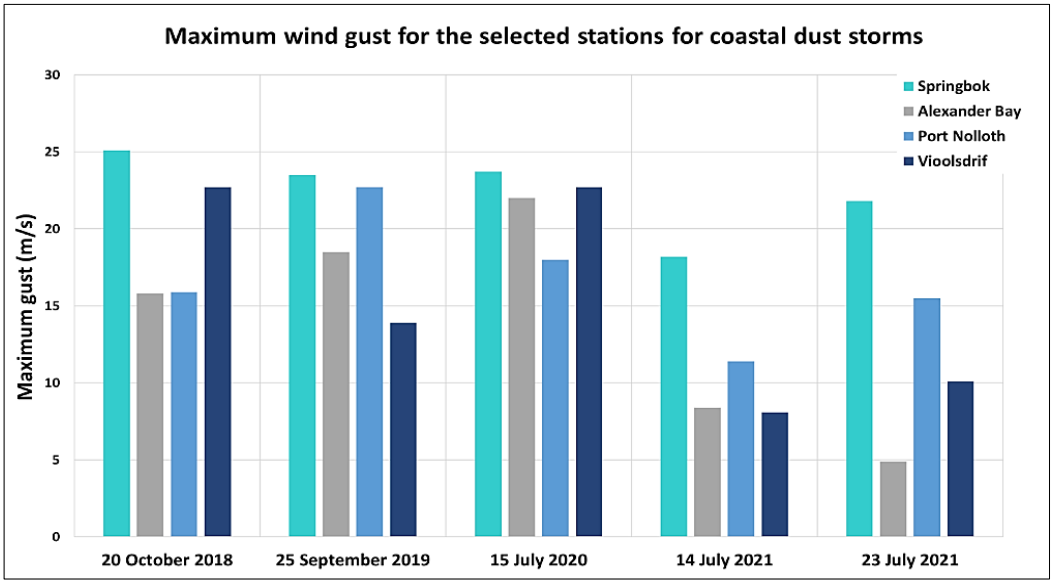

Figure 4.14: Maximum wind gust for each station selected for analysis on the day of the DS event for each event.

The main wind direction for each DS event ranged from easterly, north-easterly, and south-easterly, as seen in the two DS shown in figures 4.15a and 4.15b (also see appendix 3). What was evident was that the wind direction for all the DS events had an easterly component. The DS with the shortest duration indicated in figure 4.15b (14 July 2021) had the weakest easterly component for the two stations directly along the coast. In other words, wind speed for the easterly component for both Port Nolloth and Alexander Bay was less than 5 m/s, whereas the DS with the longest duration had stronger easterly components, reaching between 8 and 12 m/s for Port Nolloth and between 12 and 16 m/s for Alexander Bay.

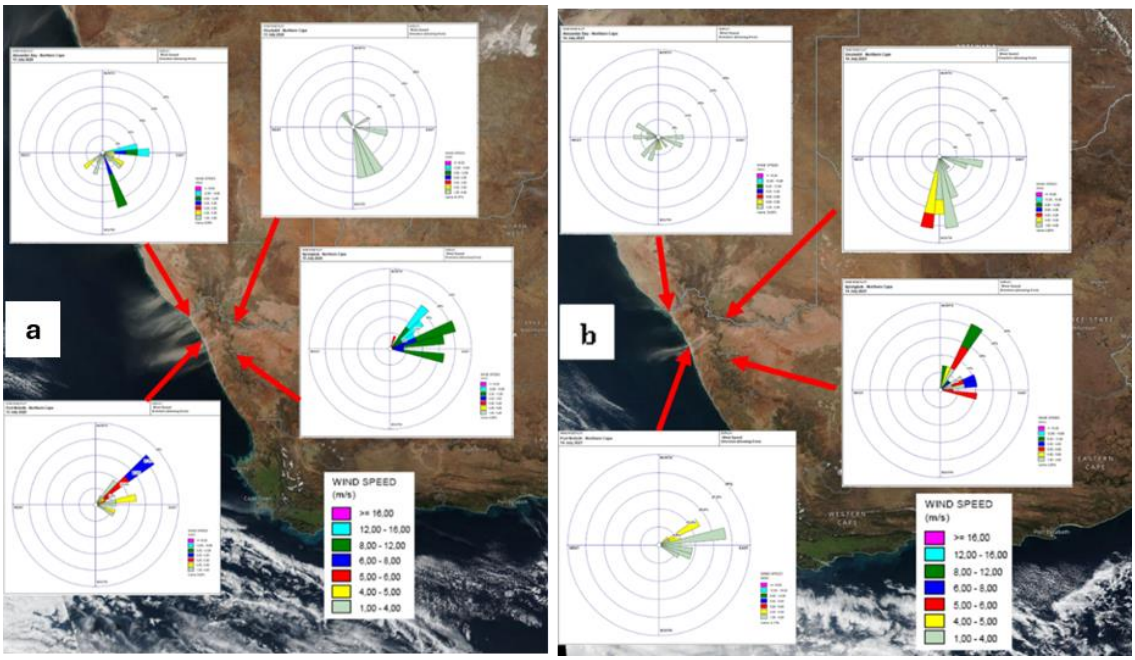

Figure 4.15: Visible satellite imagery of the DS on a) 25 September 2019 and b) 14 July 2021, with wind roses of the same day of the four stations that were used for analysis. Image Source: NASA Worldview (2020). Retrieved from https://worldview.earthdata.nasa.gov/

4.7.2.Interior DS

Wind speeds of the interior had more variations as they were associated with different weather systems. Figure 4.16 indicates the maximum wind gusts for interior DS cases. The strongest winds were observed with DS associated with synoptic scale weather systems (i.e. 8 July 2021), with the daily winds speed averaging from 7 to 10 m/s, gusting between 22 and 27 m/s for all stations. The higher daily average of wind speeds indicates that the strong winds were also sustained for longer with synoptically induced DS, as compared to the winds of DS originating from thunderstorms. This also allowed for greater dispersion of dust particles. The average wind speed at the start of the interior DS is indicated on table 4.7.

Table 4.7: The wind speed (m/s) reported at each station at the start of the DS. The last row is the average wind speed (m/s) of the stations at the start of each DS.

16-Oct-14		**13-Jan-16**		**22-Aug-17**		**28-Dec-18**		**08-Jul-21**	
Start time: 14:00		**Start time: 16:00**		**Start time: 12:00**		**Start time: 19:00**		**Start time: 13:00**	
Bloemfontein Stad	8	Kimberly	6	JHB bot Tuine	4	Bloemfontein Stad	4	Beaufort-West	13
Glen College AWS	8	Fauresmith	10	JHB int. WO	6	Glen college AWS	5	Graaff-Reinet	9
Bloemhof	6	Welkom	4	Ermelo	11	Bloemhof	7	Fraserburg	11
Welkom	9			Wonderboom	3			Calvinia WO	10
								Brandvlei	8
Average (m/s)	***8***		***7***		***6***		***5***		***11***

This is an estimation, as the start time is not always accurate due to some DS being hidden by clouds. The DS of 08 July 2021 had the highest starting winds at 11 m/s and had one of the larger spatial distributions amongst the cases selected for this study. The wind direction of interior DS depends on the weather system that induced it. Prefrontal DS will have a north-westerly wind direction, whereas DS from thunderstorms are dependent on the direction of the outflow boundary (see appendix 4). In this study, of the three thunderstorm-induced DS, two were south westerly, while one easterly to north easterly, following the direction of the outflow boundary.

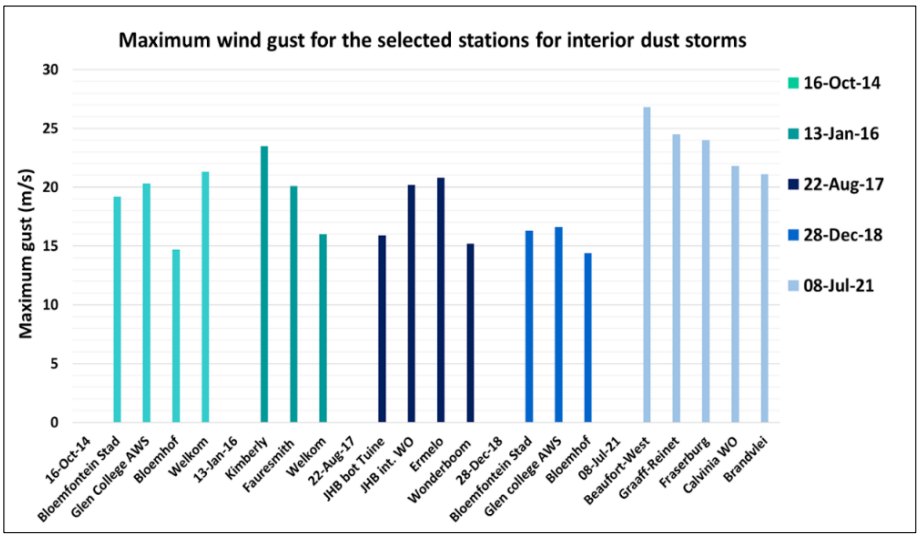

Figure 4.16: Maximum wind gust for each station selected for analysis on the day of the DS event for each event for interior DS.

4.8. Analysis of rainfall and soil moisture

4.8.1.Coastal DS

Figure 4.17 shows the soil moisture over South Africa for the coastal DS events, averaged over two days (the day before and during the DS event). Generally, the coastal areas receive their rainfall during the winter months. However, the West Coast is also one of the drier regions of South Africa, receiving less than 100 mm of rainfall in winter and spring. Table 4.8 also indicates the amount of rainfall in mm that the stations received prior to the DS event.

Table 4.8: Table indicates the amount of rainfall in mm that the stations received prior to the DS event. The cells highlighted in blue indicate the stations that have received rainfall. The amount shaded in darker blue highlights the higher rainfall amounts.

Date of dust event	Station name	2 days before	1 day before	During
20-Oct-18	Springbok	0	0	0
	Alexander Bay	0	0	0
	Port Nolloth	0	0	0
	Vioolsdrif	0	0	0
25-Sep-19	Springbok	0	0	0
	Alexander Bay	0	0	0
	Port Nolloth	0	0	0
	Vioolsdrif	0	0	0
15-Jul-20	Springbok	7	1	0
	Alexander Bay	0	0	0
	Port Nolloth	0	0	0
	Vioolsdrif	0	0	0
14-Jul-21	Springbok	28	0	0
	Alexander Bay	7	0	0
	Port Nolloth	0	0	0
	Vioolsdrif	1	0	0
23-Jul-21	Springbok	1	0	0
	Alexander Bay	0	0	0
	Port Nolloth	0	0	0
	Vioolsdrif	0	0	0

The soil moisture for all DS cases was less than 25%, with the DS on 20 October 2018 having the lower soil moisture at 12.5% and less. The DS events of 15 July 2020 and 23 July 2021 received less than 10mm of rainfall before the DS, and no rain on the day. However, the DS with the shortest duration (14 July 2021) received just under 40 mm of rainfall two days before the DS. This could have been one of the factors contributing to the short duration of the DS, possibly resulting in greater binding between soil particles, which means that they are less likely to be entrained. The soil moisture was also slightly higher for the areas where to interior stations were located (Springbok), averaging between 25 and 37%.

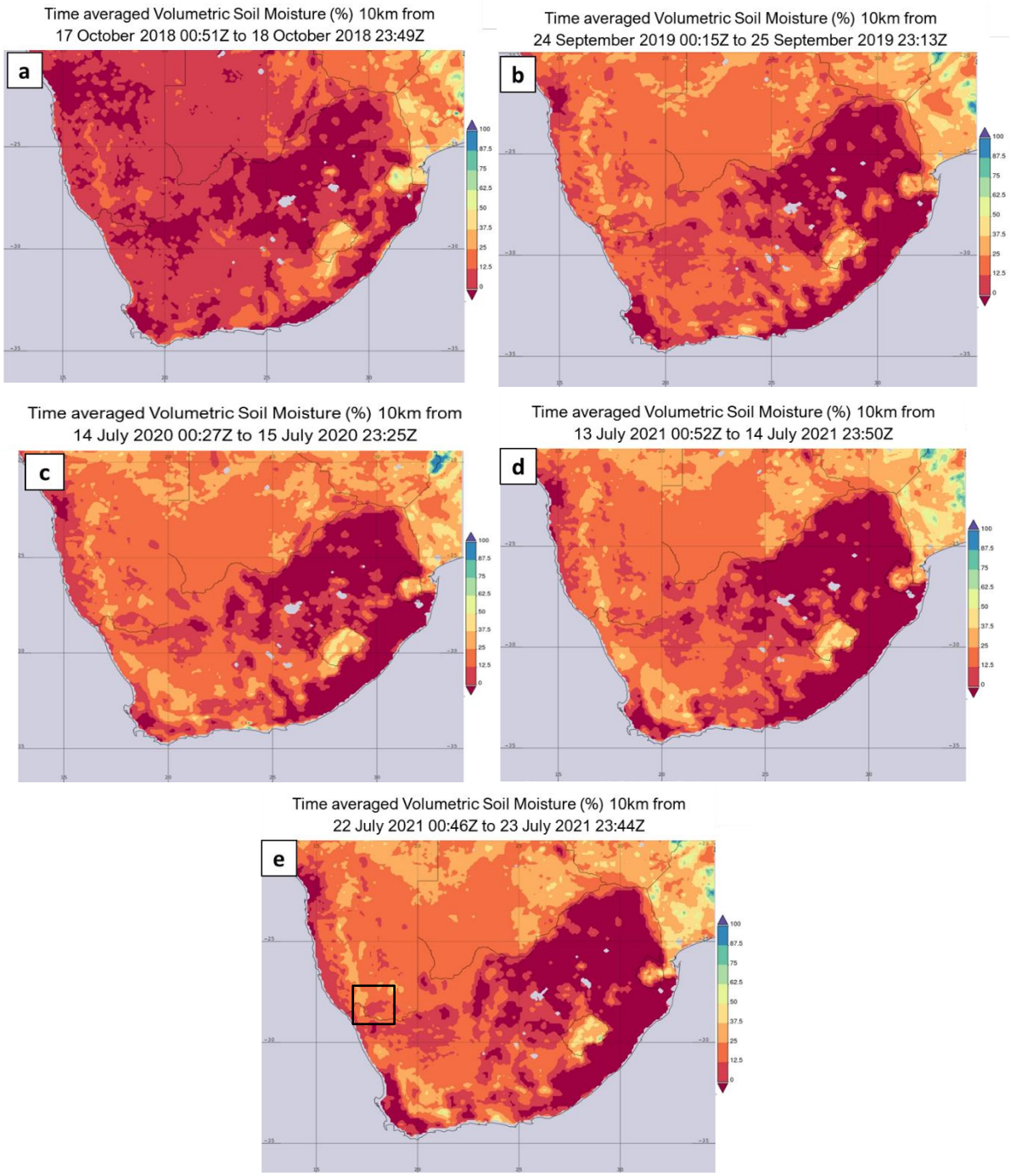

Figure 4.17: Volumetric Soil moisture (%) at a resolution of 10km averaged over two days approximately midnight to midnight for the coastal DS events a)18 to 19 October 2018, b) 24 to 25 September 2019, c) 14 to 15 July 2020, d)13 to 14 July 2021 and e) 22 to 23 July 2021.

4.8.2.Interior DS

Figure 4.18 indicates the soil moisture over South Africa for the interior DS events, averaged over two days (the day before and during the DS event). In contrast to coastal DS, interior DS events were mostly associated with rainfall except for two events. Generally, the interior areas of the country are summer rainfall areas. The rainfall amounts can range from 200 mm to 400 mm in the late spring and summer months.

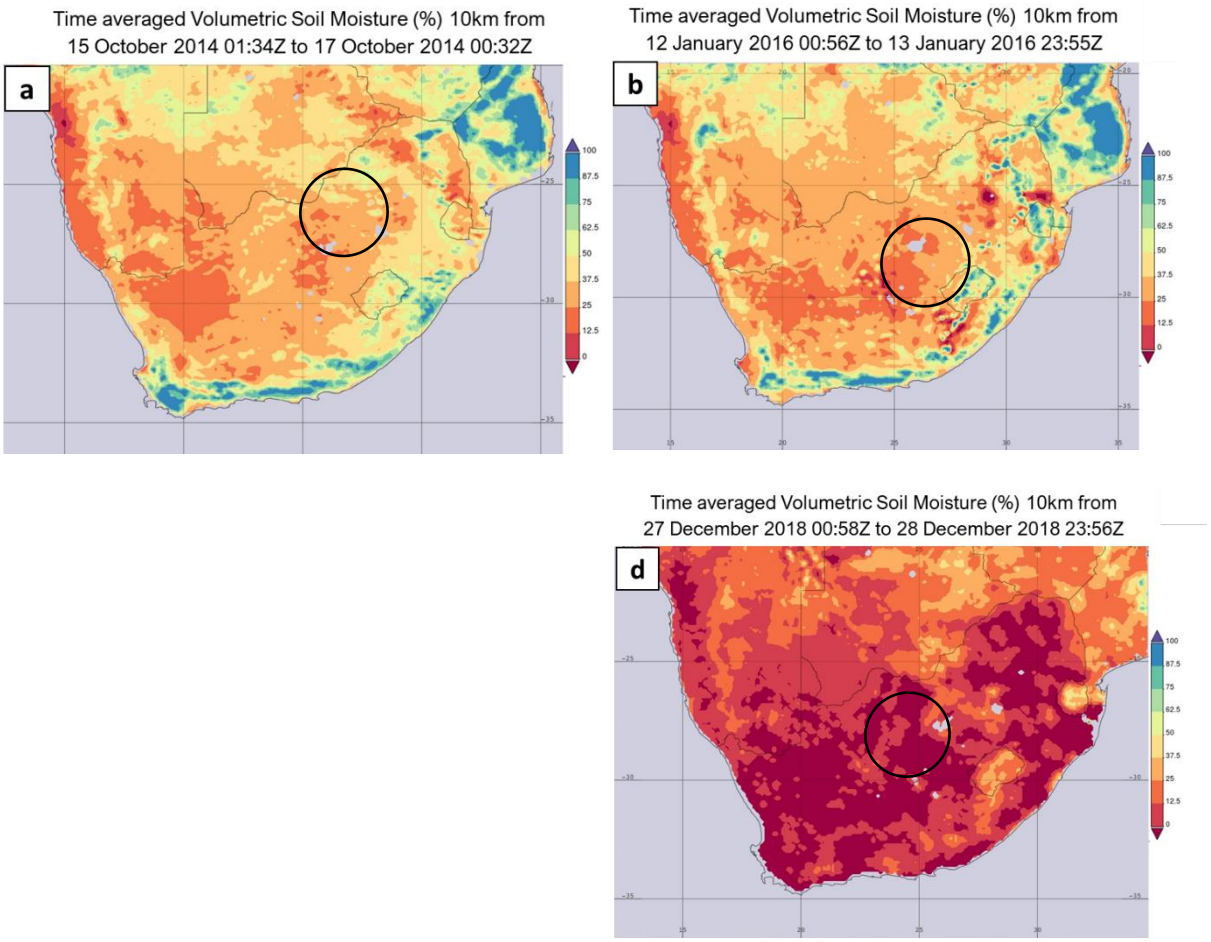

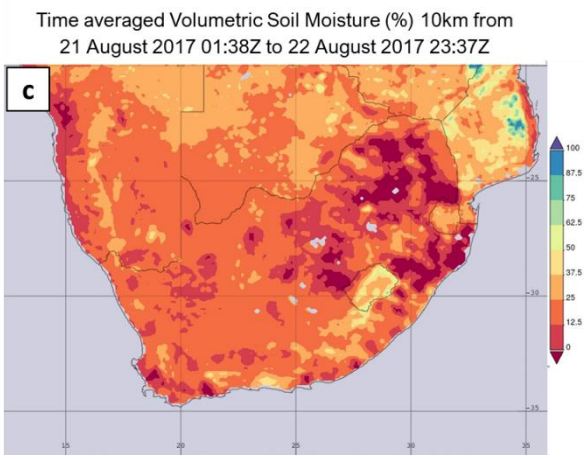

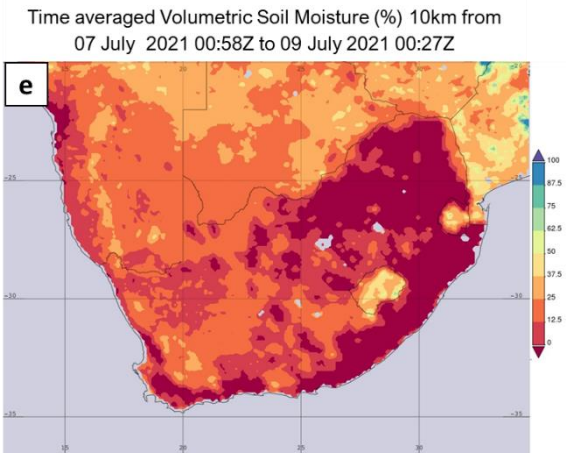

Figure 4.18: Volumetric Soil moisture (%) at a resolution of 10km averaged over two days approximately midnight to midnight for a) 15 to 16 October 2014, b)12 January 2016 to 13 January 2016 and c) 21 to 22 August 2017, d) 27 to 28 December 2018 and e) 07 to 08 July 2021.

The DS with the highest rainfall amounts was the thunderstorm-induced DS on 13 January 2016, with 44mm before the day and an additional 22mm on the day of the DS as shown in table 4.9. Although January is in the middle of the summer rainfall season, 2016 was part of the 2015/2016 drought season during the 2014-2016 El Nino which resulted in below-normal rainfall. Figure 4.18 shows the volumetric soil moisture over southern Africa during the interior DS events, where although it had been raining, the soil moisture was still low, at below 37% over the central parts of the country. Focusing on the area where the DS occurred, the soil moisture was between 12.5 and 25%. This was followed by the prefrontal DS on 8 July 2021 where rainfall was reported with the passage of the frontal band, after the DS had occurred. However, no rain was reported days prior to the DS event. This DS occurred during the winter season, and over an area where the annual rainfall is less than 300mm. The soil moisture reflected this expected dryness in figure 4.18e, with soil moisture less than 12.5% over the DS area on 8 July 2021.

Another contributing factor to the low soil moisture is that this was a prefrontal DS. Prefrontal conditions are characterized by low humidity, warmer conditions which may have contributed to increased evaporation, reducing soil moisture in the top surface of the soil. The DS events that had no rain reported before and during the DS were the thunderstorm-induced DS of 16 October 2014 with a soil moisture of less than 25%, and the postfrontal DS of 22 August 2017 with a soil moisture that is mostly 12.5%. Both events had long durations, lasting more than a day. Seasonal rainfall could have

also contributed to the low soil moisture as both occurred in seasons which do not receive high rainfall amounts.

Table 4.9: indicates the amount of rainfall in mm that the stations received prior to the interior DS events, as well as during the DS event. The cells highlighted in blue indicate the stations that have received rainfall. The area blocked out in black indicates that there was no rainfall data available.

Date of dust event	Station name	2 days before	1 day before	During
16-Oct-14	Bloemfontein Stad	0	0	0
	Glen College AWS	0	0	0
	Bloemhof	0	0	0
	Welkom	0	0	0
13-Jan-16	Kimberly	17,6	0	0,5
	Fauresmith	11,6	0	15,8
	Welkom	15,2	0,2	5,6
22-Aug-17	JHB Bot Tuine	0	0	0
	JHB int WO			
	Ermelo	0	0	0
	Wonderboom	0	0	0
08-Jul-21	Beaufort West	0	0	3,2
	Graaff-Reinet	0	0	0
	Fraserburg	0	0	0,6
	Calvinia WO	0	0	1,6
	Brandvlei	0	0	0
28-Dec-18	Bloemfontein Stad	0	0	0
	Glen College AWS	0	2,4	0,2
	Bloemhof	0	1,4	0,4

4.9. Discussion

4.9.1. Weather systems

The weather systems that produce coastal DS are a combination of the surface trough over western interior or along the west coast, with a high pressure situated south, south east or over the interior of the country. A few key findings can be highlighted regarding the combination of weather systems that cause coastal DS:

I. The duration of the DS can be linked to the strength of the high-pressure systems. The stronger the high pressure, the greater the gradient along the west, therefore creating stronger off shore winds.

II. The spatial distribution of the DS can also be linked to the strength of the high pressure system as this is a key determinant to the wind strength.

III. The wind direction remained fairly consistent with all DS events, with an easterly component, in line with the dominant weather systems.

The DS originating from mesoscale weather systems had thunderstorms with a gust front that triggered the DS, even though there were synoptic weather systems at play. The DS resulting from

synoptic scale weather systems were associated with cold fronts, being both prefrontal (ahead of the cold front) and postfrontal (after the cold front) DS.

4.9.2.Meteorological Variables

For all coastal DS, as well as synoptically induced DS over the interior, the general observation was a gradual increase in maximum temperature leading to the day of the DS event. For synoptically induced DS, the warmer maximum temperatures can be linked to the pre-frontal and post-frontal conditions associated with a cold front. However, the opposite was observed for thunderstorm-induced DS, where temperatures cooled on the day of the DS. The cloud cover and precipitation could have reduced the maximum temperature on the day of the DS.

The ΔT for most of the stations was highest during the coastal DS events, with the spring DS having the highest ΔT. There was also a general decline in the ΔT observed the day after the DS, with the highest decline observed during the spring DS events. Although not all the stations were showing the drop in ΔT the day after, one or both coastal stations in each case indicated this change. Interior DS also indicated a similar pattern, where there was a drop in ΔT the day after the DS. The maximum ΔT was reached either one day before the DS event, or on the day of the DS event.

In general, RH and T_d decreased gradually leading up to the day of the DS for the coastal DS, with RH the lowest the day after the DS. Thunderstorm-induced DS were associated with the higher RH values, compared to post frontal and prefrontal DS, which were associated the lower RH values. Thunderstorm-induced DS had higher T_d, while post frontal and prefrontal DS generally had sustained low T_d that was observed before the day of the DS event, and during the DS event.

The wind direction of interior DS depended on the weather system that induced it. The wind speed peaked on the day of the DS for all cases. Strong winds sustained for a longer period, allowing for greater dispersion of the dust particles with prefrontal and post frontal DS. Strong wind speeds were not sustained for long during thunderstorm-induced DS, which resulted in lesser dispersion of dust particles, and therefore lesser spatial distribution.

Little to no rainfall was reported during prefrontal and post frontal DS. However, thunderstorm induce DS had rainfall reported on the day of the DS, as well as before, which is not unusual as thunderstorm-induced DS occur during the summer rainfall season. In both interior and coastal DS events rainfall and soil moisture has on impact on soil moisture. The coastal DS with the shortest life span was the only case the reported rainfall before the day of the DS, possibly contributing

to the higher soil moisture average as compared to the other DS cases. This is also a similar finding with interior DS, where thunderstorm-induced DS received more rainfall and had higher soil moisture.

Finally, some significant differences in the behaviour of behaviour of the meteorological variables between DS produced by synoptic scale systems and DS produced by mesoscale systems or thunderstorms are summarised:

I. *RH*: Thunderstorm-induced DS were associated with the higher RH values, compared to post frontal and prefrontal DS, which were associated the lower RH values.
II. *Dew point temperature:* Thunderstorm induced DS had higher T_d, while post frontal and prefrontal DS generally had sustained low T_d that was observed before the day of the DS event, and during the DS event.
III. *Rainfall:* Little to no rainfall was reported during prefrontal and post frontal dust storms. However, thunderstorm induce DS had Rainfall was reported on the day of the DS, as well as before, which is not unusual as thunderstorm-induced DS occur during the summer rainfall season.
IV. *Wind speed*: Strong winds sustained for a longer period, allowing for greater dispersion of the dust particles with prefrontal and post frontal DS. Strong wind speeds were not sustained for long during thunderstorm-induced DS, which resulted in lesser dispersion of dust particles, and therefore lesser spatial distribution.

4.10. Summary

This chapter focussed on addressing the aims and objectives of the study. The focus of this dissertation is to identify the synoptic circulation associated with significant DS events over South Africa, as well as how meteorological variables evolve before, during and after significant DS over South Africa. The first aim was addressed by analysing the weather systems associated with interior and coastal DS. The findings suggest that the weather system that triggered coastal DS was similar for all coastal DS but varied for the interior DS. The analysis of meteorological variables addressed the second aim. The analysis of the meteorological variables also indicated that evolution was is linked to the larger weather system. This was evident in the analysis of wind direction. For all the coastal DS, the direction contained an easterly component, while the wind direction differed for the interior DS. Furthermore, the spatial distribution for interior DS was determined by the spatial distribution of the weather system that triggered the DS. Synoptically induced DS had a larger spatial distribution, as compared to DS triggered by mesoscale weather systems. The season in which the DS occurred in also

influenced meteorological variables such as temperature which in turn also influenced the delts T and rainfall. Overall, the findings also indicate an interdependency between meteorological variables that influence the formation and propagation of DS.

5. Chapter 5: Summary and Conclusions

This section gives a summary and conclusion for each objective listed in Chapter 1, after which the limitations and recommendations, as well as the scientific contributions of the research, are outlined.

5.1. Introduction

Sand and DS are a meteorological hazard that can threaten human health, agriculture, aviation, ground transportation, solar energy industry, air quality, and aquatic and terrestrial ecological systems (WMO, 2019). They are common in semi-arid and arid regions, with most of the natural dust source regions located in the 'dust belt' Northern Hemisphere (extending from the west coast of North Africa, across the Middle East, Central and South Asia, to China). Outside of this Sahara dust belt, there are very few inventories of DS observations in Africa, especially in South Africa (SA), as it is not a main contributor to the global dust emissions. Previous studies (Bhattachan et al., 2012, Vickery et al., 2013) on dust source regions in South Africa indicated that the south-western part of the Kalahari Desert, a natural source region, had the highest emission frequency in South Africa. Recent studies (Bekiswa, 2019; Eckardt *et al*., 2020) have now identified major dust source regions associated with anthropogenic activities such as commercial agriculture, concentrated over the central parts of South Africa, with minor source regions identified over the Northern Cape and Mpumalanga provinces.

Each DS region or source region, whether local or global, has its own local characteristics that influence DS formation, as well as the transportation and deposition as discussed in the DS cycle. Several studies (Knippertz and Stuut, 2014, Brazel, 1989, Hyde et al., 2018) identified the weather systems (both mesoscale and synoptic scale) that produce conditions necessary for DS in regions such as North Africa, the Middle East, Europe, and south western United States. Most studies identifying the weather systems that produce conditions necessary for DS have always focussed on the Northern Hemisphere, as this is where the most significant dust source regions in the dust belt are located. Although SA is not a major contributor, it is still important to understand DS in relation to weather systems that form them in relation to the climate of South Africa.

There were two main objectives of this research. The first was to identify the synoptic circulation associated with significant DS events over South Africa. The weather systems were further divided according to those that cause DS along the coast and those that cause DS over the interior. The second objective was to identify how meteorological variables evolve before, during, and after significant DS. The meteorological variables selected were wind speed and direction, temperature, RH, dew point temperature (T_d), and rainfall in conjunction with soil moisture.

The results of the research will contribute to the limited research conducted over the Southern Hemisphere, especially over South Africa, regarding DS and meteorological parameters. Ultimately, the research will assist in accurately modelling DS and their impacts on the environment. With increased information about DS and their drivers, more accurate DS forecasting systems can be developed, the appropriate efforts to mitigate damage can be put into place and effective early warning can be communicated (UNEP Global Environmental Alert Service, 2013).

5.2. Characteristics of selected dust storm cases

This study took a case study approach and selected a total of ten DS cases to analyse, with five occurring along the coastal region and the other five taking place over the interior of the country. These DS cases were identified using a combination of satellite imagery, media, and meteorological observations. The interior DS cases were then further summarised according to the weather system that produced the DS (i.e. synoptic or mesoscale weather systems). The characteristics of the DS were discussed in terms of the source regions, spatial distribution, and the duration of each DS. The coastal DS cases selected occurred between the late winter and spring months (July to October), while the interior DS cases occurred in all seasons except for autumn. This was a key factor to note, as it impacted the behaviour of meteorological variables that were analysed. Seasonal variability influences meteorological variables such as temperature, which influences humidity and rainfall. An example of the former is that increasing temperatures, coupled with a decrease in rainfall, can result in an

increased evaporation rate. This was evident in the DS that occurred on 15 July 2020, which had a maximum temperature or less than 25 for all four stations. This was cooler than the maximum temperatures of the DS storms that occurred in spring. Winter has shorter days and receives less incoming solar radiation, which can result in lower maximum temperatures, as compared to spring and summer.

The starting point of each DS was the deciding factor in the stations that were selected to analyse the meteorological parameters. The stations selected for analysis of the coastal DS were the same as they occurred over a similar region. However, the interior DS had a number of different stations selected as they had occurred in various places over the interior.

5.3. Source regions

The coastal DS selected for this study were all confined to the west coast of the country. They were classified as natural dust sources, which are areas that are naturally dominated by loose soil, little to no vegetation, and low annual rainfall. This was in line with the previous study done by (Vickery et al., 2013). The source regions of the interior DS were mainly of anthropogenic nature, which were similar to previous studies of the interior source regions (Vickery et al., 2013, Eckardt et al., 2020b). Anthropogenic source regions are largely influences by human activities such as agriculture and farming and can be exacerbated by the changes in rainfall patterns and the occurrence of drought.

5.4. Spatial distribution

The coastal DS had a similar spatial distribution along the west coast of South Africa. A notable difference is the spatial distribution of the DS that had the shortest lifespan was smaller as compared to the other DS. The DS with the shorter lifespan was blown just off the coast, whereas the other DS were blown further into the ocean. There was more variation in terms of the prevailing weather systems when it came to interior DS cases, which contributed to the significant difference in spatial distribution. The spatial distribution of thunderstorm-induced interior DS was more challenging to determine, as they were hidden under clouds. Even with this challenge, the distribution was still smaller than the distribution of synoptically induced DS. This can be linked to the size of the weather system that caused the DS. In summary, the spatial distribution of thunderstorm-induced DS was smaller than the spatial distribution of DS caused by synoptic-scale weather systems (e.g. cold fronts).

5.5. Overview of dust-producing weather systems

Coastal DS were produced by the same weather system over the same area. It was a combination of a surface trough over the western interior or along the west coast, with a high pressure

situated south, south east, or over the interior of the country. The strength of the high appears to be a key factor contributing to the duration of the DS. The stronger the high-pressure system, the greater the gradient along the west, therefore creating stronger offshore winds.

The DS originating from mesoscale weather systems had thunderstorms with a gust front that triggered the DS, even though there were synoptic weather systems at play. The DS resulting from synoptic scale weather systems were associated with cold fronts, being both prefrontal (ahead of the cold front) and postfrontal (after the cold front) DS. These findings are in line with previous studies (Goliger and Retief, 2002, Kruger et al., 2010) which identified weather systems that can produce strong winds over South Africa. In this study, weather systems identified to have produced the DS selected for analysis were as follows:

I. The combination of a surface trough extending over the west coast and a high-pressure system associated over the interior (coastal DS)
II. Cold fronts (prefrontal and post-frontal), often associated with upper troughs in winter (interior DS)
III. Cut-off low, producing thunderstorm activity that generated strong winds in spring (interior DS).
IV. Gust fronts that are generated by outflow from convective activity, mainly in summer (interior DS)

5.6. Meteorological variables

Meteorological variables play an important role in the occurrence of DS. There were a number of factors to take into consideration when looking at how the meteorological variables evolved as a DS occurs such as the weather system that caused the DS (whether it is a synoptic-scale or mesoscale weather system, the duration, and strength of the weather system associated with the DS), the season in which the DS occurred, as well as the location or source region of the DS.

5.6.1.Interior DS

The interior DS produced by mesoscale systems occurred in mid-summer (i.e. December and January), over summer rainfall areas, while the DS produced by synoptic-scale weather systems occurred in winter and early spring. This is where the season in which the DS occurred is crucial to consider. According to the literature, higher temperatures with little to no rainfall result in higher evaporation rates and lower soil moisture. However, not all DS with higher temperatures (over 30˚ C) resulted in lower soil moisture values. The DS cases induced by thunderstorm activity occurred in summer and were characterized by high temperatures. However, soil moisture was also higher than

the other DS cases since the DS occurred in an area that is a summer rainfall region, with rainfall also reported days before the DS occurred. DS from synoptic scale weather systems occurred in winter, which is a season characterized by cooler temperatures and little rainfall. Although temperatures were cooler (not higher than 27˚ C), soil moisture was lower. This can be due to the season in which they occurred. Winter is generally characterized by little rainfall over the interior of the country, which can result in lower soil moisture due to little rainfall. So, the question to consider is the importance of higher temperatures to the occurrence of DS in general.

The moisture indicators, RH and T_d, were also affected by the season in which the DS occurred. DS are associated with drier atmospheric conditions, which are depicted by low RH and T_d. This was observed with synoptic scale-induced DS, where the RH and T_d gradually decreased, being the lowest on the day of the DS. However, the opposite was observed for mesoscale-induced DS. The presence of thunderstorms associated with the mesoscale-induced DS meant that there was enough moisture in the atmosphere for their development, indicated by higher T_d and RH values. This may also mean that the general threshold for RH (40%) may not be a good indicator for DS induced by mesoscale weather systems.

The strongest wind speeds, which were also sustained for a long period, were observed with synoptic scale induced DS. This is in line with the duration of the DS, where the DS induced by synoptic scale weather systems lasted the longest. The exception was the DS associated with the cut-off low but induced by thunderstorm activity. Although the thunderstorms dissipated, the dust particles were transported further as the cut-off low moved eastwards, eventually exiting the country. Therefore, how well-developed an upper air system (such as a cut-off low) is, was found to be important to the dispersion of dust particles, even if the initial trigger of the DS is long dissipated.

5.6.2.Coastal DS

The coastal DS selected were mainly in winter and spring, which, similar to the interior DS, will have an impact on the meteorological variables. The DS that occurred in spring had higher temperatures as compared to the DS that occurred in winter. The coastal DS with the shortest life span was the only case of the reported rainfall before the day of the DS, possibly contributing to the higher soil moisture average as compared to the other DS cases. It also had the weakest high-pressure system, which in turn resulted in weaker winds and weaker gusts. The conclusion from this is that, though the strength of the high-pressure system is important as it is a determining factor of the strength of the winds, the season in which the DS occurs should be considered as this affects the behaviour of meteorological variables.

The meteorological variables evolved as would be expected. RH and T_d decreased gradually leading up to the day of the DS event, being the lowest on the day of the DS. The temperature gradually increased, being the highest on the day of the DS. The ΔT was also lower the following day for most of the DS cases, possibly indicating how the presence of dust particles affects the temperature. More than just the season, the location of the stations selected for analysis impacted the meteorological variables, resulting in differing results when compared to the interior stations. This was most evident with the RH and T_d, which were generally higher for the stations along the coast as compared to the interior stations.

Both wind direction and wind speed are important to the occurrence of DS. Coastal DS all had an easterly component to the wind direction, which is caused by the location of the weather systems that caused the DS. The DS that lasted the longest, did not have the lowest RH, T_d, or temperature, but had the strongest wind gusts and strongest high-pressure system.

5.7. Limitations in the study

There were several limitations in conducting this study. Not all the limitations were evident at the start of the research but became evident later. The limitations are as follows:

I. Sample size: The sample size is not a representative sample of all DS that occurred in South Africa. This is due to a lack of an official database that records DS cases that occurred over SA, as they are not common occurrences.

II. Data availability: There is a lack of observations regarding DS in South Africa. This can hinder certain factors of the research, such as identifying the exact start time of the DS, and the exact spatial distribution of the DS, which had to be based on calculated estimations. The lack of data availability also made it difficult to classify DS in line with the WMO as well as other studies (Abdullaev and Sokolik, 2019, Ardon-Dryer et al., 2023), who classify DS according to visibility (see section 1.2.)

III. Causation vs Correlation: It is clear that there is a relationship between meteorological variables and the occurrence of DS. However, it is not always clear which variables were the most important in causing the DS as the variables themselves are also interdependent. Not all meteorological variables were considered in this study, which may also influence the occurrence of DS.

5.8. Key questions and recommendations to consider in future work

The results of this study can be considered as a base study on the topic of meteorology and DS over South Africa that can be expanded on. Some key questions to consider in future work are:

I. What are the key variables to consider when forecasting DS, especially considering the climate of South Africa?
II. Considering that DS in South Africa are not confined to one season, does the importance of specific meteorological variables change with the season?
III. The primary weather systems have been identified. However, not all of these weather systems produce DS. So, what are the key differences in the dynamics of weather systems that produce DS and those that do not, as well as those that cause large-scale dispersion of dust particles and those that do not?
IV. Several studies focus on humidity as an indicator of how dry or moist the atmosphere is in relation to DS. Should the focus be more on T_d or even T_d depression as a more accurate indicator of how dry or moist the atmosphere is in relation to DS?
V. Is there a difference in the dust mass concentration/aerosol concentration between synoptically induced DS and mesoscale-induced DS? This could be a key contribution to health studies related to DS.
VI. Anthropogenic dust source regions were identified and aggravated during the 2015/2016 drought season. Does the recovery from the drought season and the onset of wet season impact the permanence of the anthropogenic source regions? Are anthropogenic sources seasonal?

In line with the findings of the study, these are the recommendations for further research:

I. Building on this study, a possible decision tree for forecasting DS can be created that is focussing on South Africa. Previous studies have included parameters such as RH, temperature, and windspeed (Desouza et al., 2014). However, T_d can also be a key parameter to include in a decision tree for forecasting DS. The previously identified thresholds for parameters such as RH may not be applicable to the South African climate, especially in the summer seasons when DS are often caused by thunderstorm activity, or even winter, where DS occur in cooler temperatures.
II. Research indicates that the severity of thunderstorms can be linked to DS. With such a common occurrence of severe thunderstorms over South Africa, investigating if there is a possible increased DS occurrence may lead to a further increase in severe thunderstorm occurrence.

Overall, the findings in this research have shed light on the weather systems that are responsible for DS over the interior and along the west coast of South Africa. By identifying the synoptic weather

patterns that cause DS over South Africa, further research can be done on the specific atmospheric conditions that lead to the formation of dust storms. This knowledge is important for the modelling of dust storms. The meteorological variables were analysed from the initial start of the DS. The correct meteorological conditions at the initialization of DS are extremely important for the most accurate and reliable simulations of dust storms.

ReferencesReferences

ABDULLAEV, S. & SOKOLIK, I. 2019. Main Characteristics of Dust Storm sand Their Radiative Impacts: With a Focuson Tajikistan. *Journal of Atmospheric Science Research,* 2.

AHRENS, C. D. & HENSON, R. 2019. *Meteorology today : an introduction to weather, climate, and the environment,* Boston, MA, Cengage Boston, MA.

AILI, A., KIM OANH, N. T. & ABUDUWAILI, J. 2016. Variation Trends of Dust Storms in Relation to Meteorological Conditions and Anthropogenic Impacts in the Northeast Edge of the Taklimakan Desert, China. *Open Journal of Air Pollution,* 05**,** 127-143.

ANDREAE, M. O. & ROSENFELD, D. 2008. Aerosol–cloud–precipitation interactions. Part 1. The nature and sources of cloud-active aerosols. *Earth-Science Reviews,* 89**,** 13-41.

ARDON-DRYER, K., GILL, T. E. & TONG, D. Q. 2023. When a Dust Storm Is Not a Dust Storm: Reliability of Dust Records From the Storm Events Database and Implications for Geohealth Applications. *Geohealth,* 7**,** e2022GH000699.

BEKISWA, S. O. 2019. *Characterising South Africa's major dust sources.* Master's, University of Cape Town.

BHATTACHAN, A., D'ODORICO, P., BADDOCK, M. C., ZOBECK, T. M., OKIN, G. S. & CASSAR, N. 2012. The Southern Kalahari: a potential new dust source in the Southern Hemisphere? *Environmental Research Letters,* 7**,** 024001.

BOTAI, C. M., BOTAI, J. O., DLAMINI, L. C., ZWANE, N. S. & PHADULI, E. 2016. Characteristics of Droughts in South Africa: A Case Study of Free State and North West Provinces. *Water* [Online], 8.

BRAZEL, A. J. 1989. Dust and Climate in the American Southwest. *In:* LEINEN, M. & SARNTHEIN, M. (eds.) *Paleoclimatology and Paleometeorology: Modern and Past Patterns of Global Atmospheric Transport.* Dordrecht: Springer Netherlands.

BRYANT, R., BIGG, G., MAHOWALD, N., ECKARDT, F. & ROSS, S. 2007. Dust emission response to climate in southern Africa. *Journal of Geophysical Research,* 112.

CATTO, J. L. 2016. Extratropical cyclone classification and its use in climate studies. *Reviews of Geophysics,* 54**,** 486-520.

CHAKRAVARTY, K., VINCENT, V., VELLORE, R., SRIVASTAVA, A. K., RASTOGI, A. & SONI, V. K. 2021. Revisiting Andhi in northern India: A case study of severe dust-storm over the urban megacity of New Delhi. *Urban Climate,* 37.

CHEN, S., JIANG, N., HUANG, J., XU, X., ZHANG, H., ZANG, Z., HUANG, K., XU, X., WEI, Y., GUAN, X., ZHANG, X., LUO, Y., HU, Z. & FENG, T. 2018. Quantifying contributions of natural and anthropogenic dust emission from different climatic regions. *Atmospheric Environment,* 191**,** 94-104.

CHEN, S., JIANG, N., HUANG, J., ZANG, Z., GUAN, X., MA, X., LUO, Y., LI, J., ZHANG, X. & ZHANG, Y. 2019. Estimations of indirect and direct anthropogenic dust emission at the global scale. *Atmospheric Environment,* 200**,** 50-60.

COMET, C. P. F. O. M., EDUCATION AND TRAINING. 2012. *Atmospheric Dust course* [Online]. Available: https://www.meted.ucar.edu/EUMETSAT/at_dust/index.htm [Accessed 25 June 2020].

CSAVINA, J., FIELD, J., FÉLIX, O., CORRAL-AVITIA, A. Y., SÁEZ, A. E. & BETTERTON, E. A. 2014. Effect of wind speed and relative humidity on atmospheric dust concentrations in semi-arid climates.

DE ORO, L. A. & BUSCHIAZZO, D. E. 2009. Threshold wind velocity as an index of soil susceptibility to wind erosion under variable climatic conditions. *Land Degradation & Development,* 20**,** 14-21.

DESOUZA, N., KURCHANIA, R. & QURESHI, M. 2014. Use of Decision Theory to Predict Dust Storms over New Delhi, India. *Natural Science,* 06**,** 574-582.

DESOUZA, N., SIMON, B. & QURESHI, M. 2011. Evolutionary characteristics of a dust storm over Oman on 2 February 2008. *Meteorology and Atmospheric Physics,* 114.

ECKARDT, F. D., BEKISWA, S., VON HOLDT, J. R., JACK, C., KUHN, N. J., MOGANE, F., MURRAY, J. E., NDARA, N. & PALMER, A. R. 2020a. South Africa's agricultural dust sources and events from MSG SEVIRI. *Aeolian Research,* 47**,** 100637.

ECKARDT, F. D., BEKISWA, S., VON HOLDT, J. R., JACK, C., KUHN, N. J., MOGANE, F., MURRAY, J. E., NDARA, N. & PALMER, A. R. 2020b. South Africa's agricultural dust sources and events from MSG SEVIRI. *Aeolian Research,* 47.

ELEMO, E., OGOBOR, E., AYANTUNJI, B., MANGETE, O., ÀLÀGBÉ, G., ABDULKAREEM, M., OBAROLO, A. & ONUH, B. 2021. Relationship between Relative Humidity and the Dew Point Temperature in Abuja, Nigeria. *OALib,* 08**,** 1-13.

EUMETRAIN. 2021. *South African Cold fronts* [Online]. https://resources.eumetrain.org/satmanu/CM4SH/SACF/print.htm: Eumetsat. Available: https://resources.eumetrain.org/satmanu/CM4SH/SACF/print.htm [Accessed 22 November 2022].

EUMETRAIN. n.d. *SEVIRI Dust RGB Quick Guide* [Online]. https://www-cdn.eumetsat.int/files/2020-04/pdf_rgb_quick_guide_dust.pdf: Eumetsat. Available: https://www-cdn.eumetsat.int/files/2020-04/pdf_rgb_quick_guide_dust.pdf [Accessed 16 September 2022].

FRANCIS, D., FONSECA, R., NELLI, N., CUESTA, J., WESTON, M., EVAN, A. & TEMIMI, M. 2020. The Atmospheric Drivers of the Major Saharan Dust Storm in June 2020. *Geophysical Research Letters,* 47.

GCIS 2021. *South Africa yearbook : 2020/21*, Government Communication And Information System.

GHALIB, W. A. M., MANSOOR, A. M. & PONNAPPA, S. C. 2021. Environmental Factors that Influence the Geography of Yemen Leading to Dust and Sand Storms - A Case Study. *Journal of Environmental Geography,* 14**,** 24-37.

GHERBOUDJ, I., NASEEMA BEEGUM, S. & GHEDIRA, H. 2017. Identifying natural dust source regions over the Middle-East and North-Africa: Estimation of dust emission potential. *Earth-Science Reviews,* 165**,** 342-355.

GINOUX, P., PROSPERO, J. M., GILL, T. E., HSU, N. C. & ZHAO, M. 2012. Global-scale attribution of anthropogenic and natural dust sources and their emission rates based on MODIS Deep Blue aerosol products. *Reviews of Geophysics,* 50.

GOLIGER, A. M. & RETIEF, R. V. 2002. Identification of zones of strong wind events in South Africa.

GOUDIE, A. & MIDDLETON, N. 2006. *Desert dust in the global system,* Berlin, Springer Berlin, Heidelberg.

HELMERT, J., HEINOLD, B., TEGEN, I., HELLMUTH, O. & WENDISCH, M. 2007. On the direct and semidirect effects of Saharan dust over Europe: A modeling study. *Journal of Geophysical Research: Atmospheres,* 112.

HUANG, J., WANG, T., WANG, W., LI, Z. & YAN, H. 2014. Climate effects of dust aerosols over East Asian arid and semiarid regions. *Journal of Geophysical Research: Atmospheres,* 119.

HYDE, P., MAHALOV, A. & LI, J. 2018. Simulating the meteorology and PM(10) concentrations in Arizona dust storms using the Weather Research and Forecasting model with Chemistry (Wrf-Chem).

KHAIN, A. & POKROVSKY, A. 2004. Simulation of Effects of Atmospheric Aerosols on Deep Turbulent Convective Clouds Using a Spectral Microphysics Mixed-Phase Cumulus Cloud Model. Part II: Sensitivity Study. *Journal of The Atmospheric Sciences - J ATMOS SCI,* 61**,** 2983-3001.

KIM, H. & CHOI, M. 2015. Impact of soil moisture on dust outbreaks in East Asia: Using satellite and assimilation data. *Geophysical Research Letters,* 42**,** 2789-2796.

KNIPPERTZ, P. & STUUT, P. W. 2014. *Mineral Dust-A Key Player in the Earth System*, Springer Dordrecht.

KRUGER, A. C., GOLIGER, A. M., RETIEF, J. V. & SEKELE, S. 2010. Strong wind climatic zones in South Africa. *Wind and Structures An International Journal,* 13**,** 37-55.

KRUGER, A. C., VAN STADEN, M. & PILLAY, D. L. 2016. Indicative hazard profile for strong winds in South Africa. *South African Journal of Science,* Volume 112.

LANDMAN, W., MALHERBE, J. & ENGELBRECHT, F. 2017. South Africa's present-day climate.

LEI, H. & WANG, J. X. L. 2014. Observed characteristics of dust storm events over the western United States using meteorological, satellite, and air quality measurements. *Atmospheric Chemistry and Physics,* 14**,** 7847-7857.

LI, J., CHEN, H., LI, Z., WANG, P., CRIBB, M. & FAN, X. 2015. Low-level temperature inversions and their effect on aerosol condensation nuclei concentrations under different large-scale synoptic circulations. *Advances in Atmospheric Sciences,* 32**,** 898-908.

LI, J., OKIN, G. S., HERRICK, J. E., BELNAP, J., MUNSON, S. M. & MILLER, M. E. 2010. A simple method to estimate threshold friction velocity of wind erosion in the field. *Geophysical Research Letters,* 37**,** n/a-n/a.

LI, Z., CRIBB, M., CHANG, F. L., TRISHCHENKO, A. & LUO, Y. 2005. Natural variability and sampling errors in solar radiation measurements for model validation over the Atmospheric Radiation Measurement Southern Great Plains region. *J. Geophys. Res.,* 110.

LI, Z., GUO, J., DING, A., LIAO, H., LIU, J., SUN, Y., WANG, T., XUE, H., ZHANG, H. & ZHU, B. 2017. Aerosol and boundary-layer interactions and impact on air quality. *National Science Review,* 4**,** 810-833.

MA, X., GAO, Q., JIANG, X., CHEN, S., GAN, Y., ZHANG, T., LU, X. & WANG, X. 2023. Direct Effects of Air Humidity on Dust Aerosol Production: Evidences for the Surprising Role of Electrostatic Forces. *Geophysical Research Letters,* 50**,** e2023GL103639.

MAGHRABI, A. 2017. The influence of dust storms on solar radiation data, aerosol properties and meteorological variables in Central Arabian Peninsula. *International Journal of Environmental Science and Technology,* 14**,** 1643-1650.

MAGHRABI, A. H. 2011. The Impact of the March 10, 2009 Dust Storm on Meteorological Parameters in Central Saudi Arabia. *Proceedings of the World Renewable Energy Congress – Sweden, 8–13 May, 2011, Linköping, Sweden.*

MAGHRABI, A. H. & AL-DOSARI, A. F. 2016. Effects on surface meteorological parameters and radiation levels of a heavy dust storm occurred in Central Arabian Peninsula. *Atmospheric Research,* 182**,** 30-35.

MCKENNA NEUMAN, C. 2003. Effects of Temperature and Humidity upon the Entrainment of Sedimentary Particles by Wind. *Boundary-Layer Meteorology,* 108**,** 61-89.

MCKENNA NEUMAN, C. & SANDERSON, S. 2008. Humidity control of particle emissions in aeolian systems. *Journal of Geophysical Research,* 113.

MCTAINSH, G. H. & PITBLADO, J. R. 1987. Dust storms and related phenomena measured from meteorological records in Australia. *Earth Surface Processes and Landforms,* 12**,** 415-424.

MIDDLETON, N. & KANG, U. 2017. Sand and Dust Storms: Impact Mitigation. *Sustainability,* 9**,** 1053.

MILLER, D., GRASSO, L., BIAN, Q., KREIDENWEIS, S., DOSTALEK, J., SOLBRIG, J., BUKOWSKI, J., VAN DEN HEEVER, S., WANG, Y., XU, X., WANG, J., WALKER, W., WU, T., ZUPANSKI, M., CHIU, C. & REID, R. 2019. A Tale of Two Dust Storms: Analysis of a Complex Dust Event in the Middle East. *Atmospheric Measurement Techniques* 5101-5118.

MUOFHE, T. P., CHIKOORE, H., BOPAPE, M.-J. M., NETHENGWE, N. S., NDARANA, T. & RAMBUWANI, G. T. 2020. Forecasting Intense Cut-Off Lows in South Africa Using the 4.4 km Unified Model. *Climate,* 8.

NAMDARI, S., KARIMI, N., SOROOSHIAN, A., MOHAMMADI, G. & SEHATKASHANI, S. 2018. Impacts of climate and synoptic fluctuations on dust storm activity over the Middle East. *Atmospheric Environment,* 173**,** 265-276.

NAZAROV, B. I., ABDULLAEV, S. F. & MASLOV, V. A. 2010. Studies of temperature effects of dust storms. *Izvestiya, Atmospheric and Oceanic Physics,* 46**,** 475-481.

NIDIS, N. I. D. I. S. n.d. *Soil Moisture* [Online]. Available: https://www.drought.gov/topics/soil-moisture#:~:text=As%20defined%20by%20the%20AMS,the%20pores%20of%20the%20soil [Accessed 16 September 2020].

NOVLAN, D., HARDIMAN, M. & GILL, T. 2007. *A synoptic climatology of blowing dust events in El Paso, Texas from 1932-2005*.

PETROPOULOS, G. 2013. *Remote Sensing of Energy Fluxes and Soil Moisture Content*.

PU, B., GINOUX, P., GUO, H., HSU, N. C., KIMBALL, J., MARTICORENA, B., MALYSHEV, S., NAIK, V., O'NEILL, N. T., PÉREZ GARCÍA-PANDO, C., PAIREAU, J., PROSPERO, J. M., SHEVLIAKOVA, E. & ZHAO, M. 2020. Retrieving the global distribution of the threshold of wind erosion from satellite data and implementing it into the Geophysical Fluid Dynamics Laboratory land–atmosphere model (GFDL AM4.0/LM4.0). *Atmospheric Chemistry and Physics,* 20**,** 55-81.

RAVI, S. & D'ODORICO, P. 2005. A field-scale analysis of the dependence of wind erosion threshold velocity on air humidity. *Geophysical Research Letters,* 32.

RAVI, S., D'ODORICO, P., OVER, T. M. & ZOBECK, T. M. 2004. On the effect of air humidity on soil susceptibility to wind erosion: The case of air-dry soils. *Geophysical Research Letters,* 31**,** n/a-n/a.

RAVI, S., ZOBECK, T. M., OVER, T. M., OKIN, G. S. & D'ODORICO, P. 2006. On the effect of moisture bonding forces in air-dry soils on threshold friction velocity of wind erosion. *Sedimentology,* 53**,** 597-609.

ROMANO, F., RICCIARDELLI, E., CIMINI, D., DI PAOLA, F. & VIGGIANO, M. 2013. Dust Detection and Optical Depth Retrieval Using MSG-SEVIRI Data. *Atmosphere,* 4**,** 35-47.

SELAH, A. & FRYREAR, D. W. 1995. THRESHOLD WIND VELOCITIES OF WET SOILS AS AFFECTED BY WIND BLOWN SAND. *Soil Science,* 160**,** 304-309.

SHAO, Y. 2008. Physics and Modelling Wind Erosion.

SHAO, Y., WYRWOLL, K.-H., CHAPPELL, A., HUANG, J., LIN, Z., MCTAINSH, G., MIKAMI, M., TANAKA, T., WANG, X. & YOON, S. 2011a. Dust cycle: An emerging core theme in Earth system science. *Aeolian Research,* 2**,** 181-204.

SHAO, Y., WYRWOLL, K.-H., CHAPPELL, A., HUANG, J., LIN, Z., MCTAINSH, G. H., MIKAMI, M., TANAKA, T. Y., WANG, X. & YOON, S. 2011b. Dust cycle: An emerging core theme in Earth system science. *Aeolian Research,* 2**,** 181-204.

SIMPSON, L.-A. & DYSON, L. L. 2018. Severe weather over the Highveld of South Africa during November 2016. *Water SA,* 44**,** 75-85.

TYSON, P. D. & PRESTON-WHYTE, R. A. 2000. *The Weather and Climate of Southern Africa,* South africa Oxford University Press.

UNEP 2013. Forecasting and Early Warning of Dust Storms: UNEP Global Environmental Alert Service. United Nations Environment Programme.

UNEP, WMO & UNCCD 2016. Global assessment of sand and dust storms. *In:* SHEPHERD, G. (ed.). Nairobi: United Nations Environment Programme.

VICKERY, K. J., ECKARDT, F. D. & BRYANT, R. G. 2013. A sub-basin scale dust plume source frequency inventory for southern Africa, 2005–2008. *Geophysical Research Letters,* 40**,** 5274-5279.

WANG, Z.-T. 2006. Influence of moisture on the entrainment of sand by wind. *Powder Technology,* 164**,** 89-93.

WMO, W. M. O. 2022. Aerodrome Reports and Forecasts: A Users' Handbook to the Codes. Geneva.

XULU, N. G., CHIKOORE, H., BOPAPE, M.-J. M., NDARANA, T., MUOFHE, T. P., MBOKODO, I. L., MUNYAI, R. B., SINGO, M. V., MOHOMI, T., MBATHA, S. M. S. & MDOKA, M. L. 2023. Cut-Off Lows over South Africa: A Review. *Climate* [Online], 11.

YANG, X., ZHOU, C., HUO, W., YANG, F., LIU, X. & MAMTIMIN, A. 2019. A study on the effects of soil moisture, air humidity, and air temperature on wind speed threshold for dust emissions in the Taklimakan Desert. *Natural Hazards,* 97**,** 1069-1081.

ZHANG, Y., LIU, J., XU, X., TIAN, Y., LI, Y. & GAO, Q. 2010. The response of soil moisture content to rainfall events in semi-arid area of Inner Mongolia. *Procedia Environmental Sciences,* 2**,** 1970-1978.

APPENDIX 1: 28 December 2018 Dust storm from 1730Z to 2000Z, with METARS where available

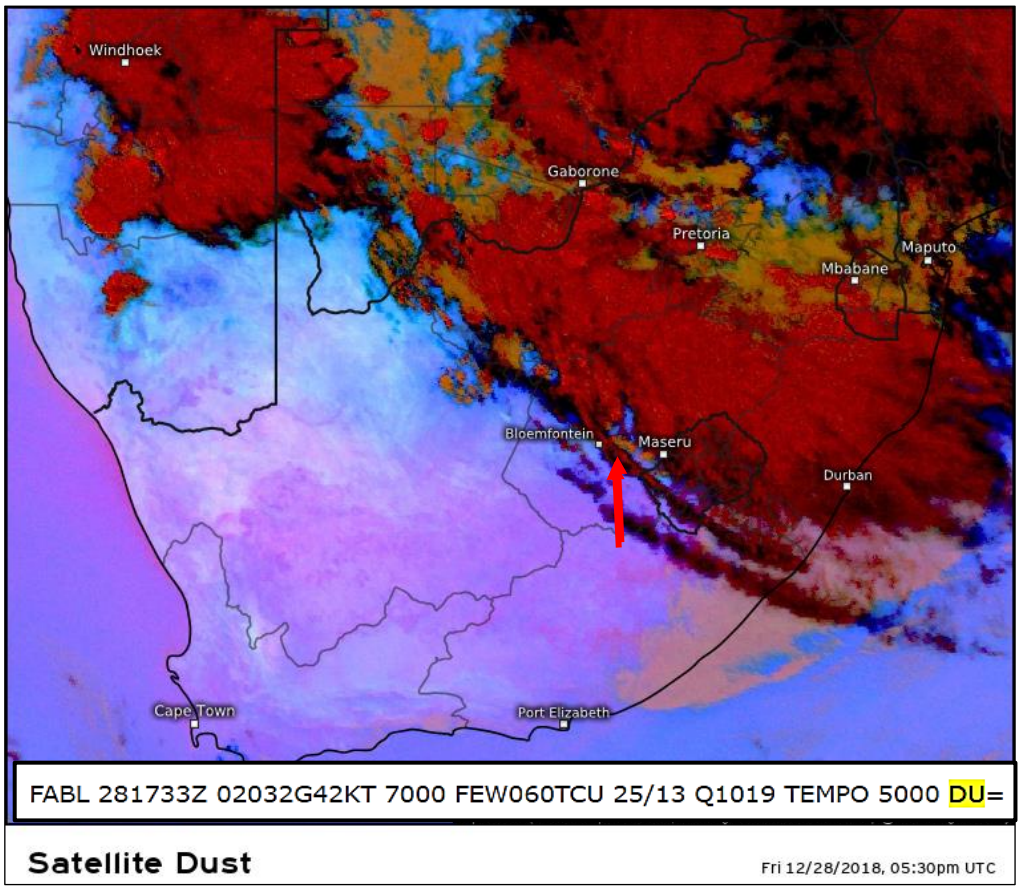

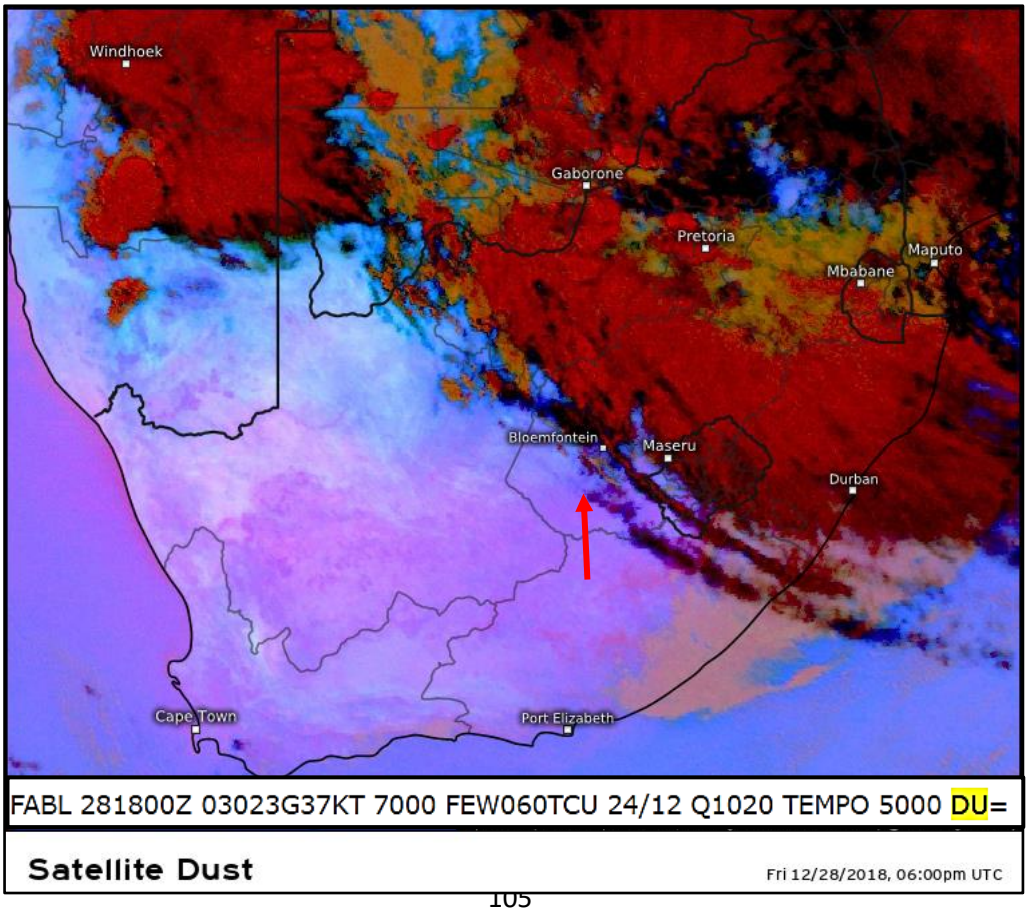

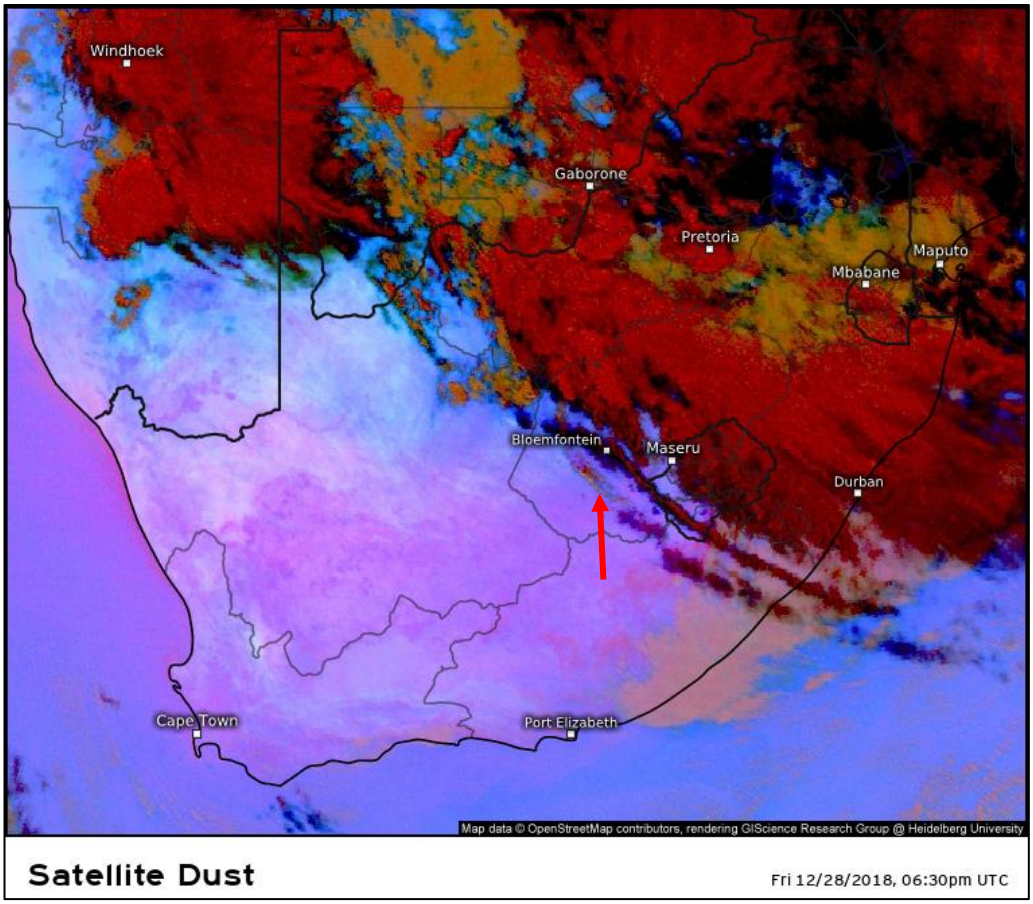
Windhoek
Gaborone
Pretoria
Maputo
Mbabane
Bloemfontein
Maseru
Durban
Cape Town
Port Elizabeth
Map data © OpenStreetMap contributors, rendering GIScience Research Group @ Heidelberg University
Satellite Dust
Fri 12/28/2018, 06:30pm UTC

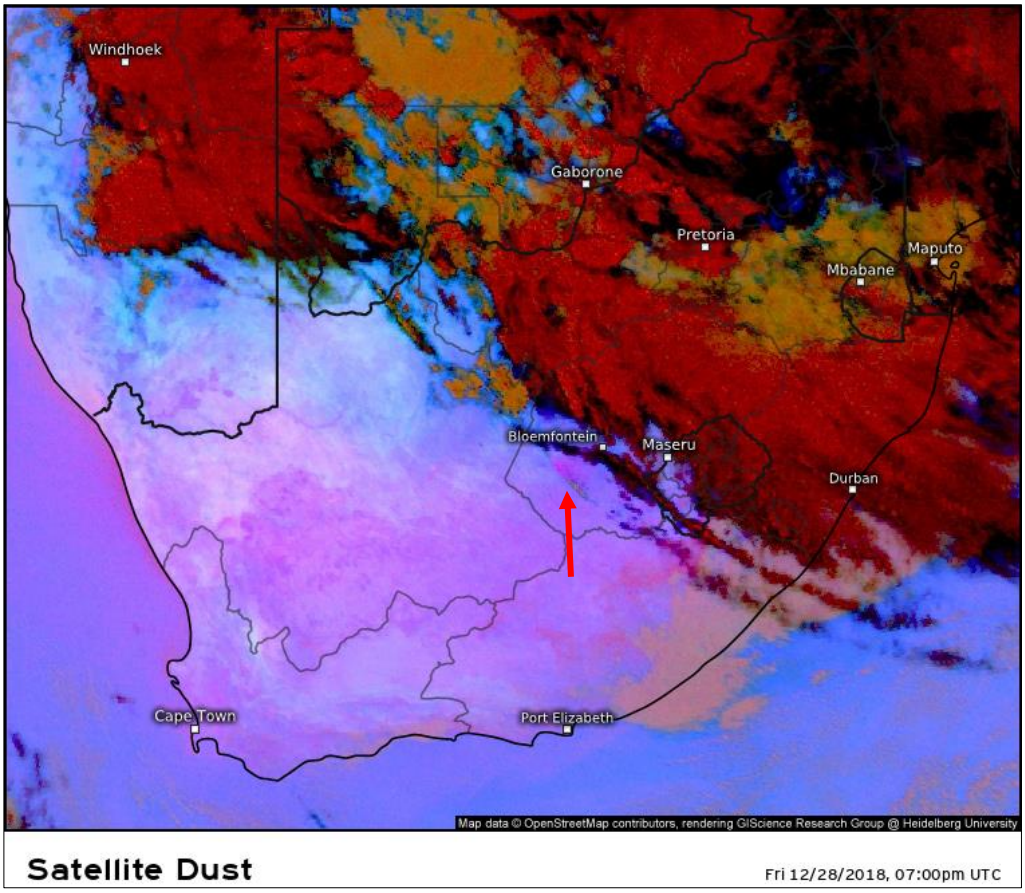
Windhoek
Gaborone
Pretoria
Maputo
Mbabane
Bloemfontein
Maseru
Durban
Cape Town
Port Elizabeth
Map data © OpenStreetMap contributors, rendering GIScience Research Group @ Heidelberg University
Satellite Dust
Fri 12/28/2018, 07:00pm UTC

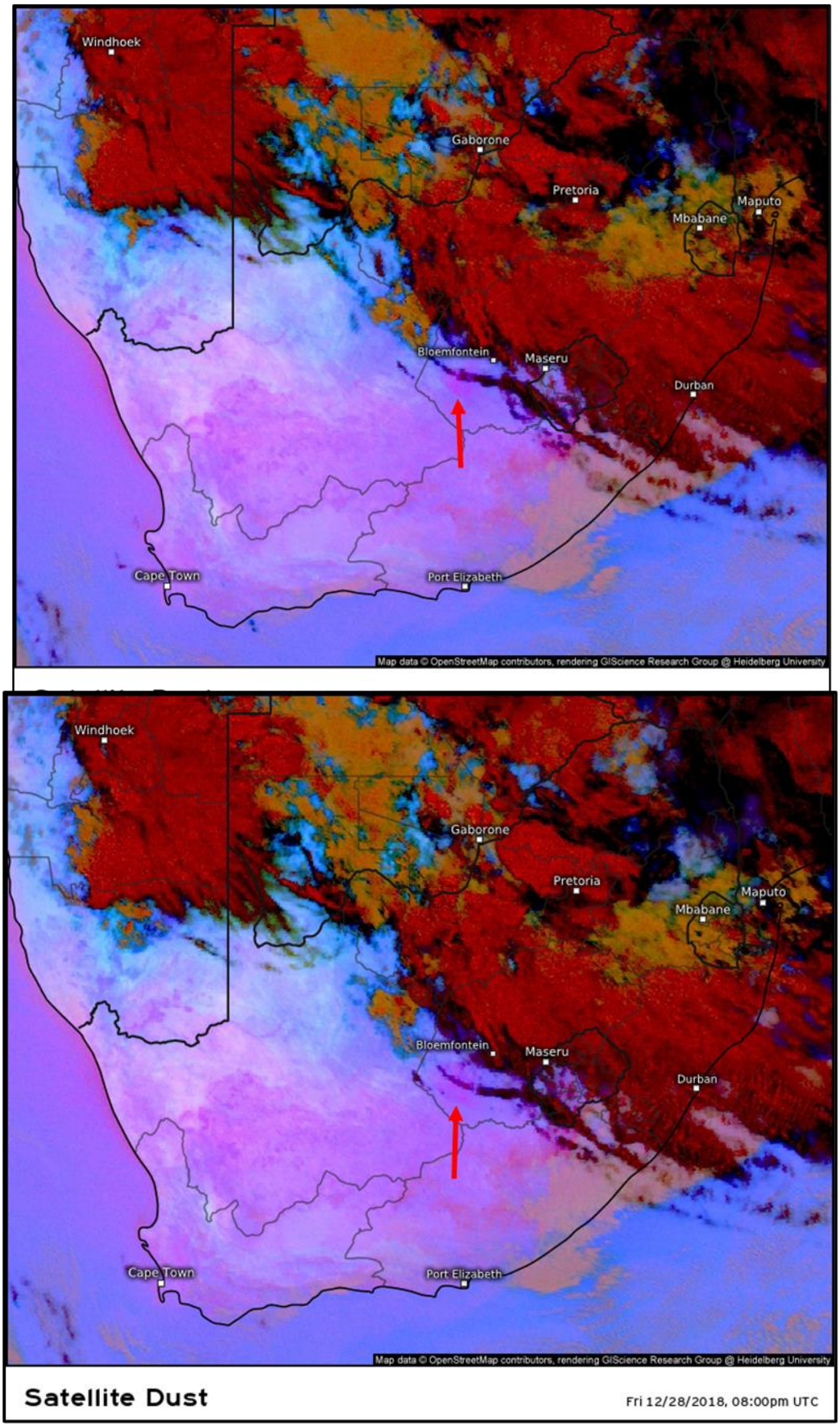
Windhoek
Gaborone
Pretoria
Maputo
Mbabane
Bloemfontein
Maseru
Durban
Cape Town
Port Elizabeth
Map data © OpenStreetMap contributors, rendering GIScience Research Group @ Heidelberg University
Windhoek
Gaborone
Pretoria
Maputo
Mbabane
Bloemfontein
Maseru
Durban
Cape Town
Port Elizabeth
Map data © OpenStreetMap contributors, rendering GIScience Research Group @ Heidelberg University
Satellite Dust
Fri 12/28/2018, 08:00pm UTC

APPENDIX 2: Dust RGB Satellite image of 16 October 2014 Dust Storm from 1030Z to 1300Z

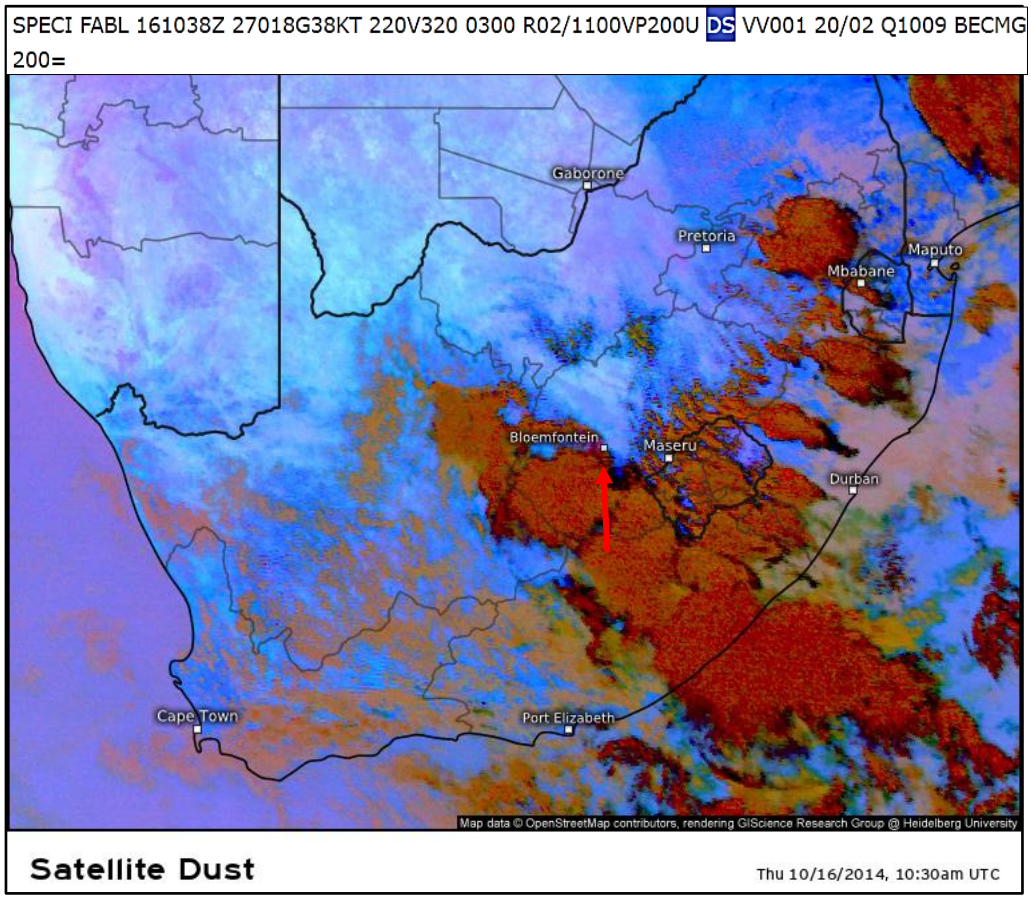

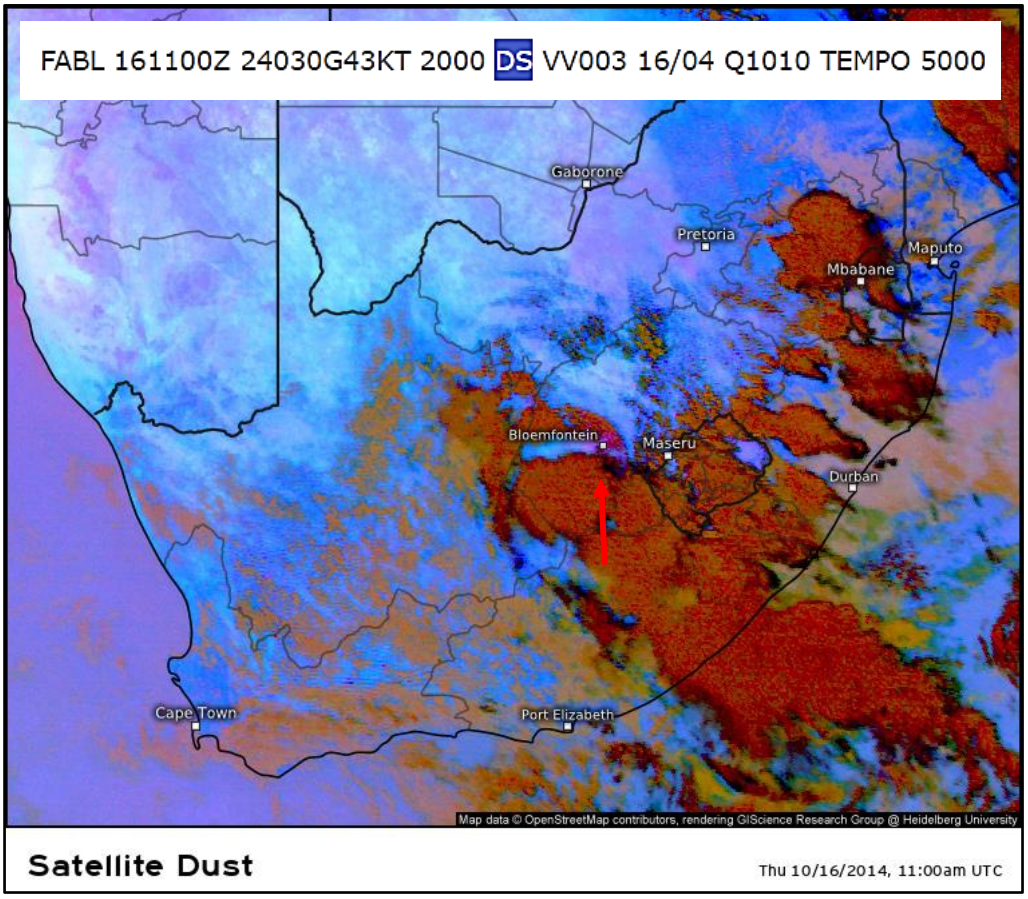
FABL 161100Z 24030G43KT 2000 DS VV003 16/04 Q1010 TEMPO 5000
Gaborone
Pretoria
Maputo
Mbabane
Bloemfontein
Maseru
Durban
Cape Town
Port Elizabeth
Map data © OpenStreetMap contributors, rendering GIScience Research Group @ Heidelberg University
Satellite Dust
Thu 10/16/2014, 11:00am UTC

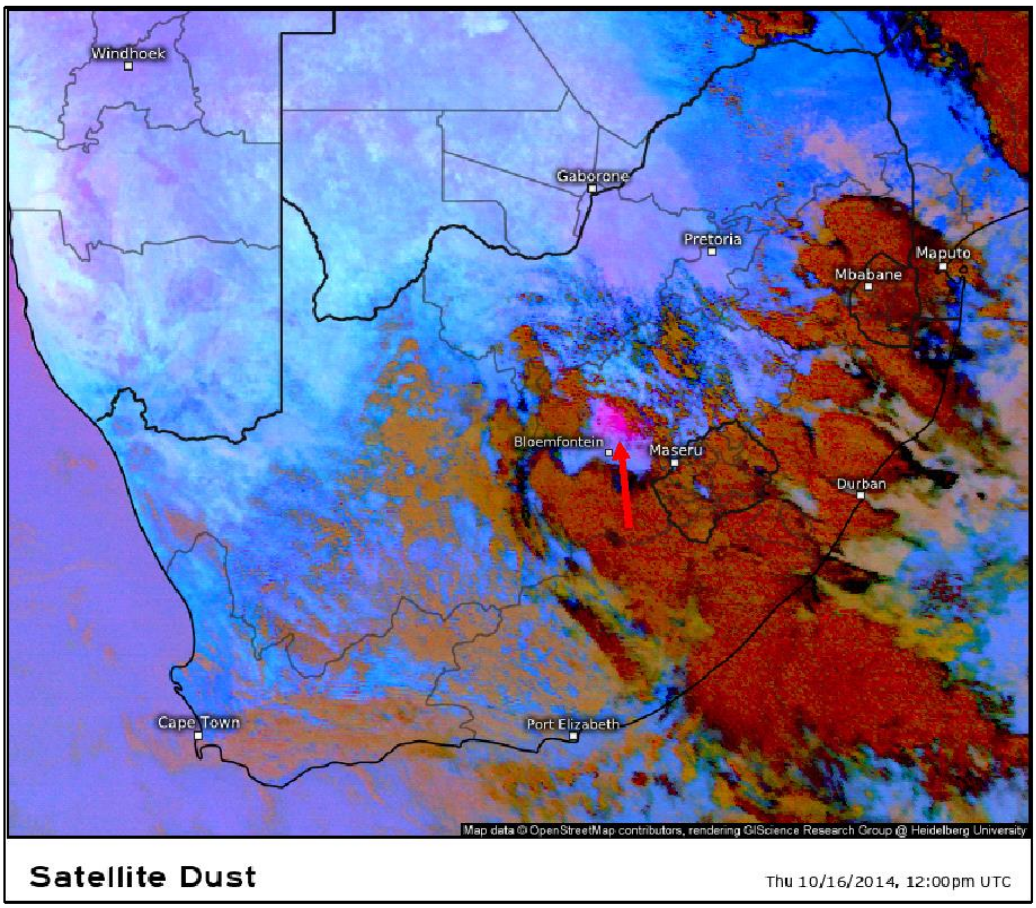
Windhoek
Gaborone
Pretoria
Maputo
Mbabane
Bloemfontein
Maseru
Durban
Cape Town
Port Elizabeth
Map data © OpenStreetMap contributors, rendering GIScience Research Group @ Heidelberg University
Satellite Dust
Thu 10/16/2014, 12:00pm UTC

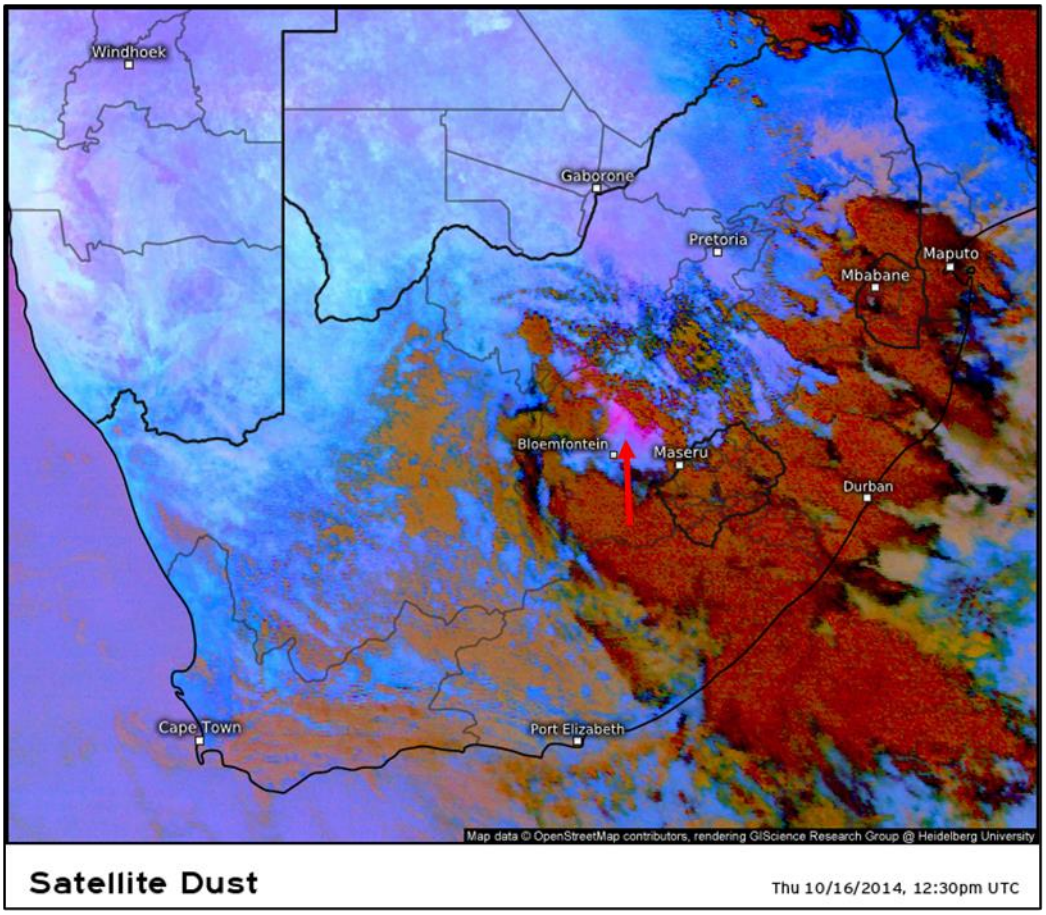
Windhoek
Gaborone
Pretoria
Maputo
Mbabane
Bloemfontein
Maseru
Durban
Cape Town
Port Elizabeth
Map data © OpenStreetMap contributors, rendering GIScience Research Group @ Heidelberg University
Satellite Dust
Thu 10/16/2014, 12:30pm UTC

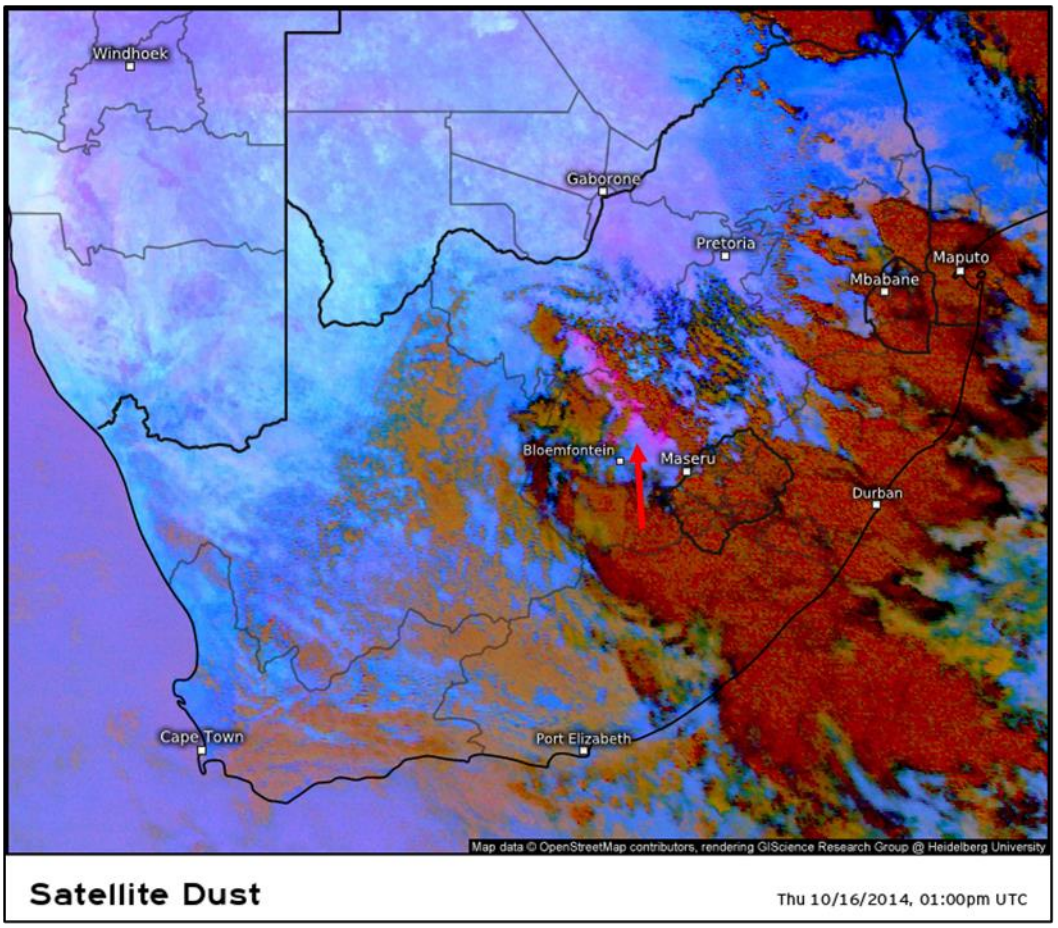
Windhoek
Gaborone
Pretoria
Maputo
Mbabane
Bloemfontein
Maseru
Durban
Cape Town
Port Elizabeth
Map data © OpenStreetMap contributors, rendering GIScience Research Group @ Heidelberg University
Satellite Dust
Thu 10/16/2014, 01:00pm UTC

APPENDIX 3: Wind roses for Coastal Dust storms

20 October 2018

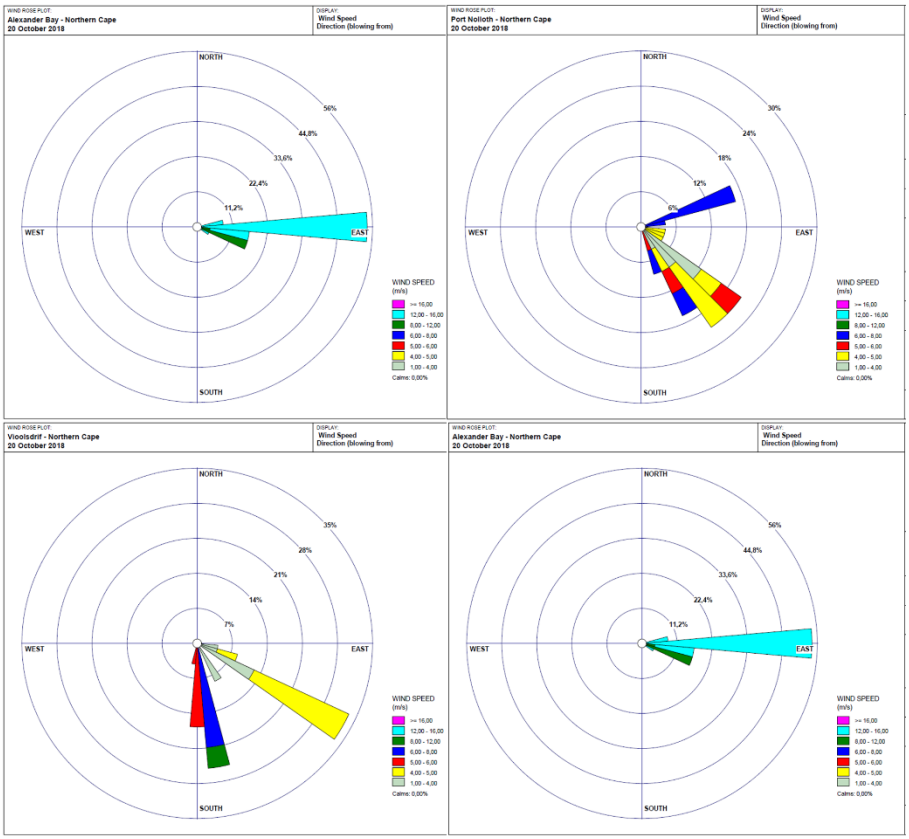

25 September 2019

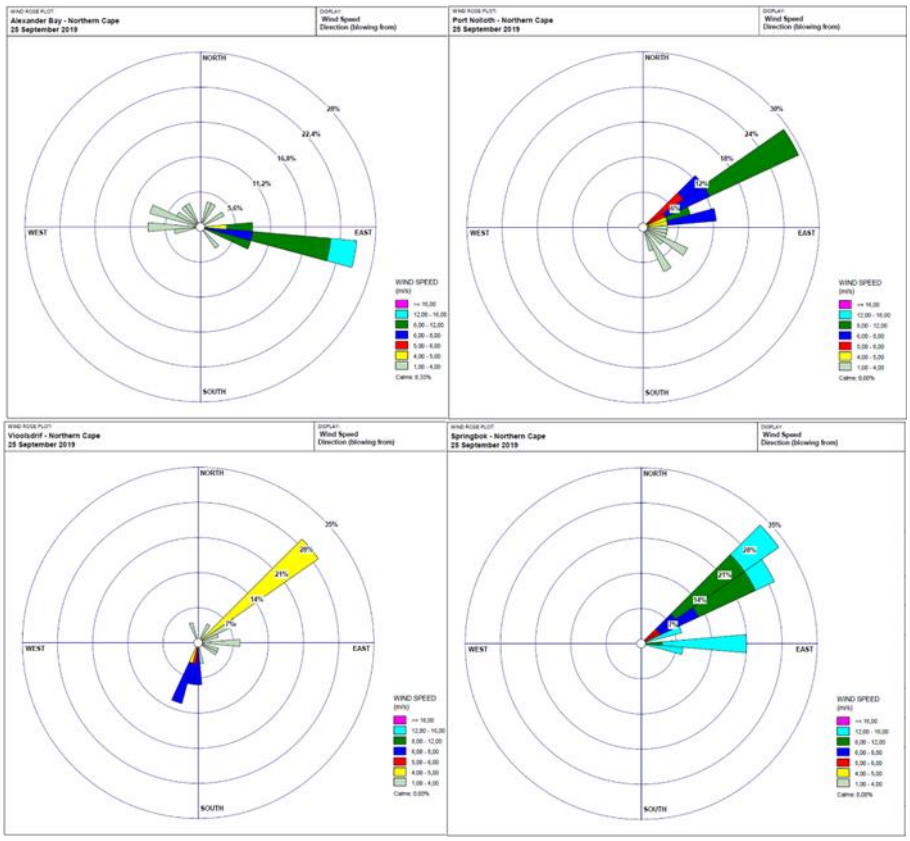

15 July 2020

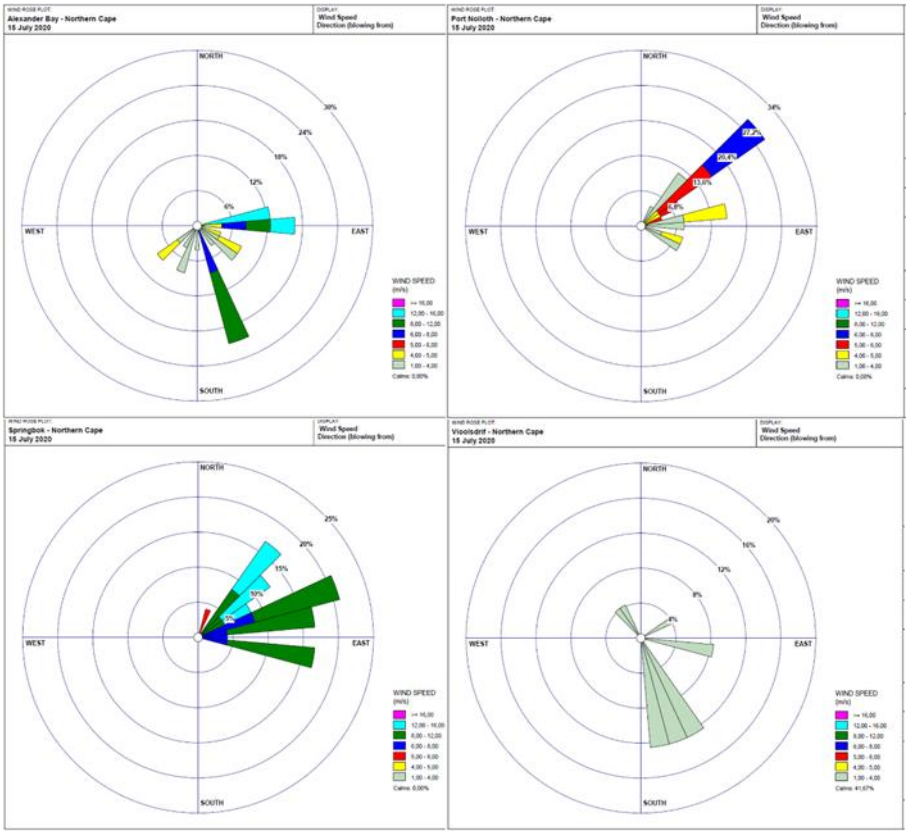

14 July 2021

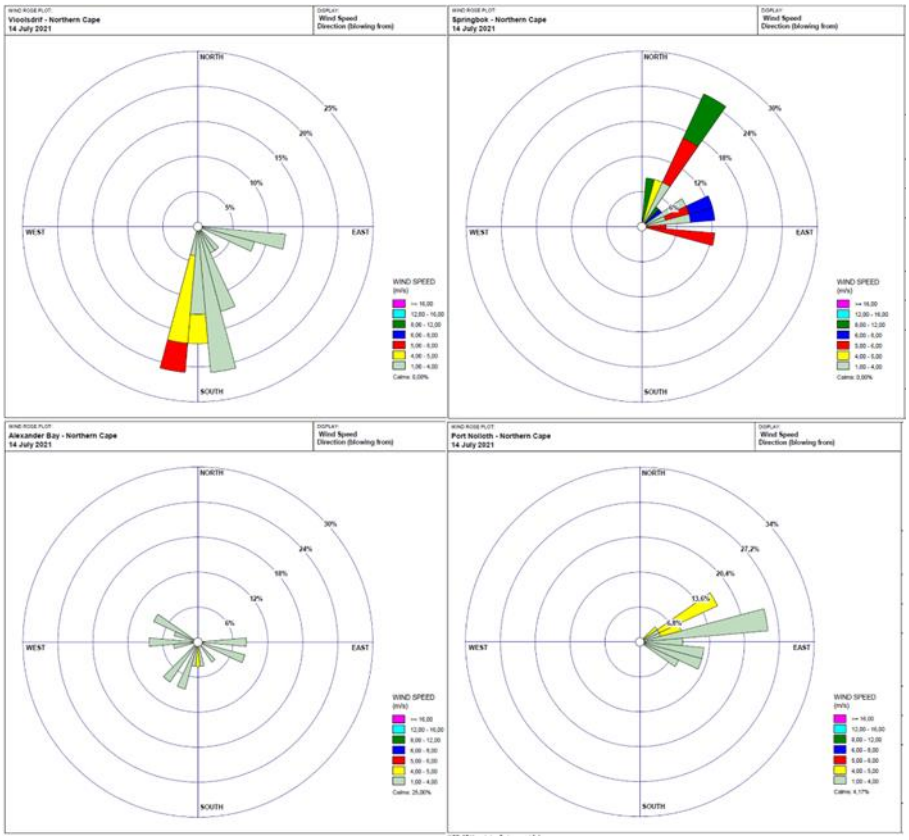

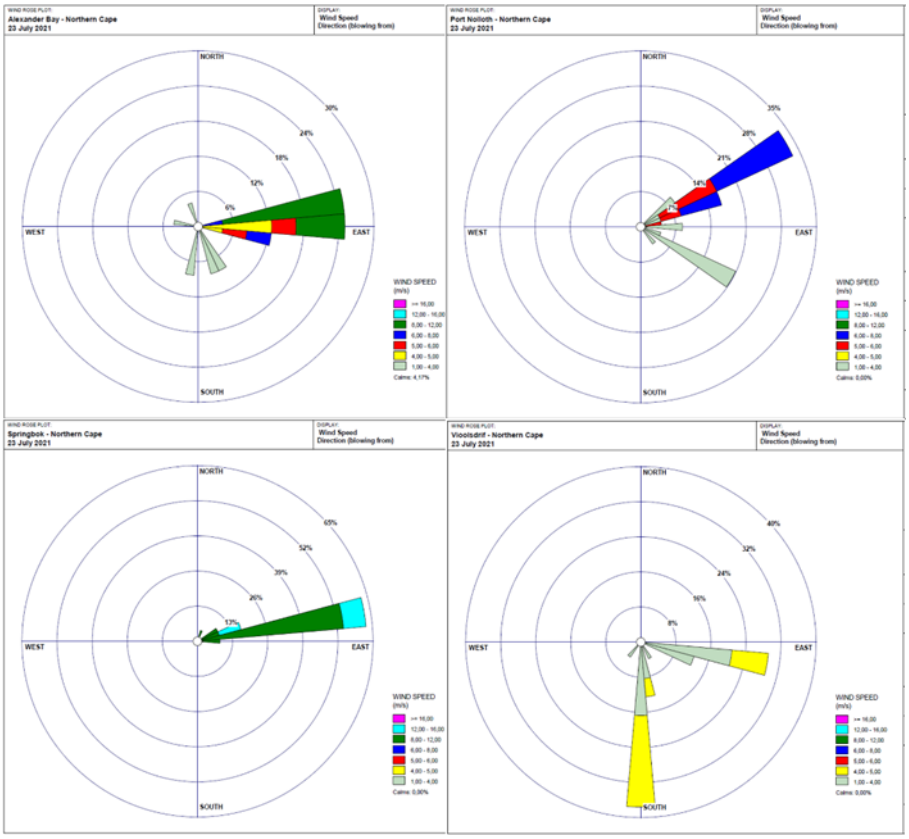
WIND ROSE PLOT:
Alexander Bay - Northern Cape
23 July 2021
DISPLAY:
Wind Speed
Direction (blowing from)
NORTH
EAST
SOUTH
WEST
WIND SPEED
(m/s)
WIND ROSE PLOT:
Port Nolloth - Northern Cape
23 July 2021
DISPLAY:
Wind Speed
Direction (blowing from)
NORTH
EAST
SOUTH
WEST
WIND SPEED
(m/s)
WIND ROSE PLOT:
Springbok - Northern Cape
23 July 2021
DISPLAY:
Wind Speed
Direction (blowing from)
NORTH
EAST
SOUTH
WEST
WIND SPEED
(m/s)
WIND ROSE PLOT:
Vioolsdrif - Northern Cape
23 July 2021
DISPLAY:
Wind Speed
Direction (blowing from)
NORTH
EAST
SOUTH
WEST
WIND SPEED
(m/s)

APPENDIX 4: Wind roses for Interior Dust storms

16 October 2014

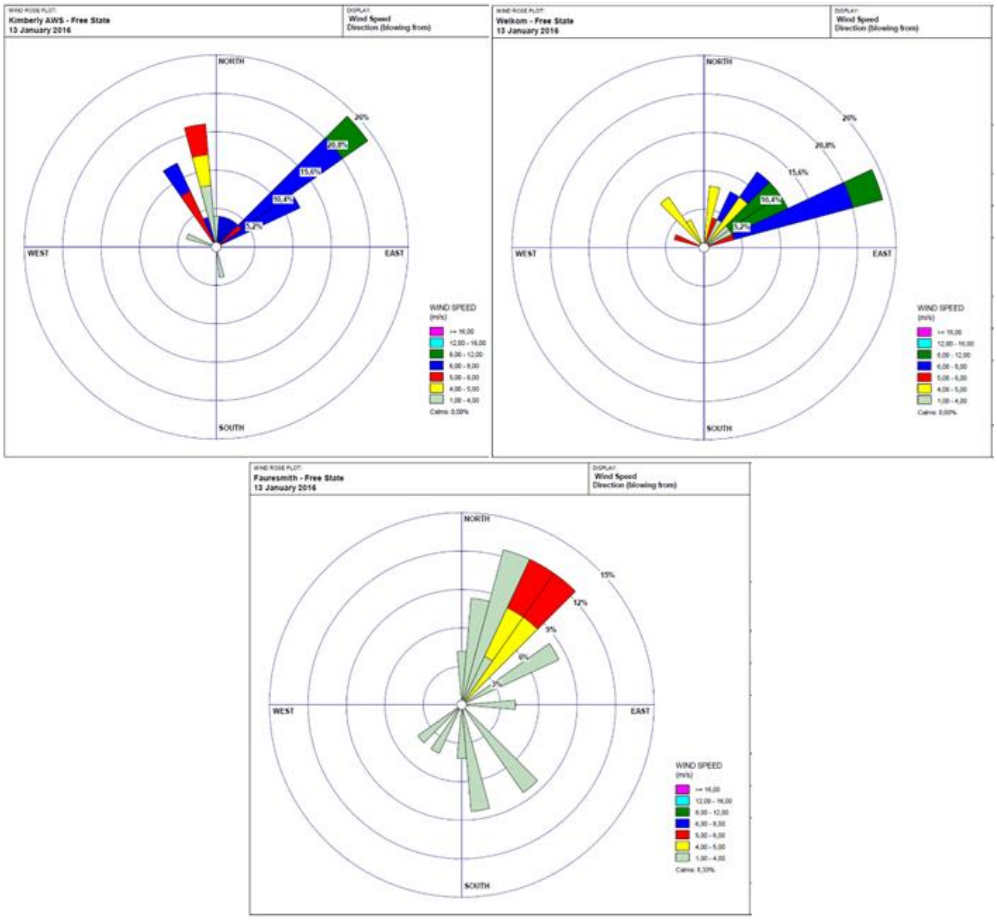

13 January 2016

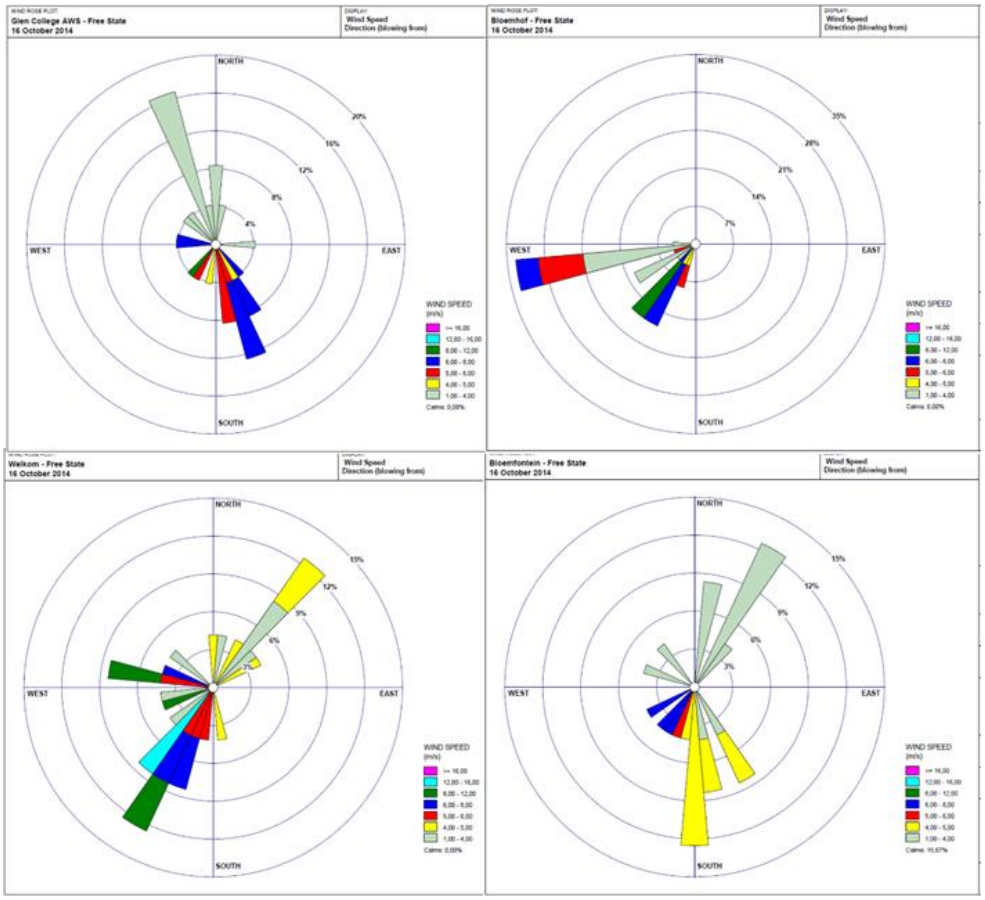

22 August 2017

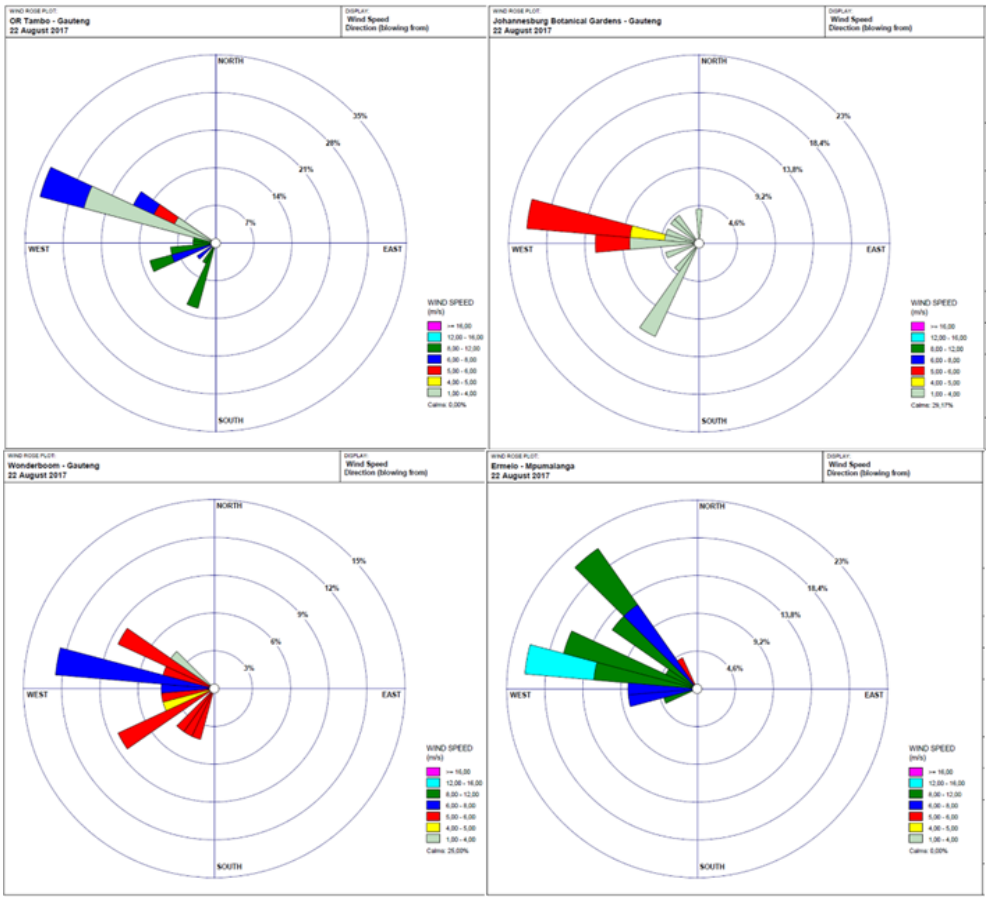

28 December 2018

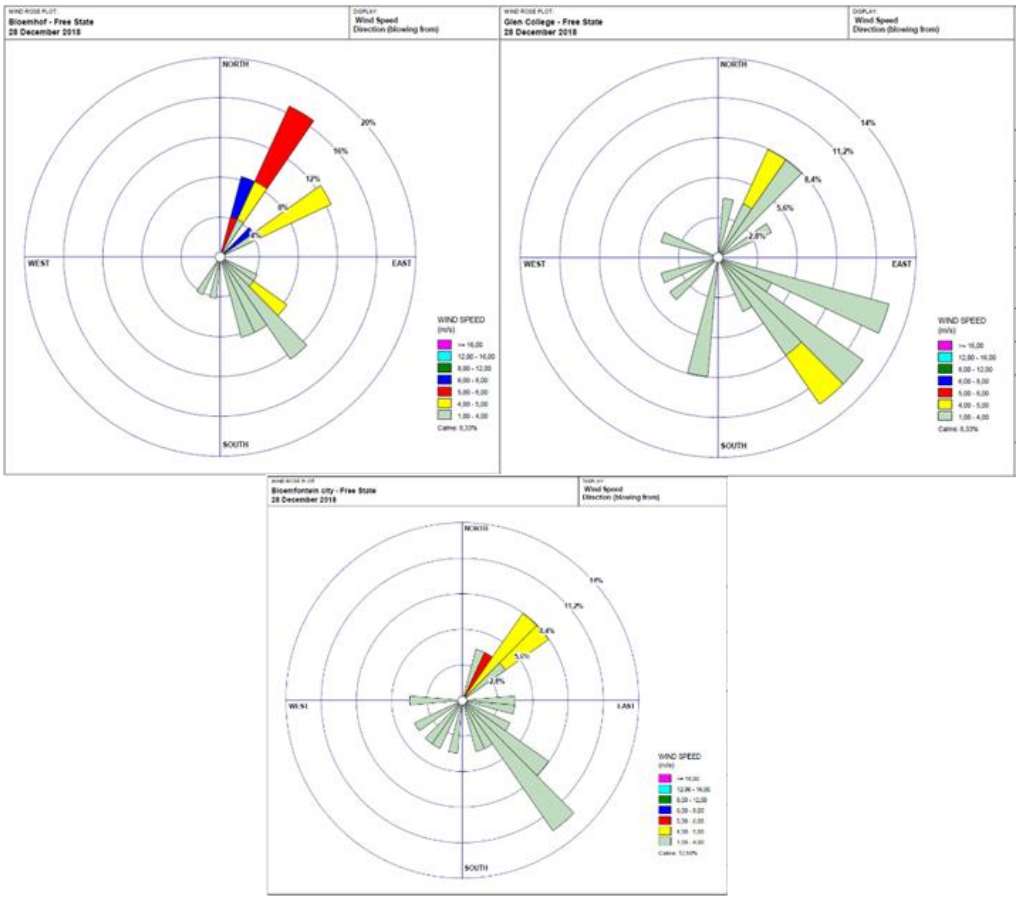

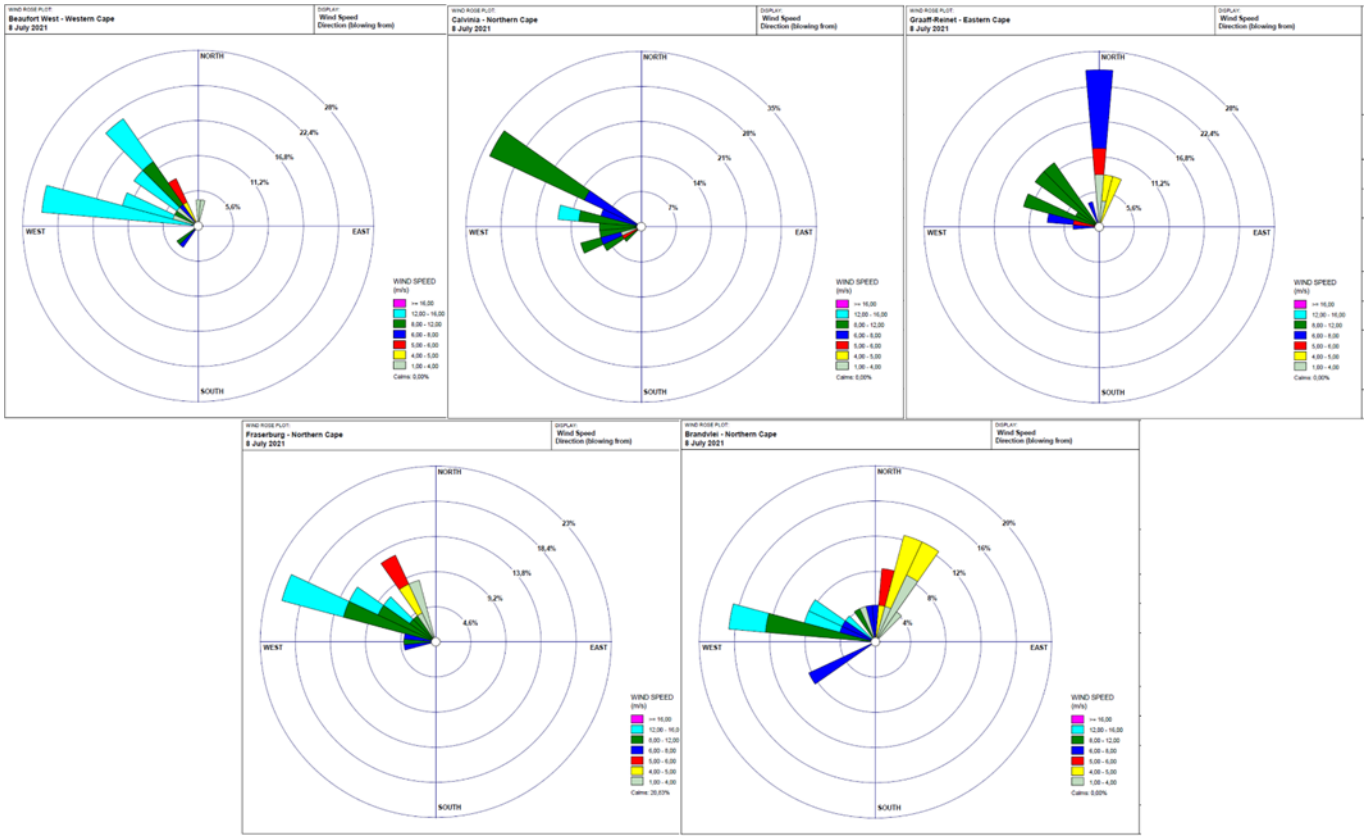
WIND ROSE PLOT:
Beaufort West - Western Cape
8 July 2021
DISPLAY:
Wind Speed
Direction (blowing from)
NORTH
EAST
SOUTH
WEST
5,6%
11,2%
16,8%
22,4%
28%
WIND SPEED
(m/s)
>= 16,00
12,00 - 16,00
8,00 - 12,00
6,00 - 8,00
5,00 - 6,00
4,00 - 5,00
1,00 - 4,00
Calms: 0,00%
WIND ROSE PLOT:
Calvinia - Northern Cape
8 July 2021
DISPLAY:
Wind Speed
Direction (blowing from)
NORTH
EAST
SOUTH
WEST
7%
14%
21%
28%
35%
WIND SPEED
(m/s)
>= 16,00
12,00 - 16,00
8,00 - 12,00
6,00 - 8,00
5,00 - 6,00
4,00 - 5,00
1,00 - 4,00
Calms: 0,00%
WIND ROSE PLOT:
Graaff-Reinet - Eastern Cape
8 July 2021
DISPLAY:
Wind Speed
Direction (blowing from)
NORTH
EAST
SOUTH
WEST
5,6%
11,2%
16,8%
22,4%
28%
WIND SPEED
(m/s)
>= 16,00
12,00 - 16,00
8,00 - 12,00
6,00 - 8,00
5,00 - 6,00
4,00 - 5,00
1,00 - 4,00
Calms: 0,00%
WIND ROSE PLOT:
Fraserburg - Northern Cape
8 July 2021
DISPLAY:
Wind Speed
Direction (blowing from)
NORTH
EAST
SOUTH
WEST
4,6%
9,2%
13,8%
18,4%
23%
WIND SPEED
(m/s)
>= 16,00
12,00 - 16,00
8,00 - 12,00
6,00 - 8,00
5,00 - 6,00
4,00 - 5,00
1,00 - 4,00
Calms: 20,69%
WIND ROSE PLOT:
Brandvlei - Northern Cape
8 July 2021
DISPLAY:
Wind Speed
Direction (blowing from)
NORTH
EAST
SOUTH
WEST
4%
8%
12%
16%
20%
WIND SPEED
(m/s)
>= 16,00
12,00 - 16,00
8,00 - 12,00
6,00 - 8,00
5,00 - 6,00
4,00 - 5,00
1,00 - 4,00
Calms: 0,00%

Appendix 5: Table of the meteorological variables during coastal dust storms

				Temperature (°C)						Dewpoint Temperature (°C)		Relative Humidity (%)				wind (m/s)		Rain (mm)		
Date of dust event	Season	Duration	Station name	Max temp	2 days before	1 day before	During	Day after	Max temp	Min Td Temp	Max Td Temp	2 days before	1 day before	During	Day after	max wind gust	Wind speed at start of DS (m/s)	2 days before DS	1 day before DS	During DS
20-Oct-18	Spring	6 hours (8.30 - 15:00)	Springbok WO	27,6	10,9	7,8	25,3	17,3	27,6	-4,4	2,9	25,9	30,6	17,5	18,4	25	12,1	0,0	0,0	0,0
			Port Nolloth	38,1	8,9	7,2	27,7	22,8	38,1	8,3	13,6	80,2	78,8	52,9	43,7	16	3,0	0,0	0,0	0,0
			Alexanderbay	35,1	13,5	14,3	14,1	16,2	35,1	9,6	13,4	73,2	72,5	54,9	44,3	16	1,0	0,0	0,0	0,0
			Vioolsdrif - AWS	36,3	17,8	18,6	13,6	15,5	36,3	-3,8	7,8	19,3	21,9	13,1	11,7	23	5,0	0,0	0,0	0,0
25-Sep-19	Spring	15 hours (05.30 - 20:00)	Springbok WO	27	13,9	11,3	11,8	9,1	27	-12,4	2,0	26,5	20	20,2	18,1	24	14,0	0,0	0,0	0,0
			Alexanderbay	38,8	13,9	11,6	26,7	24,8	38,8	0,0	8,5	69,3	70	24,4	25	19	9,0	0,0	0,0	0,0
			Port Nolloth	38	16,7	24,2	27,4	21,5	38	-3,4	8,6	55,8	53,1	33	29,6	23	2,0	0,0	0,0	0,0
			Vioolsdrif - AWS	37	12,5	12,6	13,9	15,6	37	-11,0	2,1	19,8	12	11,8	11	14	7,0	0,0	0,0	0,0
15-Jul-20	Winter	3 days (10:00 15th - 18:00 17th)	Springbok WO	12	3,8	4,8	7,2	8,6	12	-7,4	1,6	94,3	83,2	46,3	23,5	24	10,0	7,0	1,0	0,0
			Alexanderbay	24	2,3	3,8	7,6	6,5	24	-1,2	7,3	87,3	83,1	40,8	15,6	22	6,0	0,0	0,0	0,0
			Port Nolloth	24	6,7	8,1	15,7	11,7	24	-2,8	5,3	80,8	77,3	44,6	16,3	18	5,0	0,0	0,0	0,0
			Vioolsdrif - AWS	22	3,4	3,3	6,4	8,6	22	-7,4	1,6	65,2	53,2	36,9	25,4	23	3,0	0,0	0,0	0,0
14-Jul-21	Winter	3 hours (13:30 - 17:30)	Springbok WO	11	9,7	5,4	7,8	8,5	11	-1,1	6,2	85,8	79,7	52	30,6	18	9,8	28,0	0,0	0,0
			Alexanderbay	20	8,3	8,7	16,5	14,8	20	1,2	8,6	69,4	76	50,7	36,5	8	4,0	7,0	0,0	0,0
			Port Nolloth	21	8,1	8,5	14,7	15,9	21	-1,2	3,8	87,1	77,8	65,9	52,9	11	1,3	0,0	0,0	0,0
			Vioolsdrif - AWS	20	3,3	1,6	3,1	2,4	20	-4,8	1,5	56	56,3	37,5	26,7	8	3,1	1,0	0,0	0,0
23-Jul-21	Winter	2 days (09:30 23rd - 19:00 24th)	Springbok WO	13	7,5	6,9	8,0	8,3	13	-2,1	1,9	70,8	65,8	33,9	24,3	22	11,0	1,0	0,0	0,0
			Alexanderbay	24	13,3	12,9	15,6	19,2	24	0,6	5,2	69,4	66,8	28,8	19,6	5	7,0	0,0	0,0	0,0
			Port Nolloth	22	11,7	11,0	19,5	13,8	22	3,9	8,1	60	63	36,5	15	16	2,0	0,0	0,0	0,0
			Vioolsdrif - AWS	20	13,4	12,6	10,3	15,4	20	-4,3	2	43,2	44,1	24,7	17,3	10	5,0	0,0	0,0	0,0

Appendix 6: Table of the meteorological variables during interior dust storms

				Temperature (°C)						Dewpoint Temperature (°C)		Relative Humidity (%)				wind (m/s)		Rain (mm)		
Date of dust event	Season	Duration	Station name	Max temp	2 days before	1 day before	During	Day after	Max temp	Min Td Temp	Max Td Temp	2 days before	1 day before	During	Day after	max wind gust	Wind speed at start of DS (m/s)	2 days before DS	1 day before DS	During DS
Mesoscale-induced DS																				
16-Oct-14	spring	3 days	Bloemfontein Stad	19,2	21,2	16,8	15,7	12,2	19,2	-3,7	6,7	41,8	24,7	49,1	48,5	19,2	8,0	0	0	0
			Glen College AWS	20,3	25,0	19,6	17,2	13,4	20,3	-7,2	4,8	41,6	26,2	47,0	44,9	20,3	8,0	0,0	0,0	0,0
			Bloemhof	22,7	22,0	16,9	16,8	15,2	22,7	-4,6	7,9	33,1	20,7	34,0	41,4	14,7	6,0	0,0	0,0	0,0
			Welkom	21,3	19,7	13,5	15,8	14,7	21,3	-7,7	9,3	39,0	22,0	47,0	41,2	21,3	9,0	0,0	0,0	0,0
13-Jan-16	summer	a few hours	Kimberly	32,8	20,0	15,1	15,2	15,8	32,8	12,7	15,9	54,5	58,4	63,2	52,4	23,5	6,0	17,6	0,0	0,5
			Fauresmith	31,9	18,4	15,7	17,0	18,2	31,9	6,9	14,9	55,3	53,5	65,3	54,0	20,1	10,0	11,6	0,0	15,8
			Welkom	32,8	18,1	19,0	13,9	15,4	32,8	7,3	16,2	57,8	60,3	57,5	59,2	16,0	4,0	15,2	0,2	5,6
28-Dec-18	Summer	3 hours (19:30 - 22:00)	Bloemfontein Stad	35,9	17,4	19,6	17,1	13,8	35,9	1,0	12,9	16,9	22,0	38,3	58,4	16,3	4,0	0,0	0,0	0,0
			Glen College AWS	36,3	23,6	25,0	21,0	16,1	36,3	8,6	16,2	17,7	29,4	45,3	58,3	16,6	5,0	0,0	2,4	0,2
			Bloemhof	33,8	11,5	11,1	7,8	7,7	33,8	-1,4	14,5	16,7	27,1	55,8	65,5	14,4	7,0	0,0	1,4	0,4
Synoptic scale-induced DS																				
22-Aug-17	Spring	1 day (from 11:30 am)	JHB Bot Tuine	24,6	15,6	19,2	17,7	16,5	24,6	-14,6	0,7	52,1	47,5	32,5	22,7	15,9	4,0	0,0	0,0	0,0
			JHB int WO	22,8	14,4	12,1	16,6	15,3	22,8	-11,9	1,7	55,2	46,9	33,3	25,1	20,2	6,0	/	/	/
			Ermelo	22,1	16,2	17,4	18,3	19,4	22,1	-7,9	2,1	69,8	55,4	39,7	39,7	20,8	11,0	0,0	0,0	0,0
			Wonderboom	27,5	15,5	21,1	24,8	19,2	27,5	-13,9	2,8	50,4	50,7	37,0	24,2	15,2	3,0	0,0	0,0	0,0
08-Jul-21	Winter	6 hours (13:30 - 19:30)	Beaufort West	23,7	19,8	18,6	15,6	11,8	23,7	-0,2	5,9	28,8	21,0	27,5	53,3	26,8	13,0	0,0	0,0	3,2
			Graaff-Reinet	26,9	26,4	26,3	11,8	19,0	26,9	-10,7	7,5	41,0	32,3	20,5	39,6	24,5	9,0	0,0	0,0	0,0
			Fraserburg	19,9	21,8	21,0	19,8	13,0	19,9	-14,9	4,4	37,0	34,0	46,3	68,6	24,0	11,0	0,0	0,0	0,6
			Calvinia WO	17,3	15,9	20,2	12,0	11,3	17,3	-10,7	0,4	43,7	40,5	52,6	78,6	21,8	10,0	0,0	0,0	1,6
			Brandvlei	25,2	23,8	23,7	16,7	12,9	25,2	/	/	29,9	29,3	42,4	63,0	21,1	8,0	0,0	0,0	0,0

Appendix 7: Table of the difference in minimum temperature of the day after the DS and the day of the DS.

The blue indicates dates where the minimum temperature either did not change or decreased the day after the DS.

Date of dust event	Station name	Tmin (day after DS) - Tmin (day of DS)
20-Oct-18	Springbok	2
	Alexander Bay	5
	Port Nolloth	4
	Vioolsdrif	1
25-Sep-19	Springbok	5
	Alexander Bay	7
	Port Nolloth	4
	Vioolsdrif	0
15-Jul-20	Springbok	4
	Alexander Bay	9
	Port Nolloth	8
	Vioolsdrif	-1
14-Jul-21	Springbok	2
	Alexander Bay	1
	Port Nolloth	3
	Vioolsdrif	-1
23-Jul-21	Springbok	2
	Alexander Bay	9
	Port Nolloth	2
	Vioolsdrif	1